GEOLOGIC MAP OF THE LAKE JOY 7.5-MINUTE QUADRANGLE, KING COUNTY, WASHINGTON

by Joe D. Dragovich, Megan L. Anderson,
Shannon A. Mahan, James H. MacDonald, Jr.,
Coire P. McCabe, Recep Cakir, Bruce A. Stoker,
Nathan M. Villeneuve, Daniel T. Smith, and John P. Bethel

WASHINGTON
DIVISION OF GEOLOGY
AND EARTH RESOURCES
Map Series 2012-01
October 2012

WASHINGTON STATE DEPARTMENT OF
Natural Resources
Peter Goldmark - Commissioner of Public Lands

DISCLAIMER

INDEMNIFICATION

Research supported by the U.S. Geological Survey, National Cooperative Geologic Mapping Program, under USGS award number G11AC20236. The views and conclusions contained in this document are those of the authors and should not be interpreted as necessarily representing the official policies, either expressed or implied, of the U.S. Government.

WASHINGTON STATE DEPARTMENT OF NATURAL RESOURCES

Peter Goldmark—*Commissioner of Public Lands*

DIVISION OF GEOLOGY AND EARTH RESOURCES

David K. Norman—*State Geologist*
John P. Bromley—*Assistant State Geologist*

Washington Department of Natural Resources
Division of Geology and Earth Resources

Mailing Address:
MS 47007
Olympia, WA 98504-7007

Street Address:
Natural Resources Bldg, Rm 148
1111 Washington St SE
Olympia, WA 98501

Phone: 360-902-1450; *Fax:* 360-902-1785
E-mail: geology@dnr.wa.gov
Website: http://www.dnr.wa.gov/ResearchScience/GeologyEarthSciences/Pages/Home.aspx

Publications List:
http://www.dnr.wa.gov/ResearchScience/Topics/GeologyPublicationsLibrary/Pages/pubs.aspx

Washington Geology Library Catalog:
http://www.dnr.wa.gov/ResearchScience/Topics/GeologyPublicationsLibrary/Pages/washbib.aspx

Washington State Geologic Information Portal:
http://www.dnr.wa.gov/ResearchScience/Topics/GeosciencesData/Pages/geology_portal.aspx

Suggested Citation: Dragovich, J. D.; Anderson, M. L.; Mahan, S. A.; MacDonald, J. H., Jr.; McCabe, C. P; Cakir, Recep; Stoker, B. A.; Villeneuve, N. M.,; Smith, D. T.; Bethel, J. P., 2012, Geologic map of the Lake Joy 7.5-minute quadrangle, King County, Washington: Washington Division of Geology and Earth Resources Map Series 2012-01, 2 sheets, scale 1:24,000, 79 p. text, 1 Microsoft Excel file.

Published in the United States of America

Table of Contents

List of Figures

List of Tables

Plates

Geologic Map of the Lake Joy 7.5-minute Quadrangle, King County, Washington

by Joe D. Dragovich[1], Megan L. Anderson[2], Shannon A. Mahan[3], James H. MacDonald Jr.[4], Coire P. McCabe[1], Recep Cakir[1], Bruce A. Stoker[5], Nathan M. Villeneuve[1], Daniel T. Smith[6], and John P. Bethel[6]

[1] Washington Division of Geology and Earth Resources
MS 47007
Olympia, WA 98504-7007

[2] Colorado College
Department of Geology
14 E Cache La Poudre St
Colorado Springs, CO 80903

[3] U.S. Geological Survey
Box 25046, MS 974
Denver Federal Center
Denver, CO 80225-5046

[4] Florida Gulf Coast University
Department of Marine and Ecological Science
Fort Myers, FL 33965

[5] Earth Systems
19729 207th Ave SE
Monroe, WA 98272

[6] King County Department of Natural Resources and Parks
Water and Land Resource Division
201 S Jackson St
Seattle, WA 98104

INTRODUCTION

The Lake Joy map is the latest of several 7.5-minute quadrangle geologic maps, each of which represents a year-long effort to document surficial geology and geologic structures in northwestern King County and southwestern Snohomish County, a populated region that is seismically active. To further this effort, we have added detailed field observations and several types of geological analyses to existing data, including prior geologic mapping (for example, Tabor and others, 1993; Booth, 1990). We have also incorporated geotechnical findings from the Seattle Public Utilities road and bridge engineering studies, as well as surface and subsurface information from several geotechnical companies for site-specific projects. Plate 1 presents the geologic map, stratigraphic cross sections, a correlation diagram, a lidar (Light Detection and Ranging) image, and geophysical maps and models of the cross sections. Appendices A and B present radiocarbon dates and optically stimulated luminescence (OSL) and infrared stimulated luminescence (IRSL) age information for Quaternary deposits. Appendices C through H provide further geochemical and petrographic data and information about faults, neotectonics, earthquakes, potential field geophysics, sedimentary provenance, and photographs. Plate 2 and Appendix G cover earthquakes and structural features. We follow the nomenclature of Booth (1990) for glacial features, such as Vashon Stade proglacial lakes. Names of all the faults, folds, and geomorphic features shown on the geologic map, such as the Tolt River landslide complex, are informal. The term “volcanic rocks of Mount Persis” of Tabor and others (1993) is herein abbreviated to Mount Persis unit.

FAULT NOMENCLATURE, ACTIVITY, AND STRUCTURES

Geologic mapping of the Lake Joy quadrangle continues our efforts to better understand the southern Whidbey Island fault zone (SWIF) and the relation of the Carnation, Cherry Creek, Griffin Creek, Tokul Creek, and Tolt River fault zones in this quadrangle to the regional SWIF structure (Appendix H). Sherrod and others (2008) extended the SWIF eastward from the Whidbey Island area to the Maltby quadrangle west of the Monroe quadrangle (northwest of the present study area). In a series of geologic maps, we (Dragovich and others) extended the Rattlesnake Mountain fault zone (RMFZ) from the North Bend, Snoqualmie, and Fall City quadrangles northwestward through the Carnation and Monroe quadrangles and correlated this broad fault zone with the SWIF. These map reports are: Fall City (2007), Snoqualmie (2009a,b), North Bend (2009c), Carnation (2010a,b), and Monroe (2011a,b). (An overview map below the geologic map on Plate 1 shows the location of these quadrangles relative to the Lake Joy quadrangle.) In these reports, we suggest that the SWIF from the Monroe area to the south is likely a strike-slip fault zone and has some active or potentially active segments. Some of those segments align with probably active fault strands mapped by Sherrod and others (2008) to the west. Major faults of the RMFZ–SWIF in the Carnation quadrangle (directly west of the map area) include the Cherry Valley fault (CVF), Cherry Creek fault zone (CCFZ), Snoqualmie Valley faults, Rattlesnake Mountain faults, and Carnation faults nos. 1 and 2 (CF-1 and CF-2). RMF-1

is the main strand of the RMFZ, which Dragovich and others (2010a,b) correlated with the Cottage Lake lineament of the SWIF of Sherrod and others (2008). We extend the CF-1 and -2, CVF, and the CCFZ into the Lake Joy quadrangle, and thus the northeastern part of the SWIF likely traverses the southwestern part of the map area. (See Dragovich and others, 2010b, and Appendix H in this study for a discussion of individual fault strand attributes in the Carnation quadrangle.) Reverse faults in the Carnation and Monroe quadrangles include the Carnation faults and the Monroe and Fontal Road faults. We tentatively interpret these east-trending faults as restraining bend duplex structures within the northwest-trending SWIF. Associated folds, including the Tolt River anticline (Plate 1), that are subparallel to these reverse faults are likely flexural-slip anticlines and synclines. We base this interpretation on the (1) parallel structures, (2) current north–south compression of the Puget Lowland, (3) geophysical data, and (4) limited kinematic data for subsidiary fault zones. The northerly vergence of these reverse faults in the Monroe quadrangle contrasts with the southerly vergence of the Carnation faults in the Carnation quadrangle and western part of the Lake Joy map area. This opposite vergence may demark a pop-up or positive flower structure within the SWIF (Dragovich and others, 2011a,b). The northeast-trending CCFZ is conjugate to the northwest-trending SWIF and likely merges with it in the Carnation quadrangle (Dragovich and others, 2010a,b). The 1996 Duvall earthquake (max. M_L=5.3) hypocenters were at a shallow depths (~2–8 km) along the CCFZ; the quakes occurred as a swarm that was roughly centered on the intersection of the Lake Joy, Monroe, Carnation, and Sultan quadrangles (Appendices G and H; Plate 2). Major faults in the Snoqualmie quadrangle (adjacent to the south) that extend into the Lake Joy quadrangle include the Tokul Creek fault zone (TCFZ) and the Griffin Creek fault. Like the CCFZ, the TCFZ is probably a northeast-trending fault zone conjugate to the SWIF that may be locally active (Appendices G and H). Most kinematic indicators in the Lake Joy map area, such as shallow slickenlines on steep shear planes and (or) en echelon vein arrays, suggest strike-slip or oblique-slip offset along strands of the CCFZ and TCFZ (Appendix H). Reverse faulting is shown by kinematic indicators on shallowly dipping, very thick and well-exposed foliate mylonites along CF-1 at significant site 28D (Plate 1; sec. 12, T25N R7E) on the Tolt River. The CCFZ, CF-1, and parts of the TCFZ may be potentially active to active structures. For example, active faulting along the western part of the TCFZ in the center of the quadrangle is indicated by a probable Quaternary fault displacing Pleistocene deposits at significant site 108D (Plate 1; sec. 33, T26N R8E). This area is also the general location of the 1932 Tolt River earthquake (Bradford and Waters, 1934). (The center of the VI earthquake intensity contour for this quake is located at significant site TQ2 [Plate 1; sec. 20, T26N R8E]; this contour was partially based on a felt report—“practically impossible to stand”—at significant site TQ1 [sec. 33, T26N R8E] near the Tolt Regulating Basin on Plate 1).

PLEISTOCENE ALLUVIUM AND QUATERNARY STRUCTURES

Throughout the Snoqualmie River valley, ancient alluvium representing several Pleistocene nonglacial intervals is widespread; it has vertical and lateral distribution and internal structure that imply significant tectonic control of these old river deposits within the broad SWIF and along subsidiary structures. The Pleistocene Snoqualmie River sediments have a petrographic composition that is similar to that of Holocene Snoqualmie alluvium (Dragovich, 2007; Dragovich and others, 2007, 2009a,b,c, 2010a,b, 2011a,b). These Quaternary deposits (Holocene or Pleistocene), which are derived from the Snoqualmie River basin, have a distinct composition and stratigraphic fluvial style and form a mappable depositional facies over time. Here we refer to the Snoqualmie River sediments of that composition and depositional style as SP (see Appendix F). SP strata dominate ancient nonglacial deposits, such as the Whidbey Formation (unit Qcws), that are also found in the present study area. The SP has a distinct granodiorite to granite Tertiary batholith and volcanic provenance signature; deposits contain significant amounts of monocrystalline quartz (~10–20%), plagioclase, volcanic and sedimentary lithic clasts, granitic lithic clasts, potassium feldspar, and lesser, but also significant, green pleochroic hornblende and biotite (Appendix F). We also map ancient Tolt River alluvium (for example, unit Qchmp) in the quadrangle; this alluvium displays a distinct local eastern provenance similar to that for modern Tolt River alluvium. This alluvium may interfinger with SP sediments in the subsurface in the western part of the map area. We apply the growth folding and pull-apart and inverted basin models to the structures and stratigraphic relations we observe within the SWIF and extend these structural-stratigraphic concepts to Quaternary strata. For example, Dragovich and others (2009a,b) hypothesized a SWIF pull-apart basin containing Miocene volcanic rocks of Snoqualmie Falls to the south in the Snoqualmie area. This volcanism is likely the result of intrusion of the Snoqualmie batholith along SWIF strands. At the same time, the volcanic rocks of Snoqualmie Falls were being deposited in fault-controlled basins within the RMFZ strands. Dragovich and others (2007, 2009a,b,c, 2010a,b, 2011a,b), and Littke and others (2009) suggested much younger

inversion of sub-basins along the length of the SWIF in the Snoqualmie valley, whereby the Snoqualmie River has been structurally trapped within fault-controlled transpressional or transtensional basins during the Quaternary. Some of this ancient SP alluvium is anomalously thick—as much as about 800 ft (~250 m) thick in SWIF basins south of the quadrangle. Ancient SP sediment is also commonly tilted or broadly folded and is observed at many stratigraphic levels and various elevated positions along the Snoqualmie, Skykomish, and Tolt River valleys. The thickness and structural style of nonglacial SP strata suggest that they were deposited in SWIF pull-apart basins and locally uplifted to form shortened inverted basins. This transition from transtensional to transpressional basins is indirectly evidenced by the exceptional thickness of some of the alluvial basin sediments. In our hypothesis, formerly extensional pull-apart basins are uplifted as a result of kinematic changes along the fault zones and are now tilted, folded, and (or) raised in blocks between apparent subparallel faults. North of CF-1, ancient SP alluvium is apparently folded along the proposed Tolt River anticline (Cross Section B). This alluvium is currently mapped to an elevation of ~900 ft (274 m)(significant site 5W, Plate 1; sec. 7, T25N R8E). In the present study area, logs of wells in the Tolt valley directly north of CF-1 suggest that SP Pleistocene sediments are as much as 400 ft (122 m) thick, implying some structural control over sedimentation (Cross Section B). Offset along the CF-1 may be actively raising the highlands north of this fault zone. Some uplift of Olympia-age and Whidbey Formation SP deposits seems likely, given their distribution, elevation, age, and structure across the map area (Appendices B, G, and H). We surmise that the ancient Snoqualmie River valley occupied the southwest part of the quadrangle west of the Griffin Creek fault. This buried alluvial valley(s) corresponds to the topographically subdued area visible with lidar data (Plate 1, Fig. 3).

ISOSTATIC GRAVITY AND AEROMAGNETIC ANALYSES

Map-view qualitative analysis and forward modeling of potential field geophysical anomalies along cross section lines within the Lake Joy quadrangle support our interpreted stratigraphic and structural arrangement, especially at depth. High-quality aeromagnetic data define the geomagnetic anomalies (Plate 1, Figs. 1 and 2; Blakely and others, 1999), and an unpublished regional database of gravity data constrains isostatic gravity anomalies. (See Anderson and others, 2006, for an overview of this database.) In addition, new gravity data collected in the quadrangle help define smaller scale anomalies, especially along Cross Section B (Plate 1, Fig. 1; Villenueve, 2012; Appendix D). Extensive sampling and measurement of physical properties for units in this and neighboring quadrangles (Appendix D, Table D1) provide strong support for predicting anomalies produced by cross-section interpretations, as well as a means for interpreting map-view anomalies in terms of subsurface geologic units. Western mélange belt rocks (unit KJm) have low magnetic susceptibility and are moderately dense, accounting for map regions with high gravity anomalies and low magnetic anomalies (for example, anomaly KJ in Fig. 1 on Plate 1). Volcanic rocks of Mount Persis are less dense than unit KJm and generally quite magnetic. The basalts (unit Evb_p) and basaltic andesites (unit Eva_{pd}) are especially magnetic and have nearly indistinguishable density and magnetic susceptibility properties (Appendix D). Hence, such units could be interchangeable in the geophysical models and map interpretations, given slight modifications in unit geometries. Geophysical data combined with regional mapping, as well as limited exposures of granodiorite, suggest that the Index batholith (unit MOig) intrudes to a shallow level in the eastern part of the map area (Cross Section A, Plate 1). Unit MOig is slightly denser than rocks of the Western mélange belt, and its existence along the eastern side of the quadrangle, combined with thicker Mount Persis units along the western edge, produces the overall isostatic gravity gradient with decreasing anomaly values to the west. A large pluton in this region is also supported by recent regional gravity and magnetic modeling of the Puget Lowland crustal structure (Anderson and others, 2011). However, details about the geometry of the contact between units MOig and KJm are poorly constrained because of the lack of east–west transects of gravity data within the quadrangle (see gravity stations on Fig. 1, Plate 1). Spatial correlation of gravity anomaly lows with strong aeromagnetic highs supports our general interpretation that most magnetic highs are due to flows of units Evb_p and Eva_{pd} filling moderately distal to distal volcanic basins, consistent with our interpretations of aeromagnetic highs in the nearby Monroe quadrangle (Dragovich and others, 2011b). (For example, see anomalies PH1 and PH2 in Plate 1, Fig. 1, as well as thick basin-filling Mount Persis units in geophysical models in Plate 1, Fig. 2). One caveat is that there are likely metagabbro bodies within unit KJm that may produce moderate magnetic and (or) gravity highs (see unit $KJigb_w$ on Plate 1and Fig. 2). Geophysical models support the hypothesis that Mount Persis units interfinger on the structural cross sections; however, these units could have numerous configurations that would also predict the geophysical anomalies observed, and therefore the structural configuration we show is not the only possibility. On the other hand, Mount Persis basaltic units, andesite, and volcaniclastic rocks have distinguishable

physical property characteristics (Table D1); therefore, their general distribution within the cross sections is well supported by the geophysical modeling. Structurally, Carnation fault no. 1 and the subparallel Tolt River anticline are very well constrained by geophysics as a reverse fault and flexural slip-fold pair. This reverse fault records substantial south-vergent offset (Plate 1, Figs. 1 and 2, Cross Section B).

DESCRIPTION OF MAP UNITS

We used the Udden-Wentworth scale (Pettijohn, 1957) to classify unconsolidated sediments, Dickinson's (1970) terminology for sandstones, and Le Maitre and others' (2002) terminology for volcanic rocks. Clinopyroxenes are collectively described as 'augite' but may include other petrographically similar varieties. We use the time scales of the U.S. Geological Survey Geologic Names Committee (2007) and Wolfe and others (1998). Description of weathering rinds on basaltic clasts follows the methodology of Colman and Pierce (1981). Thin-section point-count data on the sand-size fractions helped differentiate several glacial and nonglacial units. An important compositional discriminator for Quaternary strata studied for this report is the average percentage of monocrystalline quartz (Qm) versus quartz-mica tectonite / polycrystalline quartz / chert (Qp) versus potassium feldspar (K-spar) normalized to just the three-component system and shown as $Qm_xQp_xPF_x$. $Qm_xQp_xPF_x$ data provided below were obtained from Dragovich (2007) and Dragovich and others (2009b, 2010a,b), as well as by petrographic examination of 21sand samples from the Lake Joy quadrangle (Appendix F). Percentages given for individual mineral or lithic grains given below are not normalized and represent the whole clast population.

Quaternary Sedimentary Deposits

HOLOCENE NONGLACIAL DEPOSITS

af **Artificial fill**—Mixed-earth materials, including sand and gravel fill and natural deposits that have been disturbed at major construction sites where the original strata have been significantly obscured; includes artificial fill damming the Tolt Regulating Basin. May locally contain modified land.

Qp **Peat**—Loose or soft peat, muck, and organic silt and clay, with local thin beds of tephra, including the Mazama ash (Knoll, 1967; Broecker and others, 1956). Peat is also interstratified with alluvial deposits along Griffin and Canyon Creeks and in other low-energy-river valleys, upland depressions, and kettles over low-permeability glacial deposits. Most of these places were mapped using lidar, topographic maps, and previous mapping of Booth (1990). Yount and others (1980) and Broecker and others (1956) reported radiocarbon ages of 7,000 and 11,900 yr BP from peat in a Moss Lake bog east of Lake Joy at age sites 269A and 269B (Plate 1). The younger age at core sample site 269A (depth 14 ft [4.2 m]) was determined from peat directly below Mazama ash. The older age is from peat directly overlying probable unit Qgl_r blue clay at a core depth of 22 ft (6.7 m).

Qa, Qoa **Tolt River alluvium**—Cobble and boulder gravel, pebble gravel, sand, and gravelly sand, and lesser silt, peat, and organic sediments; sands are bluish gray; clasts are subrounded to rounded; sediment is loose, sorted, and well stratified; wood debris and detrital wood are common. Sands (68–70% SiO_2) are lithic rich and contain significant volcanic metasandstone and metachert lithic grains eroded from local Tertiary volcanic rocks and the Western mélange belt. The sands also contains significant granitic lithic grains with less, but appreciable quantities of, monocrystalline and polycrystalline quartz, plagioclase, and some K-spar (1–2%)(Appendix F). Eastern provenance unit Qa is similar to Vashon recessional outwash and ancient Tolt River alluvium nonglacial sediments (Hamm Creek unit Qc_{hmp}). Some lithic grains are K-spar-bearing true granite, and most are likely derived from reworking of Vashon recessional outwash and unit Qc_{hmp} alluvium. Tolt River alluvium is estimated at 10 to 50 ft (3–15 m) thick on the basis of sparse subsurface information (Cross Section B). Unit Qoa is older Tolt River alluvium similar to the well-stratified and -sorted, loose boulder- and gravel-dominated sediment in unit Qa, but it is elevated above the modern flood plain and generally separated from unit Qa by a topographic scarp. These terraced bodies are mapped along the Tolt River valley walls and are inset against Pleistocene deposits or bedrock. We show only the most conspicuous unit Qoa bodies. Contacts were verified using field mapping, lidar elevation information, and previous mapping by Booth (1990), who also mapped a few unit Qoa bodies along the river. Holocene tectonic uplift may have contributed to the isolation of these elevated terraces.

However, some of the terraced alluvium that is substantially elevated above the Tolt River may be latest Pleistocene fluvial outwash (see unit Qgof).

Qls **Landslide deposits (Holocene to latest Pleistocene)**—Diamicton or boulder gravel with minor sand or gravel beds where locally modified by stream processes. Sediments are loose or soft and are typically poorly sorted and unstratified. Clasts are angular to subangular where derived from bedrock. The unit contains mostly rounded clasts where landslides originated in Quaternary deposits. Landslides include rock falls, lateral spreads, slump-earthflows, debris slumps, and debris flows, but also a few areas of thick colluvium (see landslide classification system of Varnes, 1978a,b). This unit may include chaotic, stratified slump blocks or debris-flow aprons originating in unstable recessional deposits perched on hillsides, particularly kames and recessional deltas. Not shown are deposits in the numerous narrow, steep debris-flow chutes evident on lidar imagery. Some landslides may have been initiated during late Pleistocene deglaciation. The lateral-spread geometry of many of these large landslides may be the result of shaking associated with nearby faults (for example, along CF-1); examples are the deep-seated landslides along the Tolt River, such as the Tolt River landslide complex shown on Figure 3 (Plate 1).

Qaf **Alluvial fan deposits (Holocene to latest Pleistocene)**—Debris-flow diamicton, alluvial gravel, boulder gravel, and sand. Sediment is loose, mostly poorly to moderately sorted and massive to moderately stratified. The reduced gradient where streams emerge from confining valleys causes some of the sediment load to be deposited as a fan. Deposits mapped as unit Qaf are distinguished from those in unit Qls by their location and regular lobate geomorphology visible with the aid of lidar imagery.

PLEISTOCENE GLACIAL AND NONGLACIAL DEPOSITS

Vashon Stade of the Fraser Glaciation

Puget lobe continental ice advanced south across the Puget Lowland and covered the map area. Vashon deglaciation in the map area commenced about 14,000 yr BP along the Cascade Range foothills directly to the east, and the map area was fully deglaciated by about 13,500 yr BP (Porter and Swanson, 1998). The Puget lobe ice front receded across the map area in a northwesterly direction, leaving recessional outwash facies. Many of these facies are laterally and vertically gradational and commonly interfinger. During ice recession, a series of ice-marginal lakes and connecting glaciofluvial channels formed in the wake of the retreating ice lobe. The geometry, inset relations, and elevation of these deposits reflect successive lowering of base level as lower valleys became ice-free and emerging spillways migrated westward and northward; this resulted in younger inset or terraced recessional deposits graded to these spillways (Knoll, 1967; Booth, 1990; Porter and Swanson, 1998). Glacial Lake Snoqualmie, an ice-dammed lake that covered Snoqualmie valley during deglaciation (Mackin, 1941; Booth, 1990; Dragovich and others, 2007, 2009a,c, 2010a,b, 2011a,b), controlled the elevation of recessional outwash bodies such as the Tolt River outwash complex above the Tolt River in the southwestern part of the map area. Booth (1990) subdivided recessional outwash deposits into five stages of deglaciation and emphasized the importance of both ice-marginal and subglacial meltwater paths. For example, some of the small southwest-trending valleys traversing the glacial uplands evident on Figure 3 (Plate 1) may be the result of meltwater erosion and sedimentation in subglacial tunnels. Our mapping confirms that ice-marginal meltwater followed several elevated pathways during glacial recession, depositing ice-contact, fluvial, deltaic, kame, and lake sediments.

Most recessional sediments contain significant local mélange belt and Tertiary volcanic detritus, but also appreciable metasandstone, meta-argillite, metachert, volcanic lithic clasts, and lesser granite, greenstone, amphibolite, and serpentinite lithic grains and some hornblende and pyroxene. Glacial sands have a low monocrystalline-quartz grain content and a relatively high polycrystalline quartz to monocrystalline quartz ratio (Dragovich, 2007; Dragovich and others, 2009b, 2010a,b, 2011a,b). Compared to modern and ancient SP strata, average recessional sands have minor but distinct potassium feldspar contents (1–8%) (Appendix F) via the presence of K-spar-bearing granitic lithic grains. This somewhat elevated K-spar content contrasts with the composition of outwash in the Carnation and Monroe quadrangles (Dragovich and others, 2010a,b, 2011a,b). The difference is probably because the Index and Grotto batholithic sources are closer to these recessional deposits than they are to the same unit in the quadrangles to the west; furthermore, both the granites and arkosic metasandstones of the Western mélange belt are *upstream* in the southwest-directed glaciofluvial recessional pathways.

Vashon Recessional Deposits

Qgl_r **Recessional glaciolacustrine (glacial lake) deposits**—Silt, clayey or sandy silt, and silty sand, typically with scattered dropstones. Sediments are loose or soft and massive or laminated to thinly bedded and locally display varve-like rhythmites and lenses or beds of sand or gravel. Kame lake deposits locally display some soft-sediment deformational features such as tilted or deformed bedding. These sediments were deposited in small proglacial lakes formed in kames or other upland ice-marginal settings. Upward-fining sequences record waning lake sedimentation in small proglacial lakes. Upward-coarsening sequences may begin as glacial-lake deposits (units Qgl_r and Qgos) and grade into overlying deltaic (unit Qgod) and fluvial (unit Qgof) deposits as a result of progradation of the large Tolt outwash complex delta to the west into Glacial Lake Snoqualmie in the southwestern part of the map area. Broecker and others (1956) reported a radiocarbon date of 11,900 yr BP from peat overlying soft blue clay at Moss Lake in the western part of the map area east of Lake Joy (age site 269B on Plate 1). This clay is probably unit Qgl_r and indicates that the area was fully deglaciated before 11,900 yr BP, consistent with regional age information.

Qgos **Outwash sand**—Sand and pebbly sand, with some interbeds of silty sand, silt, or gravel; sands are typically dark blue-gray, weathering brownish gray. Sediments are loose or soft and vary from unstratified to weakly stratified to plane-bedded, laminated, and, rarely, crossbedded. Vertical and horizontal fining trends indicate mostly shallow-water glaciolacustrine deposition. Unit Qgos complexly interfingers with recessional lake deposits (unit Qgl_r), fluvial deposits (unit Qgof), and deltaic deposits or kame deltaic deposits (unit Qgod). Some unit Qgos sands coarsen upward into unit Qgod sands and gravels, and they locally fine downward to unit Qgl_r silty lake deposits due to deltaic progradation, as in the Tolt River Valley outwash complex (TVO complex; Fig. 3, Plate 1).

Qgod **Deltaic outwash and kame deltas**—Sandy cobble gravel, gravel, pebbly sand, and minor sand; sands are typically dark blue-gray to light gray, weathering to yellowish brown or brownish gray. Sediments are loose, moderately to well sorted, and well stratified in thin to very thick beds. Deltas have high-amplitude planar foreset beds graded to temporary ice-dammed lake levels. This unit includes fairly small kame deltas (for example, unit Qgod in the Tolt Regulating Basin ice-contact complex) or ice-free deltas (for example, the TVO complex). Gravels (unit Qgof) that cap deltas were fed by upland braided rivers, which vigorously incised the newly exposed and unstable upland surfaces. The varying elevation of proglacial lakes controlled the altitude of many delta tops, recessional channels, and the distribution of most glaciolacustrine deposits; ice receded in a north-northwesterly direction, and delta tops occupied successively lower elevations over time. Non-kame deltas, such as the TVO complex, lack evidence for near-ice deposition and are mostly younger than ice-contact deposits to the east and northeast. The TVO complex is capped by fluvial outwash (unit Qgof) and prograded significantly into Glacial Lake Snoqualmie directly west of the map area (Dragovich and others, 2010a,b); it forms a lobate delta front in the Snoqualmie valley termed the Tolt River delta by Knoll (1967). The delta complex has a glaciofluvial-delta-front interface elevation of ~300 to 420 ft (91–128 m) in the Tolt River valley, higher than the interface elevation of ~280 to 300 ft (85–91 m) directly west of the Lake Joy quadrangle.

Qgof **Fluvial outwash deposits**—Cobble and boulder gravel, gravel, pebbly sand, and interbeds of sand and rare silt; sands are grayish brown, weathering olive-yellow. Sediment is loose and moderately to well stratified and commonly contains medium to very thick subhorizontal beds that have local bar or ripple crossbedding, imbricated gravel, and rip-up clasts. This unit lacks ice-contact sedimentary structures and other geomorphic and stratigraphic evidence for nearby ice, but some unit Qgof outwash grades laterally into ice-contact deposits. For example, the unit Qgik kame fluvial deposits east of the Tolt Regulating Basin grade to the east into valley train unit Qgof deposits that lack the pitted or sparsely kettled outwash surface of the kames. Unit Qgof forms topset beds on deltas (unit Qgod), including the fluvial facies of the TVO complex. Inset fluvial outwash terraces in unit Qgof record fluvial incision as base levels dropped and meltwater incised into older glacial deposits. These terraces record ancient southwest-trending recessional meltwater pathways that generally decrease in elevation to the southwest. For example, fluvial terraces in the TVO complex are likely graded to dropping Glacial Lake Snoqualmie

lake levels in the Snoqualmie valley to the west of the map area, where the Tolt River delta has inset terraces, as well as nested deltas (Dragovich and others, 2010a,b). Thus, the elevation of Glacial Lake Snoqualmie, which may have occupied the lower Tolt River valley in the southwest part of the map area, had a major geomorphic control over recessional outwash deposition.

Qgic **Ice-contact deposits, undivided**—Cobble and boulder gravel, gravel locally containing diamicton, silty pebbly gravel and sand, pebbly sand, and silt. Sediment is loose and mostly moderately stratified, medium to very thickly bedded, and variously sorted; abrupt grain-size changes are common. Ice-contact primary structures include oversteepened and contorted bedding and other ice-shear or slump features producing variously dipping strata. Soft melt-out, flow, and water-laid diamictons are interstratified with granular supraglacial, englacial, and subglacial meltwater deposits (see subglacial depositional model of Booth, 1984, 1986, 1990). The upper surface is typically hummocky and contains numerous kettle depressions. The Tolt Regulating Basin ice-contact complex has several mappable ice-contact facies, including ice-marginal fluvial-deltaic kames, hummocky dead-ice facies, and an arcuate ridge at significant site 18V (Plate 1; sec. 28, T26N R8E) that might be a moraine. The dead-ice deposits of the complex grade eastward from kame deposits to recessional outwash fluvial deposits (unit Qgof). More broadly, various types of ice-contact deposits form north-northeast-trending belt(s) across the map area, implying an ice terminus that waned or stagnated one or more times during deglaciation (this study; Booth, 1990; Knoll, 1967). Some of the smaller isolated unit Qgic deposits likely accumulated where active ice lobes were stable long enough for debris to accumulate and do not necessarily represent ice stagnation. Includes unit Qgi of Dragovich and others (2007, 2009b). Locally divided into:

Qgik **Ice-contact kames**—Cobble and boulder gravel, gravel, sand and pebbly sand, and rare lenses of diamicton (mostly flow till or melt-out till from buried sediment-laden ice blocks). The sands are typically dark yellowish gray to gray. Sediments are loose, moderately to well stratified, medium to very thickly bedded, and commonly display till or silt rip-up clasts, cross-bedding, cut-and-fill structures, and localized oversteepened or slumped bedding. This unit is mostly fluvial kame deposits but may include some undivided kame delta deposits. Kames were mapped where sedimentary structures, geomorphology, and (or) geologic setting imply lateral ice buttressing. Included are kame deposits in the eastern part of the Tolt Regulating Basin ice-contact complex, where a pitted fluvial outwash plain records fluvial deposition around and on stagnant ice blocks along an ice margin (Fig. 3, Plate 1). In the western part of the complex, the fluvial kame deposits grade laterally into or overlie divided kame deltas (unit Qgod) and (or) proglacial lake deposits (units Qgos and Qgl_r), forming coarsening-upward deposits. In other areas, receding or wasting ice impinged upon highlands, leaving more isolated kame deposits.

Qgog **Outwash gravel deposits, undivided**—Bouldery pebble cobble gravel to pebbly sand; loose; massive to crudely bedded; mostly ice-contact deposits, including kame outwash bodies, but may include any of the gravelly Vashon recessional facies, including fluvial outwash. (See unit Qgof.) We were unable to assign a depositional environment to these gravelly recessional deposits because they are poorly exposed. Inset unit Qgog in the lower Tolt River valley is likely fluvial outwash graded to Glacial Lake Snoqualmie.

Vashon Advance Proglacial and Subglacial Deposits

Deposits of the Vashon Stade of the Fraser Glaciation of Armstrong and others (1965) are widely distributed across the study area. Glacial ice and meltwater deposited drift and carved the southern Puget Lowland into a complex geomorphology that provides insight into latest Pleistocene glacial processes. Throughout the map area, drumlins and flutes show that Puget lobe ice advanced from northwest to southeast (Fig. 3, Plate 1). Ice advance over this part of the lowland occurred about 14,500 yr BP and blocked ancient rivers, creating extensive temporary lakes across much of the map area (Mackin, 1941; Booth, 1990). Facies relations among river and delta deposits (unit Qga_v) and lake deposits (unit Qgl_v), as well as their thickness and areal distribution, indicate that one or more large proglacial lakes progressively occupied significant portions of the map area during ice advance. (See also Knoll [1967] and Dragovich and others [2007, 2009a,c, 2010b, 2011a] for such lakes and similar deposits in nearby quadrangles.) Advance outwash (average $\sim Qm_{40}Qp_{54}PF_6$) and lake deposits are similar to other glacial outwash deposits;

petrography and geochemistry of these polycrystalline quartz-rich sediments indicate a mixed arc and Western mélange belt source (Appendices C and F). Advance outwash contains less monocrystalline quartz and K-spar than nonglacial deposits that have a modern or ancient Snoqualmie River basin provenance (SP). However, two sands (67–70% SiO_2) deposited upon older SP sediments have a transitional petrographic and geochemical signature; they are also distinctly less lithic rich than modern or ancient Tolt River fluvial sediments (Appendix F). Vashon deposits are typically fresh to only slightly weathered; basalt clasts have no to very thin weathering rinds (commonly <0.5 mm). Bedding in advance outwash and lake deposits commonly has a primary dip generally southeast, reflecting glaciofluvial or deltaic deposition into temporary glacially dammed lakes or into steep-gradient and high-energy braided streams sloping away from the advancing ice front. Thus, dips of Vashon strata on the geologic map show subtle paleocurrent directions and primary bedding sloping away from the ice as foreset beds on deltas or the lee side of fluvial bar deposits and probably do not indicate significant tectonic tilting. This differs from the ancient alluvial nonglacial deposits (for example, unit Qc_{ws}), which are overbank (flood) sediments having subhorizontal primary bedding.

Qgt_v **Lodgment till**—Unstratified mixture of clay, silt, sand, and gravel (diamicton), and rare lenses of sand and gravel; grayish blue to very dark gray, locally slightly weathered to mottled yellow-brown; sand-silt matrix-supported; unsorted; dense; accreted at the base of the Vashon ice and thus typically displays a friable shear fabric. Clasts are both northern-sourced and local and rounded to subangular. Angular clasts are present where this unit directly overlies bedrock. Till is generally from 5 to 50 ft 1.5–15 m) thick (Cross Section A) but may locally reach 140 ft (43 m) thick (Cross Section B) in the western part of the map area. Till on the uplands unconformably overlies advance deposits, older Quaternary deposits, and bedrock. Subvertical sand dikes pervade till at significant site 2C (Plate 1; sec. 24, T26N R7E).

Qga_v **Advance outwash**—Sandy and pebbly gravel, sand and cobble gravel, and local silt interbeds. Sands are typically dark green-gray, weathering to yellowish brown, light yellowish brown, or pale brown. Sediments are dense and typically well sorted and stratified in thin to very thick beds; there are local (laminated) silt interbeds, as well as rip-up clasts, deltaic and bar foreset beds, cut-and-fill structures, and rare ice-shear structures. Advance outwash is complexly interlayered with, conformably overlies, or may locally underlie glacial-lake deposits (unit Qgl_v). It is most commonly overlain by Vashon lodgment till (unit Qgt_v) along a sharp contact. Advance outwash deltaic deposits are locally prevalent and may also include some kame or other ice-contact sediments deposited between advancing ice and restricting highlands or as subglacial ice tunnel deposits. Composite sections of fluvial-deltaic advance outwash and glacial-lake deposits are fairly thick where fluvial-deltaic deposits prograded into restricted proglacial lakes during ice advance (Cross Section B). Radiocarbon dates for this unit from south and west of the map area are 14,450 to 14,560 yr BP (Porter and Swanson, 1998; Associated Earth Sciences, Inc., 2003; Dragovich and others, 2007).

Qgl_v **Advance glaciolacustrine deposits**—Silt, clayey silt, pebbly silt, and diamicton, locally with very thin to thick beds of sand. Sediment is stiff or dense and typically contains scattered dropstones and beds or lenses of till-like massive diamicton that may be iceberg melt-out till or flow till. Stratification and sorting vary, and sediments are massive to thinly bedded, laminated, or varved. Some exposures are mostly diamicton with thin, wispy interbeds of silt or laminated silt and sand. Unit Qga_v typically overlies unit Qgl_v regionally, but unit Qga_v underlies thick successions of unit Qgl_v in some areas; elsewhere, the two units are complexly interbedded. Some outcrops expose contorted or folded bedding and rare sand dikes. Recumbently folded sand, silt, and clay beds are common around significant site 28M (Plate 1; sec. 14, T25N R7E) in the southwest part of the map area. These folds typically verge east-southeast, subparallel to the Vashon ice flow direction, and thus have an orientation and geometry consistent with a glacial ice-shear origin. Knoll (1967, p. 67) also observed, “overridden and deformed proglacial lake [Vashon] clays” in the area. Conversely, sand dikes at significant site 204T (Plate 1; sec. 11, T25N R7E) that intrude unit Qgl_v silt beds may be the result of earthquake liquefaction (Appendices E, G, and H). Unit Qgl_v includes some of the transitional beds of Booth (1990) and correlates with the Lawton Clay mapped elsewhere in the Puget Lowland.

Pre-Fraser Glacial and Nonglacial Deposits

Qc_{ol} **Sediments of the Olympia Nonglacial Interval**—Boulder to pebble gravel, sand, silt, and clayey silt, with local peat and organic sediments. Sands are moderately weathered to yellowish brown or yellowish gray. Sediments are dense, very thickly to thinly bedded, and moderately to well stratified and sorted. Subhorizontal, very thick beds of channel gravel with bar and cut-and-fill structures are the norm. Sands (SiO_2 ~75%) have a predominantly felsic arc geochemical affinity (Appendix C), are lithic rich, and have a local eastern provenance. Sands contain significant local mélange belt metamorphic and Tertiary Mount Persis unit volcanic clasts and fewer but appreciable granitic lithic, hornblende, and pyroxene grains. Unit Qc_{ol} is exposed in the east-central and southeastern part of the map area and is similar to both modern (unit Qa) and ancient Tolt River alluvium (unit Qc_{hmp}). It includes locally derived ancient alluvium that was deposited by overall westerly flowing streams or rivers (Appendix F). We obtained a radiocarbon age of 30,550 ±1,930 yr BP from organic sediments in unit Qc_{ol} along North Fork Tolt River near the eastern margin of the map area at age site 111C (Table A1). Multiple radiocarbon dates and OSL ages (17.5–51.5 ka) have been obtained from Olympia-age sediments in quadrangles south, west, and northwest of the map area by Dragovich and others (2007, 2009a,b,c, 2010a,b, 2011a,b), Associated Earth Sciences, Inc. (2001a,b, 2002a,b, 2003, 2004, 2005, 2007), Saltonstall and others (2003), and Minard and Booth (1988). We speculate that unit Qc_{ol} in the Lake Joy and Carnation quadrangles likely formed broad alluvial fans similar to the modern Tolt River fan at Carnation where the Tolt meets the Snoqualmie River.

Qc_{ws} **Whidbey Formation, Snoqualmie River facies**—Sand, silt, silty sands, and lesser pebbly sand, clay, and organic sediments, including peat; contains weathered (clay-rich) tephra beds in a few places near the Tolt River landslide complex. Sands are light yellowish brown to pale yellow to bluish gray, and silts are a distinctive orange-gray to dark olive-brown. Most exposures are laminated to medium-bedded sands and silts that contain thin beds or laminae of clay. Sediments are dense or hard, well sorted, and well stratified. Charcoal, disseminated organic matter, flattened sticks and logs, trough-and-ripple crossbedding, and plane or graded beds are common. Although uncommon in this quadrangle, liquefaction structures such as flutes, flames, sand dikes, dish structures, folds, and chaotic bedding are observed more regionally in this unit (Dragovich and others, 2010a,b, 2011a,b). These ancient Snoqualmie River basin provenance (SP) sands are lithic poor and dominantly contain abundant monocrystalline quartz (~20%), K-spar (12–15%), and lesser but significant amounts of granitic lithic clasts, hornblende, pyroxene, and mica, as well as a few sedimentary and volcanic lithic clasts. These SP sands (61–74% SiO_2) have an arc affinity and only minor sedimentary or metamorphic input (Appendices C and F). Unit Qc_{ws} is exposed in the west-central part of the map area, east of the Tokul Creek fault zone, which shows that the Snoqualmie River valley traversed that part of the area prior to the regional Possession Glaciation. (See Fig. 3 on Plate 1.) Subsurface data suggest that unit Qc_{ws} reaches 400 ft (122 m) in thickness and may interfinger with ancient Tolt River alluvial fan deposits (unit Qc_{hmp}) in this area (Cross Section B). The Whidbey Formation is likely faulted, folded, and uplifted across CF-1 and the Tolt River anticline (Plate 1; see also Appendices G and H, "Pleistocene Alluvium and Quaternary Structures" above, and Cross Section B). Unit Qc_{ws} is mapped to an elevation of 890 ft (271 m) at significant site 5W (Plate 1; sec. 7, T25N R8E), likely as a result of hanging wall uplift along CF-1 (Appendix H). We obtained two infinite radiocarbon dates of >43,500 yr BP at date sites 22E and 22H (Plate 1 and Table A1). We also obtained IRSL ages of 85.8 ±7.36 ka (~86,000 yr BP), 79.3 ±6.88 ka, 113 ±9.04 ka, and 143 ±4.48 ka at age sites 44C-1, 44C-2, 44A-1, and 44A-2, respectively (Plate 1; Appendix B); the quartz OSL was saturated and could not be used to compare with the IRSL data. The 143 ka age at site 44A-2 is anomalously old for the Whidbey Formation and likely is in error. (Samples 44A-2 and 44A-1 are from the same stratigraphic level and 200 ft apart.) Unit Qc_{ws} is more weathered, both petrographically and in outcrop, east of the Tolt River, consistent with a general westerly younging direction suggested by data from OSL age sites 44A and 44C. Available age, weathering, and stratigraphic information suggest that a younger unit Qc_{ws} SP fluvial sequence on the west is inset against an older unit Qc_{ws} alluvium. OSL ages of 101, 107, 120, 122, and 128 ka and several infinite radiocarbon dates were obtained from unit Qc_{ws} in the adjacent Carnation and Monroe quadrangles (Dragovich and others, 2010a,b, 2011a,b; also see Dragovich and others, 2007, 2009a,b, for previous mapping and dating of the

Whidbey Formation south of the map area.) We correlate these strata with the Whidbey Formation (~80,000–130,000 yr BP) on the basis of age, weathering, composition, and stratigraphic position.

Qc_{hmp} **Hamm Creek unit of Troost and others (2005), Mount Persis volcanic facies**—Cobble gravel, boulder cobble gravel, pebble gravel, and lesser sand, silt, and peat interbeds. Sands are light gray to greenish gray and weather to a light yellowish brown. Clasts are subangular to subrounded, and ripple or bar crossbedding and graded and scoured bedding are present in places. Sediments are very dense or hard and moderately to well stratified and sorted. Very thick beds of moderately stratified gravel and cobble gravel that have a weathered coarse sand matrix and flattened organic fragments, logs, or sticks are typical. Gravel clasts are dominantly andesite to basalt; chert, quartzite, granite, and metamorphic clasts, including meta-argillite and other clasts from the mélange belt, are less common. Weathering rinds on basalt clasts are 0.5 to 5.0 mm (avg. 2.6 mm) thick. Sands are distinctly lithic rich and dominantly contain volcanic lithic clasts (~50–75%) along with some metasandstone, meta-argillite, granite, metachert, K-spar (~1–8%), polycrystalline and monocrystalline quartz, plagioclase, and lesser but significant hornblende, pyroxene, and opaque mineral grains. Sands have an overall andesitic to rhyolitic composition and were predominantly derived from an arc source (Appendix C). Mount Persis volcanic provenance is indicated by the andesite to basalt in the gravel and sand deposits and overall westerly paleoflow indicators. The moderate to strong weathering observed in the field has been confirmed both petrographically and geochemically (Appendix C; Nesbitt and Young, 1984; Dragovich and others, 2011b). Unit Qc_{hmp} is mapped in the southwestern part of the study area where it is as much as 300 ft (91 m) thick locally and apparently thins to the west. Stratigraphic style and dominance of coarse gravel and cobbles suggest deposition by a moderate- to high-energy braided river and (or) as large alluvial fans. We envision an ancient Tolt River drainage system emanating from the highlands to the east, similar to the modern Tolt River, and deposition along the interface between the ancient Tolt River and Snoqualmie valleys. This locally derived ancient alluvium is also similar in its setting to unit Qc_{wp} in the Carnation quadrangle, which has a local, but Puget Group, provenance ($Qm_{35-42}Qp_{50-60}PF_{5-8}$). It is also somewhat analogous compositionally to Vashon recessional outwash, which also has an easterly sediment component. Our structural information suggests that unit Qc_{hmp} is likely folded along the Tolt River valley directly north of CF-1 (Cross Section B). Bedding in the unit is gently to distinctly tilted at most sites and is faulted at significant site 108D (Plate 1; sec. 33, T26N R8E) near Tokul Creek fault no. 3 (Appendices E and H). Many of the weathered pre-Fraser or old tills described by Knoll (1967), for example, significant site "ot?" on Plate 1 (sec. 6, T25N R8E), are correlated with our unit Qc_{hmp}. These deposits contain substantial amounts of andesite clasts and have a pseudo-matrix as a result of weathering. We obtained infinite radiocarbon dates (>43,500 yr BP) from wood at date sites 26F, 108A, and 114T (Plate 1; Table A1). We also obtained a minimum IRSL age of >165 ka at age site 44B (Plate 1), consistent with the strong weathering characteristics of this unit (Appendix B). (See Dragovich and others, 2011a,b, for previous mapping of the Hamm Creek unit northwest of the map area.)

$Qc_h?$ **Hamm Creek unit of Troost and others (2005), Snoqualmie River facies (Cross Section B only)**—Unit $Qc_h?$ is mapped at depth on Cross Section B. These buried silt, sand, and organic beds are lithologically similar to unit Qc_{ws} and contain sand, silt, and peat, suggesting an older nonglacial fluvial SP(?) unit. We speculate that these deposits might be the Hamm Creek unit and that units $Qc_h?$ and Qc_{hmp} interfinger locally on Cross Section B, analogous to modern Tolt River alluvium interfingering with Snoqualmie River alluvium along the Tolt River alluvial fan at the City of Carnation. The tentative correlation of units $Qc_h?$ and Qc_{hmp} with the Hamm Creek unit is made on the nonglacial lithologic characteristics, age, and weathering characteristics.

Qgd_{pd} **pre–Double Bluff glacial drift**—Poorly exposed clayey silty gravel (till) in two small areas in the western part of the map area (sec. 14, T25N R7E; sec. 31, T26N R8E); reddish brown; massive and poorly sorted; medium dense to dense; contains subrounded clasts of andesite, basaltic andesite, and basalt, and lesser gabbro, granite, amphibolite, tuff, and ultramafite. Basalt clasts are distinctly weathered (0.8–5 mm rinds). Weathering characteristics and stratigraphic position suggest a mid- to early Pleistocene age, older than Double Bluff glacial deposits, which are significantly less weathered regionally.

Qgn_{pf} **Pre-Fraser glacial and nonglacial deposits, undivided (Pleistocene to Pliocene?)(Cross Section B only)**—Dense to very dense gravel, boulder gravel, sand, silt, clay, and diamicton; locally contains peat or organic sediments. This undivided unit is shown in the subsurface below organic-bearing nonglacial strata of the Whidbey Formation or Hamm Creek unit. The few wells or boreholes that penetrated this unit drilled into significant diamicton or hardpan suggestive of early(?) Pleistocene glacial strata. However, available data are limited and can only be used to suggest undivided ancient glacial or nonglacial deposits. Dragovich and others (2007, 2009c, 2010a,b), Booth (1990), and Knoll (1967) also describe outcrops of old and undivided glacial and nonglacial deposits elsewhere in the Snoqualmie valley area, including the highly weathered tills and outwash in unit Qgn_{pf} of Dragovich and others (2009a,b) directly south of the map area. We correlate subaerial exposures of unit Qpf of Booth (1990) with one or more of our units Qgd_{pd}, Qc_{hmp}, and Qc_{ws} on the basis of field, petrographic, geochemical, and other observations.

Tertiary Volcanic, Intrusive, and Sedimentary Rocks

MOig **Granite to granodiorite (Miocene to Oligocene)**—Massive granite to granodiorite (~71% SiO_2); dark or light gray, weathers yellowish brown; contains euhedral to subhedral and mostly equigranular plagioclase (~35%), K-spar (~25%), and quartz (~25%), and minor altered hornblende, biotite, white mica, and opaque minerals. We mapped this hypidiomorphic, granular, medium- to coarse-grained intrusion east of the Tokul Creek fault near the southeastern border of the quadrangle, where it intrudes rocks of the Western mélange belt. One sample has medium-K calc-alkaline affinities (Appendix C). Correlation with the granitic Miocene to Oligocene Snoqualmie, Grotto, or Index batholiths widely exposed northeast, east, and south of this quadrangle is indicated by the composition of these massive granitic rocks. Although we did not observe intrusive contacts with the Western mélange belt, the granitic composition and massive nature (lacks foliation) is inconsistent with the composition and structure of the metatonalite and metagabbro of the older mélange belt intrusions. Unit MOig intrusions shown at depth on Cross Section B are consistent with both the geophysical data (Plate 1, Figs. 1 and 2; Appendix D) and regional mapping (Dragovich and others, 2009a,b,c; Tabor and others, 1993, 2000; Erikson, 1969).

Evs_p **Volcanic rocks of Mount Persis of Tabor and others (1993), undivided (Eocene)**—Interbedded andesitic to basaltic flows, and lesser andesitic to rhyolitic tuff, tuff breccia, and breccia, volcanic to tuffaceous sandstone and siltstone, lahar deposits, volcanic conglomerate, shale, organic-rich siltstone, and coal (Tabor and others, 1993; Dragovich and others, 2009a,b, 2010a,b, 2011a,b). Flows vary from andesite to basaltic andesite and, locally, to dacite and basalt. Rocks are locally strongly altered, particularly near tectonic zones (units tz and tz_h), but also away from fault zones, suggesting that some alteration is related to magmatic fluids. Widespread alteration of volcanic rocks of Mount Persis (unit Evs_p) also suggests that larger shallow unit MOig intrusive bodies pervade the Tokul Creek fault zone as shown on Cross Section A. The geochemistry of this unit suggests that it originated from a medium-K calc-alkaline continental arc that had an enriched mafic source that underwent crustal assimilation as the magma evolved (Appendix C). Volcaniclastic and epiclastic sections are mostly moderately to well stratified and typically contain tuff beds. The dominance of tuffs and volcanic-rich sedimentary rocks over coarse volcanic breccias and flows in areas west and south of the map area suggests a more distal volcanic depositional setting there (Dragovich and others, 2009a,b, 2010a,b). Two observations point to a volcanic center or centers along the eastern edge of the Monroe quadrangle and (or) north to northeast of the present study area or perhaps in the northern part of the present study area: (1) the dominance of flows and coarse breccia mapped by Tabor and others (1993) around Mount Persis and the Youngs Creek headwaters north-northeast of the Lake Joy quadrangle; and (2) volcanic facies relations along the eastern part of the Monroe quadrangle and in the Sultan quadrangle north-northeast and north and northwest of this quadrangle (see unit Ei_p and Dragovich and others, 2011a,b). The Mount Persis unit rocks unconformably overlie the Western mélange belt across the present study area (Cross Sections A and B; Tabor and others, 1993; Danner, 1957). Directly to the southwest, west, and northwest of the map area, along the easternmost part of the Seattle basin and within the broad SWIF, the Mount Persis unit underlies younger Tertiary strata (Dragovich and others, 2007, 2009a,b, 2010a,b, 2011a,b; Sherrod and others, 2008). Tabor and others (1993) assigned a late Eocene age to the Mount Persis unit on the basis of (1) a

poor apatite fission-track age (47.4 Ma), (2) a hornblende K-Ar age (38.1 Ma), and (3) their observation that the Mount Persis unit is intruded by the Index batholith (34 Ma) and mafic dikes (33 Ma) northeast of the map area. Dragovich and others (2009a,b, 2011a,b) obtained U-Pb single zircon ages of 36 ±2.3 Ma (late Eocene) and 43.7 ±1.0 Ma (mid-Eocene) from tuffs in the adjacent Snoqualmie and Monroe quadrangles, respectively. The distribution of the volcanic deposits and the available age information suggest that Mount Persis volcanism spans several million years (~36–47 Ma) and may involve several intrusive centers. We suspect that the Mount Persis unit thins to the southwest, where it is dominated by distal volcaniclastic and tuffaceous strata interbedded with distal basalt and basaltic andesite flows. Although the Mount Persis unit likely originally thinned to the west and south, it now thins to the east across the current map area because of uplift and subaerial erosion of the volcanic rocks within the TCFZ (Cross Section A). The transition from proximal to distal Mount Persis volcanism occurs in the Lake Joy quadrangle; proximal volcanic strata (mostly flows and an intrusive complex) in the northeast part of the map area generally grade to distal volcaniclastic strata and mafic flows in the southwestern part of the map area (Cross Section B). Locally divided into:

Eva_p **Volcanic rocks of Mount Persis, andesite flows**—Andesite and minor dacite flows; bluish to greenish gray, dark green, or gray or dark gray, weathered or altered to dark reddish gray or brown-gray, maroon-gray, or yellow-brown-gray. Flows are typically massive but locally exhibit flow structure, including aligned phenocrysts, microlites, amygdules, or vesicles; flow breccia, altered flow tops, and well-formed columns are rare. These two-pyroxene flows contain phenocrysts of plagioclase commonly with augite ± hypersthene and rare quartz microphenocrysts. Several flows contain (chloritized) hornblende, and a few also contain (chloritized) biotite. Glomerophyric textures and oscillatory-zoned plagioclase are common. Locally, rocks are moderately to strongly propylitically altered near tectonic zones (units tz and tz_h). Flows are ~30 to 100+ ft (~9–30+ m) thick (Cross Sections A and B). Very thick flows are likely compound lava flows. Flows in the northern part of the area are lenticular canyon flows that invaded ancient volcanic highlands. The more distal depositional setting of the southern part of the map area evokes a flow model onto more open plains or where braided stream valleys were overrun. Cross Sections A and B show a higher percentage of andesitic flows to the north, consistent with regional field information indicating an overall greater amount of proximal volcanic rocks to the northeast (Tabor and others, 1993; Dragovich and others, 2010a,b, 2011a,b).

Eva_{pd} **Volcanic rocks of Mount Persis, dark basaltic andesite flows**—Basaltic andesite to andesite flows; may include rare basalt flows; typically dark gray to bluish gray to very dark gray, weathered or altered to reddish gray, reddish brown, or brownish yellow. Flows are typically fine grained but show subtle flow structure defined by aligned phenocrysts or microlites, amygdules, or vesicles. Well-formed columns and pillows are rare. Thick compound flows are common. Unit Eva_{pd} contains phenocrysts of plagioclase and augite ± hypersthene with significant disseminated opaque grains (≤15%) that color the rock dark gray. Some flows have (chloritized) hornblende and rare biotite, and a few flows have sparse blocky plagioclase phenocrysts (~1–2 mm) surrounded by microlite crystals. Unit Eva_{pd} is typically almost holocrystalline and has glomerophyric microphenocryst patches and chloritized or sericitized interstitial glass. We separated unit Eva_{pd} from basalts (unit Evb_p) and andesites (unit Eva_p) in the field by the amount and composition of the phenocrysts and rock color. However, outcroppings of the mafic flows are megascopically similar, dark, fine-grained rocks that are difficult to classify in the field and thus, many unit Eva_{pd} exposures had to be classified via petrographic and geochemical analyses. Also, because of this similarity, some basalt flows may have been mapped as unit Eva_{pd}. Also, although most of these dark volcanic rocks are demonstrably volcanic flows, we cannot exclude the possibility that some of these rocks are dikes or sills.

Evb_p **Volcanic rocks of Mount Persis, basalt flows**—Basalt to basaltic andesite; dark gray or reddish or greenish gray; weathered or altered to very dark grayish brown or light olive-brown.

The flows are typically fine grained and massive but locally show flow structure defined by aligned phenocrysts or microlites, amygdules (≤3 cm), or vesicles. Thick compound flows are common, but well-formed columns are rare. Pillows, scoria, and hyaloclastic basalt at significant site 10T (Plate 1; sec. 17, T26N R8E) are likely the result of a basalt flow entering a lake. This unit contains phenocrysts of plagioclase and augite ± hypersthene, typically with (chloritized) hornblende. Unit Evb_p is glassy to holocrystalline and has glomerophyric microphenocryst patches; microscopic flow alignment is common. As for unit Eva_{pd}, basalt flows are dark and generally lack megascopic plagioclase phenocrysts. However, outcroppings of the mafic flows are dark, fine-grained rocks that are typically difficult to classify in the field. Thus we classified many dark flows by both petrographic and geochemical analyses. We mapped a few well-exposed basaltic dikes in the eastern part of the map area. Dragovich and others (2011a,b) inferred, on the basis of limited field evidence and geophysics, that basalt flows are common in the subsurface in the western part of the Monroe quadrangle northwest of the present map area; they surmised that their low viscosity resulted in pooling of basalt flows on flatter plains bordering volcanic highlands. Both field mapping and geophysical modeling (magnetic highs) in this quadrangle support the model that units Eva_{pd} and Evb_p flowed into fairly distal volcanic environments. (See geophysical information on Plate 1 and Appendix D.)

Evt_p **Volcanic rocks of Mount Persis, tuffs**—Crystal vitric and crystal lithic to lithic andesitic to rhyolitic tuffs, typically light to dark gray to bluish gray to light yellowish brown. Lithic tuff beds are typically greenish. Tuff beds are locally semivesicular and commonly form thick to very thick beds between flows; they are typically massive, but some beds are crudely compositionally banded (gradations of crystal, glass and lithic contents). Our limited petrographic information indicates that the more felsic tuffs are composed of euhedral to anhedral quartz and plagioclase phenocrysts in yellowish to light greenish glass and locally contain plagioclase microlites and (or) ash to lapilli-size pumice fragments (≤5 cm). Some tuff beds are lithic-rich and grade from andesitic lapilli tuffs to lithic volcanic breccia of unit $Evbx_p$. Propylitic alteration of tuffs is common. Dragovich and others (2009b,c, 2011a,b) obtained U-Pb single zircon ages of 36 ±2.3 Ma (late Eocene) and 43.7 ±1.0 Ma (mid-Eocene) from rhyolitic pumiceous tuffs in the Snoqualmie and Monroe quadrangles.

$Evbx_p$ **Volcanic rocks of Mount Persis, volcanic breccia**—Dacitic to andesitic lithic tuff breccia with lesser (crystal) lithic lapilli tuff and lesser agglomerate or volcanic conglomerate; multicolored with red, green, and black to gray volcanic clasts and matrix; weathered gray-brown to dark green-gray to gray. Breccia beds are generally very thick, massive, and moderately to poorly sorted. Some breccia beds contain some dark-gray basaltic andesite to basalt clasts, and a few contain exotic greenstone, metasandstone, and metachert clasts derived from nonvolcanic sources (Danner, 1957). Breccia is typically poorly exposed, but it likely represents pyroclastic flow deposits, including dome collapse breccia; it locally includes thinner flow breccia beds or bedded pyroclastic surge deposits. Some moderately sorted breccia beds that contain subangular to subrounded andesite to basalt clasts are probable lahars, similar to unit Evl_p in the adjacent Carnation and Monroe quadrangles (Dragovich and others, 2010a,b, 2011a,b). Unit $Evbx_p$ clasts in the those quadrangles are either (1) two-pyroxene andesites that are petrographically and geochemically similar to the Mount Persis andesite flows, or (2) semivesicular light-green dacite clasts (~66% SiO_2)(Dragovich and others, 2009a,b, 2010a,b). In the adjacent Monroe quadrangle, breccia clasts appear to be mostly (hornblende) dacite (~68–70% SiO_2)(Dragovich and others, 2011a,b). Thin interbeds of epiclastic volcanic sandstones in a few outcrops show that some very thick breccia units are the result of emplacement of stacked pyroclastic deposits into a restricted basin. The dacitic composition of the clasts in the Carnation and Monroe map areas (Dragovich and others, 2010a,b, 2011a,b) suggests that part of the unit may correlate with the extensive hornblende-phyric dacite breccia unit mapped by Tabor and others (1993) northeast of the map area.

Evc$_p$ **Volcanic rocks of Mount Persis, volcaniclastic rocks**—Lithic and feldspatholithic volcanic to tuffaceous sandstone, silty sandstone, and siltstone that has some interbeds of volcanic conglomerate, volcanic pebble conglomerate, tuff and lapilli tuff, shale, organic siltstone, and coal; generally light yellowish brown to very pale brown to light bluish gray to greenish gray sandstone, and some dark red to reddish brown volcanic siltstone. Volcanic sediments are mostly well sorted and stratified and contain angular to subrounded grains; strata vary from massive to medium to thickly bedded. The common plane-and-ripple crossbedding is typical of fluvial environments. A few only moderately sorted and massive to crudely graded sand and pebbly sand beds could be hyperconcentrated flood (lahar runout) deposits. Also, some pumiceous tuff beds in volcaniclastic stratigraphic sections that display rare antidune crossbedding could be interbedded pyroclastic surge deposits. Fossil leaves, stems, and fragments of black to brown, carbonized petrified wood are common and consist mostly of fragments of broadleaf trees and stems similar to modern *Equisetum* (Dragovich and others, 2010b; Danner, 1957). Most volcaniclastic rocks are rich in volcanic lithic grains and contain abundant basaltic andesite to dacite clasts, but they also locally contain altered volcanic glass, plagioclase, hornblende, pyroxene, and a few exotic grains of polycrystalline quartz and sedimentary lithic grains. The compositional spectrum of volcaniclastic rock types includes crystal-rich sediments with significant subangular to angular plagioclase, volcanic quartz, and various amounts of fragmental pumice that are probably fluvially reworked crystal-vitric ash-flow tuffs; sandstone dominated by angular microlitic volcanic grains may be reworked lithic ash-flow tuffs. Sandstones rarely have a mixed volcanic and Western mélange belt (unit KJm) provenance (Dragovich and others, 2009b) and contain some metachert, metasandstone, or meta-argillite clasts. Danner (1957) described andesitic boulder conglomerates with shale lenses, which are likely fluvial deposits, directly north of the map area; most conglomerate contains subrounded clasts dominated by basalt, andesite, and dacite, and, locally, some metachert, jasper, greenstone, and metasandstone. In the northern part of the map area, unit Evc$_p$ likely represents stream deposits within a dissected volcanic highland setting. In this moderately proximal volcanic setting, the lenticular fluvial beds are largely surrounded by more direct volcanic deposits like flows, tuffs, and breccias. We also now suspect that unit ΦEc in the northernmost part of the Snoqualmie quadrangle is correlative with unit Evc$_p$ and likely represents exposed distal Mount Persis sedimentary deposits similar to those in the southern part of the Lake Joy quadrangle. In this distal-plain setting, tuffs, mafic flows, and volcanic-rich sedimentary rocks are more common than coarse volcanic breccias and felsic flows (Cross Section B; Dragovich and others, 2011a,b). Because volcanic sediments are generally more erodible than lava flows and breccias, these rocks tend to be recessive or covered by colluvium and Quaternary deposits and thus rarely crop out; well or boring lithologic logs suggests that volcanic sandstone and shale are more common in the subsurface than exposures would indicate (Cross Sections A and B).

Ei$_p$ **Volcanic rocks of Mount Persis, North Fork Creek intrusive complex**—Interlayered gabbro, andesite, basaltic andesite, and basalt. These rocks are greenish gray to light greenish gray and weathered or altered to pale brown or olive-brown, dusky red, or pale yellow. Gabbros are locally banded or layered on a scale of centimeters and texturally range from fine to coarse grained to rarely almost pegmatitic phaneritic rocks. Intrusive relations are varied in this hypabyssal intrusive complex. Some gabbros form thick to thin sills or dikes between the andesite, basaltic andesite, and basalt aphanitic rocks (aphanites) of the complex. Elsewhere, the contact between the gabbros and the mafic aphanites is gradational, suggesting that the many aphanites are also intrusive; both the thin wispy aphanite intrusive apophyses (offshoots) in gabbroic bodies and the holocrystalline porphyritic texture of some andesites imply hypabyssal intrusion and nonvolcanic action. Both the aphanites and the gabbros of the complex are extensively propylitically altered and contain some primary plagioclase surrounded by abundant chlorite, opal (or secondary quartz), and epidote. Some rocks also contain K-spar, zeolites, and sulfide minerals. Silicification was petrographically confirmed for the gabbros (~57–59% SiO_2) and aphanites (~58% SiO_2) of the complex (Appendix C). The

alteration of the complex may be the result of hydrothermal fluids along nearby faults and (or) by hydrothermal cells adjacent to the complex. See unit Ei_p or basalt and gabbro in the Mount Persis unit described by Dragovich and others (2011a,b) and Plummer (1964) to the northwest and east of the map area, respectively.

Mesozoic Low-Grade Metamorphic Rocks (Prehnite–Pumpellyite Facies)

KJm **Western mélange belt of Tabor and others (1993), undivided (Cretaceous to Jurassic)**—Dominantly meta-argillite, metasandstone, greenstone, metagabbro, metachert, and meta-diabase, and minor metatonalite, slate, phyllite, marble, and rare ultramafite, metaquartz diorite, hornblendite, and (banded) amphibolite (Fuller, 1925; Danner, 1957; Dragovich and others, 2007, 2009a,b,c, 2010a,b, 2011a,b). Most metasedimentary rocks were deposited as turbidites along an accretionary wedge (Jett, 1986; Jett and Heller, 1988). Although mélange rocks are exposed in the southeasternmost part of the map area, geophysical modeling, subsurface data, and mapping indicate that the Mount Persis unit unconformably overlies the mélange belt across much of the map area (Cross Sections A and B). Locally divided into:

$KJmv_W$ **Western mélange belt metavolcanic rocks**—Greenstone derived from metamorphosed andesite tuff, flows, and rare volcanic breccia; greenish gray. Tabor and others (2000) described boudins of metamorphosed quartz-porphyry dikes(?) in faintly foliated greenstone south of the study area. Metamorphosed flows are mostly massive to moderately foliated metabasaltic andesite along with lesser metabasalt or meta-andesite that display rare amygdaloidal texture and pillow structures (Dragovich and others, 2009a,b,c). This unit contains plagioclase and actinolized pyroxene phenocrysts in a chloritic matrix, typically with minor quartz and opaque minerals. Only the larger greenstone bodies are shown on the map; the thin metatuff interbeds observed in the metasedimentary rocks of the mélange belt are not shown. Metatuff is calc-alkaline (Dragovich and others, 2009a,b,c).

$KJms_W$ **Western mélange belt metasedimentary rocks**—Marine lithofeldspathic to feldspatholithic subquartzose metasandstone, silty metasandstone, meta-argillite, and metachert and minor metaconglomerate, chert pebble metaconglomerate, metatuff, and metasandstone; typically greenish gray to dark gray or gray-green and weathered to brown; meta-argillite typically black or greenish or bluish black to dark gray. Clasts are subrounded to angular; graded bedding and load casts are locally preserved. Very thin to very thick meta-argillite beds are interbedded with metasandstone and form much of the mélange belt matrix. This matrix is pervasively deformed (intensely folded rocks with transposed bedding), easily eroded, and rarely exposed. Less-deformed metasedimentary sequences are commonly well stratified. Rocks are typically moderately foliated and partly recrystallized, and they commonly have a synkinematic metamorphic fabric defined by aligned white mica and moderately aligned relict clasts. Metamorphic minerals are white mica, actinolite/ tremolite, epidote or clinozoisite, chlorite ± pumpellyite, and prehnite. Relict clasts include mixtures of plagioclase, monocrystalline quartz, chert (locally enclosing radiolarians), polycrystalline quartz, and K-spar with volcanic and sedimentary lithic clasts. Detrital biotite or muscovite is locally conspicuous, and rip-up clasts of meta-argillite can be observed locally. Sand composition corresponds to the detrital K-spar-bearing arkosic petrofacies and lithic petrofacies of Jett and Heller (1988), but it probably includes some cherty petrofacies. (See arkosic petrofacies mapping of Tabor and others, 1993, and Jett, 1986, near the eastern boundary of the map area. See Dragovich and others, 2009b,c, for the geochemistry of metasandstones directly south of the map area.) These metasedimentary rocks were deposited as turbidites along an accretionary wedge, although *Equisetum* fossils found by Dragovich and others (2009a) indicate a shallow marine or terrestrial meta-argillite locally. C. D. Blome (USGS, in Walsh, 1984) reported Cretaceous or Jurassic radiolarians (*Sethocapsa*?) from metasandstone south of the study area. Tabor and others (1993, 2000) reported Cretaceous to Jurassic ages for the Western mélange belt, including a late Jurassic radiolarian age from a metachert bed at age site 8F (Plate 1). Dragovich and others (2009a,b) obtained a minimum U-Pb detrital zircon population age of

~96 Ma from a single bed in a well-stratified and thinly to thickly bedded feldspathic metasandstone–meta-argillite sequence directly south of the study area, where clast angularity suggests first-cycle sedimentation for most of the grains. This minimum population age confirmed that these turbidites are as young as Cretaceous. A U-Pb detrital-zircon age population peak of ~147 Ma, along with lesser amounts of detrital grains as old as Triassic (230 Ma), indicate that the source rock(s) for the turbidites is Mesozoic.

$KJigb_W$ **Western mélange belt metagabbro**—Metagabbro; greenish gray (Tabor and others, 1993, 2000; Fuller, 1925). Rocks are medium to coarse grained, massive or slightly foliated to locally schistose. The unit generally contains plagioclase with actinolized clinopyroxene or hornblende and opaque minerals. Metamorphic minerals include actinolite, prehnite, pumpellyite, chlorite, epidote, sphene, and calcite (Dragovich and others, 2009a,b,c). Metagabbro about 1 mi north of Little Si in the Snoqualmie quadrangle south of the map area yielded a U-Pb age of ~152 Ma (Tabor and others, 1993).

Holocene to Tertiary Tectonic Zones

tz, tz_h **Tectonic zone**—Cataclasite, fault breccia, clay-rich fault gouge, (proto)mylonite, or moderately to strongly slickensided, fractured, and veined rocks in fault zones; yellowish to variously colored, mottled, and altered. Dragovich and others (2007, 2009a,b,c, 2010a,b, 2011a,b) map similar tectonic zones along faults northwest, west, and south of the map area (see Appendices E, G and H for further fault, liquefaction, earthquake, and geophysical information). Unit tz_h is mappable zones of hydrothermal alteration. These rocks are commonly yellowish or reddish brown, white, or red or dark red and display principally propylitic alteration mineral assemblages but rarely include phyllic and potassic zone assemblages. Alteration minerals include chlorite and calcite, locally with some opal or secondary quartz, zeolites, white mica, biotite, clays, and K-spar. Sulfide mineralization is locally conspicuous (for example, significant sites 32D [sec. 8, T26N R8E] and 209Q [sec. 16, T26N R8E] on Plate 1). Most unit tz_h alteration is structurally controlled, but some may be related to hydrothermal alteration associated with Tertiary intrusions, such as near units Ei_p and MDig (see Cross Section B, unit MDig, and 'Isostatic Gravity and Aeromagnetic Analyses').

ACKNOWLEDGMENTS

This geologic map was funded in part by the U.S. Geological Survey (USGS) National Cooperative Geologic Mapping Program under award no. G11AC20236. We thank: Jonathan M. Lees (University of North Carolina) for software and scripts to generate earthquake focal mechanism plots and analyze earthquake data spatially; Jackie Caplan-Auerback (Western Wash. Univ.) and Glyn Williams-Jones (Simon Fraser Univ.) for assistance with the gravity survey; Harrison Gray (USGS, Denver) for help with OSL sand sampling; Daniel Huang (Seattle Public Utilities, Project Mgt and Engineering Divn) and Julie Stangell (Hancock Forest Management) for logistical help; Ray Wells (USGS) for laboratory support; Diane Cornelius, Rick Conrey, and Charles Knaack (WSU) for geochemical analyses of samples; and Kevin Auxier for major property access and sampling. We thank Curtis Koger (Associated Earth Sciences, Inc.), Taryn Sass and Claire Gibson (Seattle Public Utilities, Project Mgt and Engineering Divn), as well as Sue Kahle and Theresa Olsen (USGS, Water Resources Divn) for subsurface geologic information. We also thank our Washington Division of Geology and Earth Resources colleagues: Trevor Contreras for help with GIS and the gravity survey, Tim Walsh for help with the lidar data and a review, Dave Norman for help with the gravity survey, Jessica Czajkowski for GIS and editing help; Stefanie Kinnamon for logistical support, and Lee Walking for assistance with references.

REFERENCES CITED

Anderson, M. L.; Blakely, R. J.; Brocher, T. M.; Pratt, T. L.; Wells, R. E.; Haugerud, R.; Bush, M., 2006, Structure of the Seattle uplift from seismic, gravity, magnetic, geologic, and geomorphic data: Eos (American Geophysics Union Transactions), v. 87, no. 52, Supplement, Abstract T41A-1554.

Armstrong, J. E.; Crandell, D. R.; Easterbrook, D. J.; Noble, J. B., 1965, Late Pleistocene stratigraphy and chronology in southwestern British Columbia and northwestern Washington: Geological Society of America Bulletin, v. 76, no. 3, p. 321-330.

Associated Earth Sciences, Inc., 2001a, Proposed borrow pit dewatering impact analysis, Trilogy at Redmond Ridge, King County, Washington: Associated Earth Sciences, Inc., 1 v.

Associated Earth Sciences, Inc., 2001b, Subsurface exploration, geologic hazard, and geotechnical engineering report, Trilogy at Redmond Ridge, Project B vault, West Snoqualmie Valley Road NE and Novelty Hill Road, King County, Washington: Associated Earth Sciences, Inc., 1 v.

Associated Earth Sciences, Inc., 2002a, Final hydrogeologic and geotechnical assessment report—Pegasus Thoroughbred Training Center, King County, Washington: Associated Earth Sciences, Inc., 1 v.

Associated Earth Sciences, Inc., 2002b, Hydrogeologic assessment—Plat of Cromwell Plateau, Snohomish County, Washington. *In* Associated Earth Sciences, Inc., 2010, Monroe quadrangle reports: Associated Earth Sciences, Inc., 10 p.

Associated Earth Sciences, Inc., 2003, Proposed Snoqualmie Ridge II project—Environmental impact statement—Technical report on geology, soils, and groundwater: Associated Earth Sciences, Inc., [Kirkland, Wash., under contract to] Quadrant Corporation, 1 v.

Associated Earth Sciences, Inc., 2004, Environmental impact statement—Technical report on geology, soils and ground water, Redmond Ridge East UPD/FCC and Panhandle preliminary plat, King County, Washington: Associated Earth Sciences, Inc., 1 v.

Associated Earth Sciences, Inc., 2005, Proposed Snoqualmie Ridge II N1 and N2 infiltration ponds—Technical report on geology and groundwater: Associated Earth Sciences, Inc, [Kirkland, Wash., under contract to] Quadrant Corporation, 1 v.

Associated Earth Sciences, Inc., 2007, Summary of SRS-1 No. 1 infiltration pond, general geologic hazard, and geotechnical engineering recommendations, recreation complex, Redmond Ridge East, King County, Washington: Associated Earth Sciences, Inc., 1 v.

Barker, D. S., 1979, Trondhjemite—Definition, environment and hypotheses of origin. *In* Barker, D.S., editor, Trondhjemites, dacites and related rocks: Elsevier, p. 1-12.

Bhatia, M. R.; Crook, K. A. W., 1986, Trace element characteristics of graywackes and tectonic setting discrimination of sedimentary basins: Contributions to Mineralogy and Petrology, v. 92, no. 2, p. 181-193.

Blakely, R. J., 1995, Potential theory in gravity and magnetic applications: Cambridge University Press, 441 p.

Blakely, R. J.; Wells, R. E.; Weaver, C. S., 1999, Puget Sound aeromagnetic maps and data: U.S. Geological Survey Open-File Report 99-514, version 1.0. [http://geopubs.wr.usgs.gov/open-file/of99-514/]

Booth, D. B., 1984, Glacier dynamics and the development of glacial landforms in the eastern Puget Lowland, Washington: University of Washington Doctor of Philosophy thesis, 217 p., 1 plate.

Booth, D. B., 1986, The formation of ice-marginal embankments into ice-dammed lakes in the eastern Puget Lowland, Washington, U.S.A., during the late Pleistocene: Boreas, v. 15, no. 3, p. 209-264.

Booth, D. B., 1990, Surficial geologic map of the Skykomish and Snoqualmie Rivers area, Snohomish and King Counties, Washington: U.S. Geological Survey Miscellaneous Investigations Series Map I-1745, 2 sheets, scale 1:50,000, with 22 p. text. [http://pubs.er.usgs.gov/publication/i1745]

Bradford, D. C.; Waters, A. C., 1934, The Tolt River earthquake and its bearing on the structure of the Cascade Range: Seismological Society of America Bulletin, v. 24, no. 1, p. 51-62.

Broecker, W. S.; Kulp, J. L.; Tucek, C. S., 1956, Lamont natural radiocarbon measurements, III: Science, v. 124, no. 3213, p. 154-165.

Cann, J. R., 1970, Rb, Sr, Y, Zr, and Nb in some ocean floor basaltic rocks: Earth and Planetary Science Letters, v. 10, no. 1, p. 7-11.

Colman, S. M.; Pierce, K. L., 1981, Weathering rinds on andesitic and basaltic stones as a Quaternary age indicator, western United States: U.S. Geological Survey Professional Paper 1210, 56 p.

Danner, W. R., 1957, A stratigraphic reconnaissance in the northwestern Cascade mountains and San Juan Islands of Washington State: University of Washington Doctor of Philosophy thesis, 3 v. [562 p.], 7 plates.

Dickinson, W. R., 1970, Interpreting detrital modes of graywacke and arkose: Journal of Sedimentary Petrology, v. 40, no. 2, p. 695-707.

Dragovich, J. D., 2007, Sand point count and geochemical data in the Fall City and Carnation 7.5-minute quadrangles, King County, Washington: Washington Division of Geology and Earth Resources Open File Report 2007-3, 2 Microsoft Excel files and 6 p. of text. [http://www.dnr.wa.gov/Publications/ger_ofr2007-3_fallcity_supplement.zip]

Dragovich, J. D.; Anderson, M. L.; MacDonald, J. H., Jr.; Mahan, S. A; DuFrane, S. A.; Littke, H. A.; Wessel, G. R.; Saltonstall, J. H.; Koger, C. J.; Cakir, Recep, 2010a, Supplement to the geologic map of the Carnation 7.5-minute quadrangle, King County, Washington—Geochronologic, geochemical, point count, geophysical, earthquake, fault, and neotectonic data: Washington Division of Geology and Earth Resources Open File Report 2010-2, 42 p., 8 digital appendices. [http://www.dnr.wa.gov/Publications/ger_ofr2010-2_carnation_supplement.zip]

Dragovich, J. D.; Anderson, M. L.; Mahan, S. A.; Koger, C. J.; Saltonstall, J. H.; MacDonald, J. H., Jr.; Wessel, G. R.; Stoker, B. A.; Bethel, J. P.; Labadie, J. E.; Cakir, Recep; Bowman, J. D.; DuFrane, S. A., 2011a, Geologic map of the Monroe quadrangle, King and Snohomish Counties, Washington: Washington Division of Geology and Earth Resources Open File Report 2011-1, 1 sheet, scale 1:24,000, with 24 p. text. [http://www.dnr.wa.gov/Publications/ger_ofr2011-1_geol_map_monroe_24k.zip]

Dragovich, J. D.; Anderson, M. L.; Walsh, T. J.; Johnson, B. L.; Adams, T. L., 2007, Geologic map of the Fall City 7.5-minute quadrangle, King County, Washington: Washington Division of Geology and Earth Resources Geologic Map GM-67, 1 sheet, scale 1:24,000. [http://www.dnr.wa.gov/Publications/ger_gm67_geol_map_fallcity_24k.zip]

Dragovich, J. D.; Littke, H. A.; Anderson, M. L.; Hartog, Renate; Wessel, G. R.; DuFrane, S. A.; Walsh, T. J.; MacDonald, J. H., Jr.; Mangano, J. F.; Cakir, Recep, 2009a, Geologic map of the Snoqualmie 7.5-minute quadrangle, King County, Washington: Washington Division of Geology and Earth Resources Geologic Map GM-75, 2 sheets, scale 1:24,000. [http://www.dnr.wa.gov/Publications/ger_gm75_snoqualmie_24k.zip]

Dragovich, J. D.; Littke, H. A.; Anderson, M. L.; Wessel, G. R.; Koger, C. J.; Saltonstall, J. H.; MacDonald, J. H., Jr.; Mahan, S. A.; DuFrane, S. A., 2010b, Geologic map of the Carnation 7.5-minute quadrangle, King County, Washington: Washington Division of Geology and Earth Resources Open File Report 2010-1, 1 sheet, scale 1:24,000, 21 p. text. [http://www.dnr.wa.gov/Publications/ger_ofr2010-1_geol_map_carnation_24k.zip]

Dragovich, J. D.; Littke, H. A.; MacDonald, J. H., Jr.; DuFrane, S. A.; Anderson, M. L.; Wessel, G. R.; Hartog, Renate, 2009b, Geochemistry, geochronology, and sand point count data for the Snoqualmie 7.5-minute quadrangle, King County, Washington: Washington Division of Geology and Earth Resources Open File Report 2009-4, 35 p. text, 3 Microsoft Excel files. [http://www.dnr.wa.gov/Publications/ger_ofr2009-4_snoqualmie_suppl.zip]

Dragovich, J. D.; Mahan, S. A.; Anderson, M. L.; MacDonald, J. H., Jr.; Wessel, G. R.; DuFrane, S. A.; Cakir, Recep; Bowman, J. D.; Littke, H. A., 2011b, Analytical data from the Monroe 7.5-minute quadrangle, King and Snohomish Counties, Washington—Supplement to Open File Report 2011-1: Washington Division of Geology and Earth Resources Open File Report 2011-2, 58 p., 2 plates, 2 Microsoft Excel files. [http://www.dnr.wa.gov/Publications/ger_ofr2011-2_monroe_supplement.zip]

Dragovich, J. D.; Walsh, T. J.; Anderson, M. L.; Hartog, Renate; DuFrane, S. A.; Vervoot, Jeff; Williams, S. A.; Cakir, Recep; Stanton, K. D.; Wolff, F. E.; Norman, D. K.; Czajkowski, J. L., 2009c, Geologic map of the North Bend 7.5-minute quadrangle, King County, Washington, with a discussion of major faults, folds, and basins in the map area: Washington Division of Geology and Earth Resources Geologic Map GM-73, 1 sheet, scale 1:24,000. [http://www.dnr.wa.gov/Publications/ger_gm73_geol_map_northbend_24k.zip]

du Bray, E. A.; John, D. A., 2011, Petrologic, tectonic, and metallogenic evolution of the ancestral Cascades magmatic arc, Washington, Oregon, and northern California: Geosphere, v. 7, no. 5, p. 1102-1133.

Erikson, E. H., Jr., 1969, Petrology of the composite Snoqualmie batholith, central Cascade mountains, Washington: Geological Society of America Bulletin, v. 80, no. 11, p. 2213-2236, 1 plate.

Floyd, P. A.; Leveridge, B. E., 1987, Tectonic environment of the Devonian Gramscatho basin, south Cornwall—Framework mode and geochemical evidence from turbiditic sandstones: Journal of the Geological Society [London], v. 144, no. 4, p. 531-542.

Floyd, P. A.; Shail, R.; Leveridge, B. E.; Franke, W., 1991, Geochemistry and provenance of Rhenohercynian synorogenic sandstones—Implications for tectonic environment discrimination. *In* Morton, A. C.; Todd, S. P.; Haughton, P. D. W., Developments in sedimentary provenance studies: Geological Society [London] Special Publication 57, p. 173-188.

Frost, B. R.; Barnes, C. G.; Collins, W. J.; Arculus, R. J.; Ellis, D. J.; Frost, C. D., 2001, A geochemical classification for granitic rocks: Journal of Petrology, v. 42, no. 11, p. 2033-2048.

Fuller, R. E., 1925, The geology of the northeastern part of Cedar Lake quadrangle with special reference to the de-roofed Snoqualmie batholith: University of Washington Master of Science thesis, 96 p., 4 plates.

Galloway, W. E., 1974, Deposition and diagenetic alteration of sandstone in northeast Pacific arc-related basins—Implications for greywacke genesis: Geological Society of America Bulletin, v. 85, issue 3, p. 379-390.

Harper, G. D., 1995, Pumpellyosite and prehnitite associated with epidosite in the Josephine ophiolite—Ca metasomatism during upwelling of hydrothermal fluids at a spreading axis. *In* Schiffman, P.; Day, H., editors, Low grade metamorphism of mafic rocks: Geological Society of America Special Paper 296, p. 101–122.

Harper, G. D.; Bowman, J. R.; Kuhns, R., 1988, A field, chemical, and stable isotope study of subseafloor metamorphism of the Josephine ophiolite, California–Oregon: Journal of Geophysical Research, v. 93, no. B5, p. 4625-4656.

Humphris, S. E.; Thompson, G., 1978, Trace element mobility during hydrothermal alteration of oceanic basalts: Geochimica et Cosmochimica Acta, v. 42, no. 1, p. 127-136.

Jensen, L. S., 1976, A new cation plot for classifying subalkalic volcanic rocks: Ontario Division of Mines Miscellaneous Paper 66, p. 22.

Jett, G. A., 1986, Sedimentary petrology of the western melange belt, north Cascade Range, Washington: University of Wyoming Master of Science thesis, 85 p.

Jett, G. A.; Heller, P. L., 1988, Tectonic significance of polymodal compositions in melange sandstones, western melange belt, north Cascade Range, Washington: Journal of Sedimentary Petrology, v. 58, no. 1, p. 52-61.

Johnson, D. M.; Hooper, P. R.; Conrey, R. M., 1999, XRF analysis of rocks and minerals for major and trace elements on a single low dilution Li-tetraborate fused bead: Advances in X-ray Analysis, v. 41, p. 843-867. [http://www.sees.wsu.edu/Geolab/note/V41_91.pdf]

Knaack, C.; Cornelius, S.; Hooper, P., 1994, Trace element analysis of rocks and minerals by ICP/MS: Department of Geology Washington State University Open-file Report, December 1994, 18 p.

Knoll, K. M., 1967, Surficial geology of the Tolt River area, Washington: University of Washington Master of Science thesis, 91 p., 1 plate.

Le Maitre, R. W.; Streckeisen, A.; Zanettin, B.; Le Bas, M. J.; Bonin, B.; Bateman, P., eds., 2002, Igneous rocks—A classification and glossary of terms; 2nd ed.: Cambridge University Press [Cambridge, U.K.], 256 p.

Lees, J. M., 1999, Geotouch—Software for three and four-dimensional GIS in the earth sciences**:** Computers & Geosciences, v. 26, no. 7, p. 751-761.

Lees, J. M., 2007, RFOC—Graphics for spherical distributions and earthquake focal mechanisms, graphics for statistics on a sphere, as applied to geological fault data, crystallography, earthquake focal mechanisms, radiation patterns, ternary plots and geographical/geological maps: Comprehensive R Archive Network (CRAN). [accessed May 31, 2011, at http://streaming.stat.iastate.edu/CRAN/web/packages/RFOC/index.html].

Lees, J. M., 2008, GEOmap—Topographic and geologic mapping: Comprehensive R Archive Network (CRAN) [accessed May 31, 2011, at http://streaming.stat.iastate.edu/CRAN/web/packages/GEOmap/index.html].

Littke, H. A.; Dragovich, J. D.; Anderson, Megan; Hartog, Renate; Wessel, G. R.; Dufrane, S. A.; Walsh, T. J.; MacDonald, J. H., Jr.; Cakir, Recep, 2009, Geologic map of the Snoqualmie 7.5-minute quadrangle, King County, Washington—Active faulting, basin inversion and Miocene volcanic extrusion of the Snoqualmie batholith along the Rattlesnake Mountain fault zone [abstract]: Geological Society of America Abstracts with Programs, v. 41, no. 7, p. 457.

Mackin, J. H., 1941, Glacial geology of the Snoqualmie–Cedar area, Washington: Journal of Geology, v. 49, no. 5, p. 449-481.

McDonough, W. F.; Sun, S. S., 1995, The composition of the Earth: Chemical Geology, v. 120, p. 223-253.

McLennan, S. M., 1989, Rare earth elements in sedimentary rocks—Influence of provenance and sedimentary processes: Reviews in Mineralogy and Geochemistry, v. 21, no. 1, p. 169-200.

McLennan, S. M., 1993, Weathering and global denudation: Journal of Geology, v. 101, no. 2, p. 295-303.

McLennan, S. M., 2001, Relationships between the trace element composition of sedimentary rocks and upper continental crust: Geochemistry, Geophysics, Geosystems, v. 2, no, 4, p. 1021-1045, doi:10.1029/2000GC000109.

McLennan, S. M.; Hemming, S.; McDaniel; D. K.; Hanson, G. N., 1993, Geochemical approaches to sedimentation, provenance, and tectonics. *In* Johnson, M. J.; Basu, A., eds., Processes controlling the composition of clastic sediments: Geological Society of America Special Paper 284, p. 21-40.

McLennan, S. M.; Taylor, S. R.; McCulloch, M. T.; Maynard, J. B., 1990, Geochemical and Nd-Sr isotopic composition of deep-sea turbidites; Crustal evolution and plate tectonic associations: Geochimica et Cosmochimica Acta, v. 54, no. 7, p. 2015-2050.

Minard, J. P.; Booth, D. B., 1988, Geologic map of the Redmond quadrangle, King County, Washington: U.S. Geological Survey Miscellaneous Field Studies Map MF-2016, 1 sheet, scale 1:24,000. [http://ngmdb.usgs.gov/Prodesc/proddesc_5609.htm]

Nesbitt, H. W., 2003, Petrogenesis of siliciclastic sediments and sedimentary rocks. *In* Lentz, D. R., ed., Geochemistry of sediments and sedimentary rocks—Evolutionary considerations to mineral deposit-forming environments: Geological Association of Canada, GeoTex 4, p. 39-51.

Nesbitt, H. W.; Young, G. M., 1984, Prediction of some weathering trends of plutonic and volcanic rocks based upon thermodynamic and kinetic considerations: Geochimica et Cosmochimica Acta, v. 48, no. 7, 1523-1534.

Nesbitt, H. W.; Young, G. M., 1989, Formation and diagenesis of weathering profiles: Journal of Geology, v. 97, no. 2, p. 129-147.

O'Connor, J. T., 1965, A classification for quartz-rich igneous rock based on feldspar ratios: U.S. Geological Survey Professional Paper 525-B, p. B79-B84.

Pearce, J. A., 1982, Trace element characteristics of lavas from destructive plate boundaries. *In* Thorpe, R. S., ed., Andesites—Oogenic andesites and related rocks: John Wiley & Sons [Chichester, U.K.], p. 525-548.

Pearce, J. A., 1983, Role of the subcontinental lithosphere in magma genesis at active continental margins. *In* Hawksworth, C. J.; Norry, M. J., eds., Continental basalts and mantle xenoliths: Shiva Publishing [Nantwich, Great Britain], p. 230-249.

Pearce, J. A., 1996, A user's guide to basalt discrimination diagrams. *In* Wyman, D. A., ed., Trace element geochemistry of volcanic rocks—Applications for massive sulphide exploration: Geological Association of Canada Short Course Notes, v. 12, p. 79-113.

Pettijohn, F. J., 1957, Sedimentary rocks; 2nd ed.: Harper & Row, 718 p.

Plummer, C. C., 1964, The geology of the Mount Index area of Washington State: University of Washington Master of Science thesis, 62 p., 1 plate.

Porter, S. C.; Swanson, T. W., 1998, Radiocarbon age constraints on rates of advance and retreat of the Puget lobe of the Cordilleran ice sheet during the last glaciation: Quaternary Research, v. 50, no. 3, p. 205-213.

Prescott, J. R.; Hutton, J. T., 1994, Cosmic ray contributions to dose rates for luminescence and ESR dating—Large depths and long-term time variations: Radiation Measurements, v. 23, p. 497-500.

Rickwood, P. C., 1989, Boundary lines within petrologic diagrams which use oxides of major and minor elements: Lithos, v. 22, no. 4, p. 247-263.

Roser, B. P.; Korsch, R. J., 1986, Determination of tectonic setting of sandstone-mudstone suites using SiO_2 content and K_2O/Na_2O ratios: Journal of Geology, v. 94, no. 1, p. 635-650.

Roser, B. P.; Korsch, R. J., 1988, Provenance signatures of sandstone-mudstone suites determined using discriminant function analysis of major-element data: Chemical Geology, v. 67, p. 119-139.

Ross, P.-S.; Bedard, J. H., 2009, Magmatic affinity of modern and ancient subalkaline volcanic rocks determined from trace-element discriminant diagrams: Canadian Journal of Earth Science, v. 46, no. 11, p. 823-839.

Saltonstall, J. H.; Koger, C. J; Sweet, Suzanne; Thompson, S. S., 2003, Olympia age paleotopographic influences on Vashon glaciofluvial sedimentation beneath eastern Bear Creek plateau, King County, Washington [abstract]: Geological Society of America Abstracts with Programs, v. 35, no. 6, p. 109.

Sherrod, B. L.; Blakely, R. J.; Weaver, C. S.; Kelsey, H. M.; Barnett, Elizabeth; Liberty, Lee; Meagher, K. L.; Pape, Kristin, 2008, Finding concealed active faults—Extending the southern Whidbey Island fault across the Puget Lowland, Washington: Journal of Geophysical Research, v. 113, B05313, doi:10.1029/2007JB005060, 2008.

Tabor, R. W.; Frizzell, V. A., Jr.; Booth, D. B.; Waitt, R. B., 2000, Geologic map of the Snoqualmie Pass 30 x 60 minute quadrangle, Washington: U.S. Geological Survey Geologic Investigations Series Map I-2538, 1 sheet, scale 1:100,000, with 57 p. text. [http://geopubs.wr.usgs.gov/i-map/i2538/]

Tabor, R. W.; Frizzell, V. A., Jr.; Booth, D. B.; Waitt, R. B.; Whetten, J. T.; Zartman, R. E., 1993, Geologic map of the Skykomish River 30- by 60-minute quadrangle, Washington: U.S. Geological Survey Miscellaneous Investigations Series Map I-1963, 1 sheet, scale 1:100,000, with 42 p. text. [http://pubs.usgs.gov/imap/i1963/]

Telford, W. M.; Geldart, L. P.; Sheriff, R. E., 1990, Applied Geophysics, 2nd ed.: Cambridge University Press, 770 p.

Troost, K. G.; Booth, D. B.; Wisher, A. P.; Shimel, S. A., 2005, The geologic map of Seattle—A progress report: U.S. Geological Survey Open-File Report 2005-1252, version 1.0, 1 sheet, scale 1:24,000. [http://pubs.usgs.gov/of/2005/1252/]

U.S. Geological Survey Geologic Names Committee, 2007, Divisions of geologic time—Major chronostratigraphic and geochronologic units: U.S. Geological Survey Fact Sheet 2007-3015, 2 p. [http://pubs.usgs.gov/fs/2007/3015/]

Varnes, D. J., 1978a, repr. 1995, Landslide classification system. *In* Dragovich, J. D.; Brunengo, M. J., Landslide map and inventory, Tilton River–Mineral Creek area, Lewis County, Washington: Washington Division of Geology and Earth Resources Open File Report 95-1, 165 p., Plate 3. [http://www.dnr.wa.gov/publications/ger_ofr95-1_lewis_co_landslides_plates.pdf and http://www.dnr.wa.gov/publications/ger_ofr95-1_lewis_co_landslides_text.pdf]

Varnes, D. J., 1978b, Slope movement types and processes. *In* Schuster, R. L.; Krizek, R. J., editors, Landslides—Analysis and control: National Academy of Sciences Transportation Research Board Special Report 176, p. 11-33, 1 plate.

Villeneuve, N. M., 2012, Gravity survey of the Lake Joy 7.5-minute quadrangle, King County, Washington: Western Washington University Senior thesis, 1 v.

Walsh, T. J., 1984, Geology and coal resources of central King County, Washington: Washington Division of Geology and Earth Resources Open File Report 84-3, 24 p., 2 plates. [http://www.dnr.wa.gov/publications/ger_ofr84-3_central_king_co_coal_24k.pdf]

Wiemer, S., 2001, A software package to analyze seismicity—ZMAP: Seismic Research Letters, v. 72, no. 2, p. 373–382.

Wolfe, J. A.; Forest, C. E.; Molnar, Peter, 1998, Paleobotanical evidence of Eocene and Oligocene paleoaltitudes in midlatitudewestern North America: Geological Society of America Bulletin, v. 110, no. 5, p. 664-678.

Wyss, Max; Wiemer, Stefan; Zuniga, Ramon, 2001, ZMAP—A tool for analyses of seismicity patterns: [published by authors], 57 p. [http://www.earthquake.ethz.ch/software/zmap/cookbook.pdf].

Yount, J. C.; Marcus, K. L.; Mozley, P. S., 1980, Radiocarbon-dated localities from the Puget Lowland, Washington: U.S. Geological Survey Open-File Report 80-780, 51 p., 1 plate. [http://pubs.er.usgs.gov/#search:advance/page=1/page_size=100/series_cd=OFR/report_number=80-780:0]

Appendix A. Radiocarbon ages

Table A1. Radiocarbon ages in the Lake Joy and adjacent Carnation 7.5-minute quadrangles. For sample locations see 'age sites' on Plate 1 or the latitude and longitude below. Analyses were performed by Beta Analytic Inc. (Miami, Florida). Lab uncertainty values are one standard deviation (68% confidence interval) and include random errors that can be estimated by the lab but exclude uncertainties that cannot be detected by the laboratory's analytical procedures. Conventional radiocarbon ages are adjusted for measured $^{13}C/^{12}C$ ratio; 'yr BP' signifies radiocarbon years before A.D.1950. Samples for sand geochemistry (Appendix C), petrographic data and provenance (Appendix F), infrared stimulated luminescence (IRSL) and optically stimulated luminescence (OSL) sediment dating technique ages (Appendix B), and other information were collected for many of the radiocarbon sites. *Geologic units*: unit Qc_{ol}, sediments of the Olympia nonglacial interval, local provenance (Pleistocene); unit Qc_{pf}, pre-Fraser nonglacial beds in the Carnation quadrangle; unit Qc_{hmp}, nonglacial fluvial deposits locally derived dominantly from volcanic rocks of Mount Persis; and unit Qc_{ws}, nonglacial fluvial deposits (Pleistocene), Snoqualmie River provenance (Pleistocene). We report only the radiocarbon ages collected during this study. See Dragovich and others (2009b, 2010b, 2011b) for compilations of radiocarbon sites in the adjacent Snoqualmie, Carnation, and Monroe quadrangles, respectively. See Sherrod and others (2008) for radiocarbon ages from fault trenches in the Redmond and Maltby quadrangles west of the Lake Joy quadrangle. Data are organized chronologically from youngest to 'infinite' (>43,500 yr BP). AMS, radiocarbon analysis by atomic mass spectrometry for small samples; SP, Snoqualmie River basin provenance for ancient nonglacial sands.

Sample number	Analyzed organic material (geologic unit)	$^{13}C/^{12}C$ (o/oo)	Conventional radiocarbon date (yr BP)	Notes
11-111C	plant material (unit Qc_{ol})	-27.2	30,550 ±190	Site 111C is a 3-m-high erosion scar on the North Fork Tolt River immediately upstream of its confluence with Yellow Creek. The exposure reveals laminated clayey silts between weakly stratified fine sands and gravelly sand. Thin beds of disseminated plant material occur locally in the silt beds. The lower portion of the unit containing these sand and silt beds is overlain by a thick sequence of crudely stratified cobble gravel and gravel with some gravelly sand interbeds. The whole sequence is fluvial, with the fine beds interpreted as overbank deposits. Gravelly portions of the exposure have a local provenance including lithic Western mélange belt metamorphic and volcanic lithic (andesite, basalt, basaltic andesite, metasandstone, meta-argillite, and greenstone) clasts derived mostly from erosion of the local volcanic rocks of Mount Persis. AMS sample microscopically cleaned of fine modern rootlets prior to sending to Beta Analytic Inc. Measured radiocarbon age: 30,590 ±190 yr BP. Latitude and longitude: 47.72023503 and -121.75452392.
11-22E	charred materials (unit Qc_{ws})	-24.0	>43,500	Site 22E is a driveway excavation on the north side of the Tolt River valley just northeast of river mile 5. The exposure is in thin- to medium-bedded compact sand, silty sand, and silt with thin beds of laminated clay and peat with wood fragments. Sand in this exposure appears to be of ancient nonglacial Snoqualmie River provenance based on its micaceous characteristics. Larger pieces of flattened, charred bark were removed from the peat layers. The bark was broken up and scraped to remove possible modern surface contaminants. The sample was then inspected under a microscope and further potential modern organic material was removed before the sample was sent to Beta Analytic Inc. Latitude and longitude: 47.67399332 and -121.86310158. Geochemical and OSL analyses (Table B1, Sample 44C-2 at 79 ka and Sample 44C-1 at 86 ka) of sands were done from this site.
11-22H	wood (unit Qc_{ws})	-25.2	>43,500	Site 22H is a 5-m-high erosion scar on the north bank of the Tolt River near river mile 6. The exposure shows well-stratified clay and silty sand beds with numerous flattened logs. Some bedding is deformed, possibly due to liquefaction. A kilogram-size wood fragment was removed from the exposure, broken up, scraped to remove the outer layer of wood, and then examined under a microscope to remove any remaining modern organics before being sent to Beta Analytic Inc. Microscopic examination indicated low potential of contamination by modern organic materials such as rootlets. Latitude and longitude: 47.67828461 and -121.85343884.

Sample number	Analyzed organic material (geologic unit)	$^{13}C/^{12}C$ (o/oo)	Conventional radiocarbon date (yr BP)	Notes
11-26F	wood (unit Qc_{hmp})	-25.4	>43,500	Site 26F is on the north bank of the South Fork Tolt River just west of river mile 1. The outcrop shows thickly bedded pebble gravel to cobble gravel, with thick beds of compact gray silt stained red along joints. Most clasts are andesite, basalt, or basaltic andesite, consistent with the rocks of Mount Persis provenance. A log weighing almost 2 kg was removed for analysis. The log was scraped clean, broken up, and examined under a microscope to remove any remaining organic material or rootlets before being sent to Beta Analytic Inc. for radiometric dating. Microscopic examination indicated low potential of contamination by modern organic materials such as rootlets. Latitude and longitude: 47.69298806 and -121.81301485.
11-114T	charred material (unit Qc_{hmp})	-24.7	>43,500	Site 114T is a 2-m-high eroding bank on the east bank of the North Fork Tolt River just south of river mile 10. The outcrop shows a deposit of cobble gravel and pebble gravel with some thick beds of gravelly sand and numerous fragments of wood, including logs. Clasts have a local provenance and consist mostly of basalt and andesite with some metachert and meta-argillite. Basalt clasts have rinds as much as 2 mm thick. A sample of dark wood was collected for analysis. The sample was rinsed, crushed, and dried. The fragments were then examined and remaining modern organic material was removed before the sample was sent to Beta Analytic Inc. for radiometric dating. Latitude and longitude: 47.70828755 and -121.8110016.
11-108A	wood (unit Qc_{hmp})	-24.0	>43,500	Site 108A is a 4-m-high outcrop on the west bank of the South Fork Tolt River at river mile 2 in a fluvial deposit with cobble and boulder clasts in a silty sand matrix that is very compact and bluish gray; silt beds have a green hue. Clasts and sands are significantly altered to clay. Small disseminated dark pieces of wood are present throughout the exposure. Wood pieces were collected, then crushed and cleaned under a microscope to ensure all modern organics were removed before being sent to Beta Analytic Inc. for AMS dating. Latitude and longitude: 47.69310088 and -121.79326071.
11-44D	wood (unit Qc_{pf}) in the Carnation 7.5-minute quadrangle	-24.5	>43,500	Site 44D is located off of State Highway 203 in an abandoned sand and gravel pit approximately 2 mi north of the town of Carnation. The exposure shows crossbedded and plane-bedded sands and gravels offset by localized meter-scale extensional faults that trend northeast, suggesting a connection with Snoqualmie valley fault no. 3. In the absence of large deposits of wood, multiple small wood fragments were removed from different areas of the outcrop. The samples were crushed and examined under a microscope. Modern organics were removed. The sample was sent to Beta Analytic Inc. for AMS analysis. Latitude and longitude: 47.69238733 and -121.96427149. Geochemical analysis and OSL age analyses (Table B1, Sample 44D, >250 ka) were also conducted for this site.

Appendix B. Infrared and optically stimulated luminescence age data for Pleistocene nonglacial deposits

Luminescence ages for sediment samples are presented in Table B1 [1]. Table B2 provides additional sample site and sand petrography descriptions, as well as references to additional radiocarbon, geochemical, or photographic data for the samples. The petrographic and geochemical examination of the sands from the age sites, combined with deposit stratigraphy, show that the unit Qc_{ws} and Qc_{pf} samples are monocrystalline quartz–rich ancient Snoqualmie River alluvium with a strong Cascade batholith provenance (for example, Snoqualmie batholith) and have an ancient Snoqualmie River basin provenance (SP, Appendix F). Conversely, unit Qc_{hmp} is ancient Tolt River sediment with a local provenance (LP, Appendix F). The Pleistocene nonglacial character of the sampled SP and LP sediments combined with the age information (Table B1) support our correlation of the sampled strata with the Whidbey Formation or Hamm Creek unit (units Qc_{ws} and Qc_{hmp}, respectively). The luminescence ages obtained for our samples corroborate our independent field, petrographic, and geochemical interpretation that these deposits are nonglacial in origin and thus deposited between glacial episodes as ancient alluvium (Table B2).

Samples 44A-1, 44A-2, 44C-1, and 44C-2 from the southwestern part of the Lake Joy 7.5-minute quadrangle from SP strata are correlative with the Whidbey Formation (Tables B1 and B2). Samples 44A-1 and 44A-2 were 42 ft apart and were obtained from a thick sand bed in a road cut. The systematics and estimated age of 44A-2 suggest it may contain more partially bleached grains than 44A-1, giving it an older depositional age. Because the age ranges of these two samples do not overlap (104–122 ka for 44A-1 and 136–160 ka for 44A-2) and because they are likely from the same deposit, the problem may be that partial bleaching is more prevalent in certain features of each deposit sampled (for example, subaerially exposed grains from point bars versus those "dumped" into massive sand beds leading to more partially bleached grains). Because these deposits are likely ancient overbank flood deposits, perhaps some sand beds were deposited more rapidly during flooding (for example, differing facies of an overbank levee deposit).

Samples 44C-1 and *44C-2* were obtained from adjacent (~20 ft apart) exposures within similar stratigraphic levels of SP sediments. The similarity of the ages (79.3 and 85.8 ka) of these samples supports their correlation with the Whidbey Formation. It is noteworthy that Whidbey Formation samples east of the Tolt River (samples *44A-1, 44A-2)* are generally more weathered megascopically and microscopically than the formation to the west (samples *44C1, 44C-2*), consistent with the overall trend of the IRSL ages for unit Qc_{ws}. The site 44C Whidbey Formation ages (79.3 and 85.8 ka) provide a limiting age for the regional Possession glaciation, which is thought to have occurred from ~60 to 80 ka in the Puget Lowland.

Sample 44B is from a Tolt River erosional cutbank near the southwestern edge of the Lake Joy 7.5-minute quadrangle. Although the age (>165 ka) is only a minimum, we tentatively correlate this sample with the Hamm Creek unit (~188–243 ka) of Troost and others (2005) because the deposit is likely nonglacial in origin. Also, the moderate weathering of the unit suggests local deposition that is somewhat older than the Whidbey Formation and thus consistent with deposition during the next older nonglacial interval—the Hamm Creek.

Site 44D is located off State Highway 203 in the Carnation 7.5-minute quadrangle where an abandoned pit also exposes distinct SP sands and meter-scale faults with as much as 20 cm of apparent tectonic offset. The OSL and radiocarbon ages indicate that these units are middle to early Pleistocene (>250 ka), certainly beyond the range of IRSL and radiocarbon dating. Two experiments were performed, one addressing the level of saturation in the feldspar and the other addressing whether the quartz was saturated. The quartz was saturated at >200 Gray (Gy), and no age could be obtained. The IRSL from potassium feldspars was determined to be between 400 and 500 Gy, with a minimum age of at least 200 ka but more likely an age of >250 ka. The dose rate was not particularly high at ~2Gy/ka, so luminescence would have been slowly created, but the traps were still filled by at least 200 ka ago. This age information suggests that (1) Snoqualmie valley fault no. 3 is potentially active (Dragovich and others, 2010a,b), and (2) these SP deposits (Appendix F) are older than the Hamm Creek unit of Troost and others (2005).[1]

[1] Refer to Dragovich and others (2011b) for a discussion of the Infrared Stimulated Luminescence (IRSL) and Optically Stimulated Luminescence (OSL) methodologies.

Table B1. Optically stimulated luminescence (OSL) and infrared stimulated luminescence (IRSL) data and ages from the Lake Joy 7.5-minute quadrangle. This table provides elemental concentrations, cosmic and total dose rates, equivalent doses, and ages from IRSL (fine feldspars) and quartz OSL. Sample descriptions are generalized; more detailed descriptions are provided above or in Table G2. Samples are located on Plate 1. K, % potassium; Gy, Gray (unit of absorbed radiation); ka, 1000 yr. See Dragovich and others (2011b) for a discussion of OSL/IRSL methods.

Sample information	Water content (%)[a]	K (%)[b]	U (ppm)[b]	Th (ppm)[b]	Cosmic dose[c] additions (Gy/ka)	Total dose rate (Gy/ka)	Equivalent dose (Gy)	n[d]	Age (ka)[e]
44A-1 **stratified silt and sand alluvium**	20 (38)	1.29 ±0.05	1.50 ±0.11	4.68 ±0.31	0.17 ±0.01	1.76 ±0.07 2.44 ±0.09[f]	>190 275 ±6.60[f]	15 (20)	>107 113 ±9.04[f]
44A-2 **stratified silt and sand alluvium**	35 (42)	1.34 ±0.06	1.48 ±0.11	4.71 ±0.33	0.16 ±0.01	1.75 ±0.07 2.47 ±0.10[f]	366 ±3.66[f]	– – –	148 ±12.2[f]
44B **sand and cobble gravel alluvium**	20 (44)	1.59 ±0.06	2.21 ±0.14	6.75 ±0.63	0.11 ±0.01	2.13 ±0.12 3.07 ±0.17[f]	>200 >500[f]	14 (20)	>100 >165[f]
44C-1 **peat, clay, and sand alluvium**	22 (51)	2.14 ±0.06	2.04 ±0.11	8.67 ±0.62	0.15 ±0.01	2.57 ±0.11 3.56 ±0.15[f]	>190 305 ±5.31[f]	16 (20)	>75 85.8 ±7.36[f]
44C-2 **sand and silt alluvium**	5 (22)	2.51 ±0.05	2.48 ±0.11	8.59 ±0.64	0.16 ±0.01	3.44 ±0.14 4.36 ±0.18f	346 ±7.61[f]	– – –	79.3 ±6.88[f]
44D **sand and gravel alluvium**	20 (37)	1.32 ±0.06	0.96 ±0.12	3.19 ±0.34	0.11 ±0.01	1.54 ±0.08 2.02 ±0.11[f]	>500[f]	– – –	>250[f]

[a] Field moisture, with figures in parentheses indicating the complete sample saturation (percent). Ages calculated using approximately 60% of saturation values.

[b] Analyses obtained using laboratory Gamma Spectrometry (high resolution Ge detector).

[c] Cosmic doses and attenuation with depth were calculated using the methods of Prescott and Hutton (1994).

[d] Number of replicated equivalent dose (De) estimates used to calculate the mean. Figures in parentheses indicate total number of measurements made including failed runs with unusable data.

[e] Dose rate and age for fine-grained 250–180 micron sized quartz sand. Linear + exponential fit used on equivalent dose, with single aliquot regeneration. Errors to one sigma.

[f] Feldspar fine silt grains of 4–11 micron polymineral silt. Exponential fit used for multiple aliquot additive dose. Errors to one sigma. Fade tests indicate no correction. Values followed by an "f" superscript denote IRSL ages; otherwise, values denote OSL ages.

Table B2. Site and petrographic information, optically stimulated luminescence (OSL) and infrared stimulated luminescence (IRSL). Except for site 11-44D, samples are located on Plate 1. Map area, Lake Joy 7.5-minute quadrangle; SP, ancient Snoqualmie River basin provenance as further discussed in Appendix F. Some sites were revisited and thus have a new site number. For example, site 39D is the fourth field site on the 39th field day. We revisited that site as the first site on the 44th day (site 44A).

Sample # (geologic unit)	IRSL age (Table B1)	C^{14} Age (Appendix A)	Latitude & longitude (°)	Appendix C geochemistry	Site and sand (thin-section) petrography notes
11-44A-1(unit Qcws)	113 +/-9.04 ka	none	47.67277233, 121.84470423	Sample 39D	**Site Notes:** Site 44A-1 (same as site 39D) is directly south of the Tolt River near the southwestern edge of the map area. The site is on a 4-m-high road cut that was excavated to expose a 2-m x 2-m exposure of stratified silt, silty fine sand, and medium sand. A brown fine sand OSL/IRSL sample was collected 175 cm below the soil surface. **Petrography:** SP alluvial medium sand with some fine sand grains. Mostly monocrystalline quartz, plagioclase, and much pyroxene and lesser potassium feldspar, hornblende, and biotite. Volcanic lithic rich with few, but distinct granitic lithics (with internal potassium feldspar). Sands contain only a few polycrystalline quartz grains. Stratigraphy (sands, silts, peats) and composition are consistent with ancient SP (Appendix F). Percentage of volcanic lithic grains suggests contribution to these SP beds by the ancient Tolt River system. Clay weathering on some grains.
11-44A-2 (unit Qcws)	143 +/-4.48 ka	none	47.67265264, -121.84428312	Sample 44A-2	**Site Notes:** Site 44A-2 (same as site 39D) is 42 ft (13 m) east of site 44A-1. This 3-m x 3-m exposure was excavated in the 4-m-high logging road cut. The exposure revealed thick-bedded SP silt, silty fine sand, and fine and medium sand. Beds are micaceous. The brown fine sand IRSL sample was collected 217 cm below the soil. **Petrography:** Definitive ancient SP medium sand with some fine sand grains. Mostly monocrystalline quartz, plagioclase, and lesser potassium feldspar, hornblende, and biotite and much pyroxene. Volcanic lithic rich with few but distinct granitic lithics (a few granitic lithic grains have internal potassium feldspar); few polycrystalline quartz grains. Stratigraphy (sand, silt, peat) and composition are consistent with ancient SP. Volcanic lithic volume suggests a small contribution to SP in this area by the ancient Tolt River system. Clay weathering on some grains.
11-44B (unit Qcnmp)	>165 ka	none	47.67807623, -121.85334781	Sample 16A	**Site Notes:** Site 44B (same as site 16A) is a Tolt River erosional cutbank near the southwestern edge of the map area (also see site 16A). The stratigraphy is exposed by multiple debris slide erosional scars. (Lack of bedding rotation parallel to the slope suggests the stratigraphy is in place.) The site contains highly weathered, moderately stratified gravely sand, cobble gravel, and coarse sand. Sand beds are lenticular and commonly greenish blue. Many gravel clasts are strongly weathered and typically soft. Basalt gravel clasts have 3.0–3.5 mm weathering rinds. Sands are similarly weathered and "smear" when struck with a rock hammer. Most gravel beds are matrix supported except toward bottom of the outcrop, where they are clast supported. Site is overlain by well-stratified sand, silt, and peat of unit Qcws. **Petrography:** Sample of distinctly weathered sand with definitive clay weathering products of the matrix and clasts. As a result of this weathering, sands are only moderately sorted. Weathering of sand-size material results in difficult petrographic determinations of some grain types. Sand is polymictic and contains monocrystalline quartz, volcanic and metasedimentary lithic grains, polycrystalline quartz, plagioclase, a few granitic lithics, hornblende, and pyroxene. Sample has a local eastern provenance as determined in the field by gravel clast count (strong volcanic Mount Persis and Western mélange belt provenances with mostly andesite, basaltic andesite, basalt, and meta-argillite clasts) as well as sand petrography (Appendix F).

Sample # (geologic unit)	IRSL age (Table B1)	C^{14} Age (Appendix A)	Latitude & longitude (°)	Appendix C geochemistry	Site and sand (thin-section) petrography notes
11-44C-1 (unit Qcws)	85.8 +/-7.36 ka	Sample 22E (>43,500 yr BP)	47.67396441, -121.86326796	Sample 11-22E	**Site Notes:** Site 44C-1 (same as site 22E) is along a private driveway roadcut west of the Tolt River in the southwestern part of the map area. A 2-m-high roadcut exposes well-stratified, thin- to medium-bedded silty sand and sand with thin beds of clay and peat. Sand composition indicates ancient SP (micaceous and monocrystalline quartz-rich). The OSL/IRSL sample was taken at 250 cm below the soil surface. **Petrography:** Typical mineral-rich ancient SP sands with much monocrystalline quartz, plagioclase, and potassium feldspar and some biotite and hornblende grains. Volcanic lithic grains dominate the lithic grain population with some granitic lithic grains and a few sedimentary or metasedimentary lithic grains. Monocrystalline quartz content is high, distinctly greater than that of polycrystalline quartz, consistent with ancient SP alluvial compositions observed regionally. Meta-argillite content low, suggesting that contribution of clasts from the east along ancient Tolt River routes was limited or swamped by ancient SP detritus. Weathering products such as clay dominate the fine fraction of these sands.
11-44C-2 (unit Qcws)	79.3 +/- 6.88 ka	Sample 11-22E (>43,500 yr BP)	47.67394924, -121.86326796	Sample 11-22E	**Site Notes:** Site 44C-2 (same as site 22E) is located along a private driveway roadcut northwest of the Tolt River in the southwestern part of the map area. Site 44C-2 is 6 m south of site 44C-1. A 2-m-high roadcut exposes well-stratified and moderately and thin- to medium-bedded, coarse and medium sand with thin beds of silt and interbedded organic silt. Mica and monocrystalline quartz-rich sand composition indicates SP. The IRSL sample was taken at 240 cm below the soil surface. **Petrography:** Typical SP sands with much monocrystalline quartz, plagioclase, and potassium feldspar and some biotite and hornblende grains. Volcanic lithic grains dominate the lithic grain population with some granitic lithic grains and a few sedimentary or metasedimentary lithic grains. Monocrystalline quartz content is high, distinctly greater than that of polycrystalline quartz, consistent with ancient SP alluvial compositions observed regionally. Meta-argillite content low, suggesting that contribution of clasts from the east along ancient Tolt River routes was limited or swamped by ancient SP detritus. Weathering products such as clay dominate the fine fraction of these sands.
11-44D (unit Qcpf)	>250 ka	Sample 11-44D (>43,500 yr BP)	47.69238733, -121.96427149	Sample 11-20A	**Site Notes:** Site 44D (same as site 20A) is located off of State Highway 203 in the Carnation 7.5-minute quadrangle in an abandoned and re-vegetated sand and gravel pit. (See photo of site in Appendix E.) The steep pit walls expose crossbedded and planar-bedded sand, gravel, and pebble gravel. Gravel deposits locally contain silt rip-up clasts and ripple marks. The pit also exposes meter-scale faults with as much as 20 cm of apparent offset. Pit is near Snoqualmie valley fault no. 3 of Dragovich and others (2010a,b). Most bedding dips south to southeast. Scattered detrital sticks and small dark pieces of charcoalized wood were disseminated throughout the strata. An IRSL sample was taken 5 m from the top of the pit wall. **Petrography:** Medium to fine, well-sorted alluvial sand is polymictic and has significant monocrystalline quartz, plagioclase, and potassium feldspar and lesser but significant granitic lithics. Distinct SP with 15% potassium feldspar. Lithic composition is varied and includes volcanic and metamorphic clasts. Granitic lithic grains commonly contain quartz, potassium feldspar, and (or) plagioclase, indicative of a true granite source (that is, parts of the Snoqualmie batholith). Minor grains include phyllite, meta-argillite, pyroxene, and serpentinite.

Appendix C. Geochemistry of Quaternary sand deposits and the volcanic rocks of Mount Persis

Whole-rock major and trace element analyses were run on 6 glacial sands, 10 nonglacial sands, 21 samples from the volcanic rocks of Mount Persis of Tabor and others (1993)(volcanic rocks of Mount Persis, Mount Persis Unit), and 1 granite to granodiorite using X-ray fluorescence (XRF) and inductively coupled plasma source mass spectrometer (ICP-MS) at the Geoanalytical Laboratory at Washington State University (WSU). Figure C1 displays the locations of these samples. Petrographic descriptions for these samples are in Table C1. Tables C2 and C3 display the unnormalized and normalized geochemical data for these samples. (A Microsoft Excel file containing Tables C1–C3 as tabs in the spreadsheet file, "Lake Joy quadrangle_Appendix_C_Table_C1_C3.xlsx", is attached.) The normalized samples are "loss on ignition" (LOI) free (Table C3), and only these samples are plotted on geochemical diagrams. Previous reviews and interpretation of Quaternary sand and Mount Persis rock geochemistry from the Carnation, Falls City, Monroe, and Snoqualmie 7.5-minute quadrangles can be found in Dragovich and others (2011b).

Grinding of samples was done at WSU using a tungsten carbide mill for XRF analyses and iron equipment for ICP-MS analyses (Johnson and others, 1999). Estimates of accuracy and precision, as well as discussion of analytical methods for both XRF and ICP-MS at WSU, are given by Johnson and others (1999) and Knaack and others (1994), respectively. Before grinding, all Quaternary sediment samples were sieved with 2 mm (no. 10) and 0.075 mm (no. 200) sieves at the DNR laboratory in Olympia, Wash., so that only the sand-size fraction was chemically analyzed (Table C1). This was done to eliminate erroneous results that may occur from gravel-size clasts and to remove the varied amounts of silt and clay from these sandy samples. Using this technique, we provide a better comparison between the glacially and nonglacially derived sediments by comparing the composition of the sands rather than comparing sands with silty sands. The sand samples were generally from well-sorted pebbly sand or sand beds.

Some pre-Fraser age nonglacial sands displayed moderate to heavy weathering both in the field and petrographically (Table C1). These Pleistocene sands have chemical index of alteration values greater than 50, supporting chemical alteration by weathering (Table C3; Fig. C2)(Nesbitt and Young, 1989; Nesbitt, 2003). Many of the volcanic rocks of Mount Persis have petrography and geochemistry indicating that they underwent moderate to extensive hydrothermal alteration (Tables C1 and C3; Fig. C2). Many important geochemical elements are mobile under these conditions (Cann, 1970; Humphris and Thompson, 1978; Harper, 1995; Pearce, 1996). Therefore, elements that are immobile up to and including amphibolite-facies metamorphism are primarily utilized for this study. (See Pearce, 1996, for a review.)

QUATERNARY SAND GEOCHEMISTRY

Major- and trace-element geochemistry of sediments can provide invaluable information about their original tectonic setting and provenance (Roser and Korsch, 1986; McLennan and others, 1993). Biogenic $CaCO_3$ or SiO_2, high concentrations of heavy minerals or quartz, and diagenetic reactions related to burial can alter the concentrations of elements within a sedimentary sample (Galloway, 1974; Roser and Korsch, 1986, 1988; McLennan, 1989). Thus, caution should be used when making interpretations based only on geochemical analyses of sediments, and ratios should be used whenever possible. Mole ratios of CaO/Na_2O were used to confirm that the CaO values of these sands were representing a silicate phase and not strongly influenced by carbonate or phosphate (McLennan, 1993).

Holocene Nonglacial Deposits

Tolt River alluvium (unit Qa)—Three alluvial local provenance (LP) sands, including sample 09-27K from the Carnation 7.5-minute quadrangle (Dragovich and others, 2010b), plot within the arc field on the Sc vs. V diagram of Bhatia and Crook (1986)(Fig. C3). All three unit Qa samples plot transitionally between intermediate and felsic arc sources on the La/Th vs. Hf diagram of Floyd and Leveridge (1987)(Fig. C4). These samples have chondrite-normalized La/Lu ratios between 5.14 and 5.25 and Pb/Yb ratios from 3.46 to 3.99 (Fig. C5).

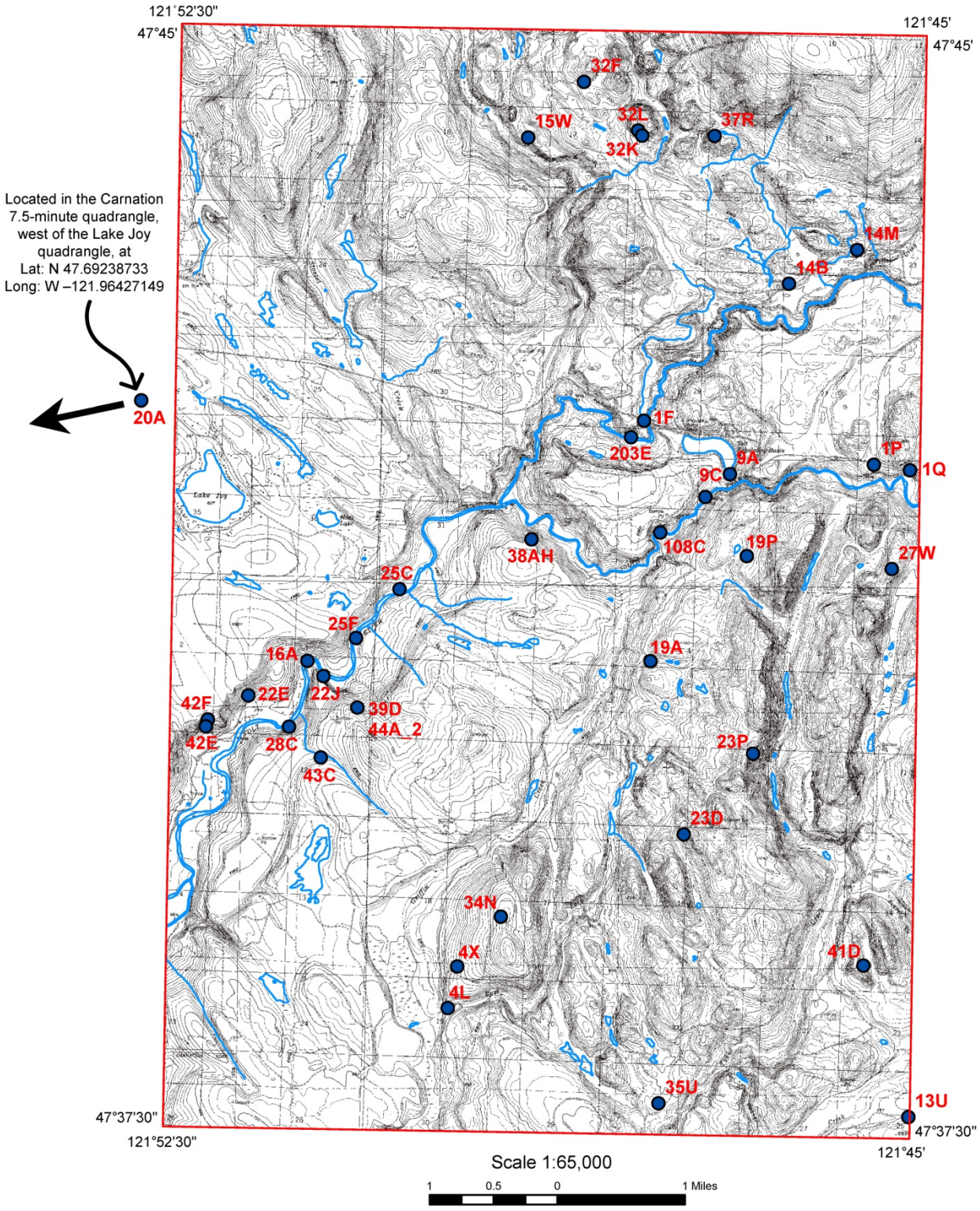

Figure C1. Geochemical sample-site locations in the Lake Joy 7.5-minute quadrangle. See Table C1 for geochemical data and other sample information including location descriptions and other sample notes. Blue lines indicate lake outlines and streams.

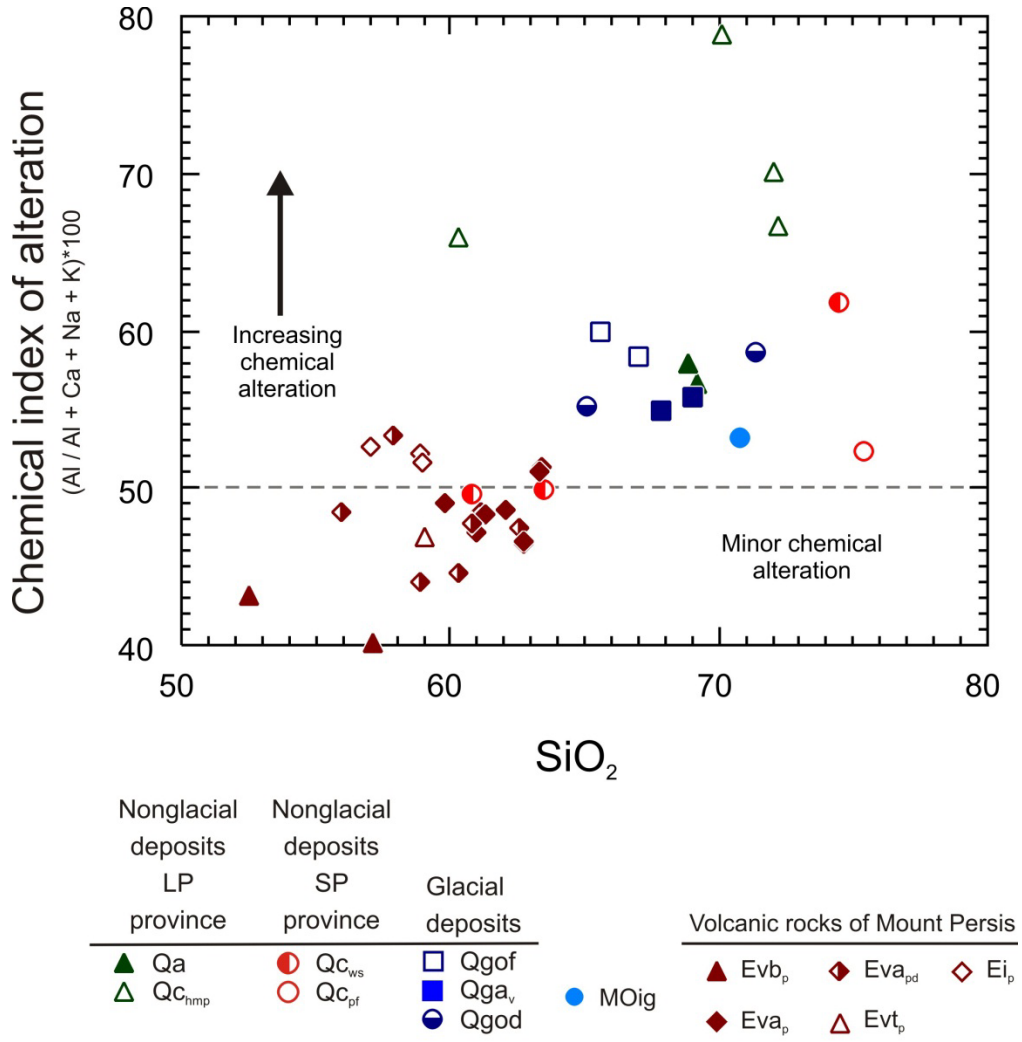

Figure C2. Chemical index of alteration vs. SiO_2 for sands from the Lake Joy 7.5-minute quadrangle. Chemical index of alteration from Nesbitt and Young (1989) and Nesbitt (2003). Data normalized LOI-free before being plotted.

Pleistocene Glacial Deposits

Deltaic outwash and kame deltas (unit Qgod)—Two delta sands plot within the arc field on the Sc vs. V diagram of Bhatia and Crook (1986)(Fig. C3). These samples plot transitionally between intermediate and felsic arc sources on the La/Th vs. Hf diagram of Floyd and Leveridge (1987)(Fig. C4). These samples have chondrite-normalized La/Lu ratios between 4.37 and 5.40 and Pb/Yb ratios from 3.39 to 4.13 (Fig. C5).

Fluvial outwash deposits (unit Qgof)—Two fluvial outwash sands plot in the arc field on the Sc vs. V diagram of Bhatia and Crook (1986)(Fig. C3). Sample 11-35U plots transitionally between intermediate and felsic arc sources on the La/Th vs. Hf diagram of Floyd and Leveridge (1987), while sample 11-203E plots close to the felsic arc source field on this diagram (Fig. C4). These samples have chondrite-normalized La/Lu ratios between 5.16 and 5.27 and Pb/Yb ratios from 2.94 to 4.65 (Fig. C5).

Tables C1–C3. Tables within this appendix contain location, petrographic, and sample descriptions (Table C1) and unnormalized and normalized geochemistry for samples (Tables C2 and C3, respectively) in the Lake Joy 7.5 minute quadrangle. Figure C1 shows the sample location in the quadrangle. Geochemically, Snoqualmie River basin provenance (SP) is very similar to that of modern alluvium and can be distinguished from glacially derived samples because: (1) nonglacial samples have higher average major element values yet lower average SiO_2 than glacial samples; (2) nonglacial samples have higher abundances of low field strength elements (for example, Pb, Ba, and Sr); and (3) nonglacial samples have higher chondrite-normalized La/Lu ratios (Dragovich, 2007; Dragovich and others, 2009b,c, 2010a,b, 2011a,b). Both the petrography and geochemistry show that nonglacial sands are predominantly derived from an arc source, whereas glacial sands are from arc sources and older accreted sedimentary and metamorphic terranes. These data are also available in an attached Microsoft Excel file.

Table C1. Geochemical sample information, including thin-section petrography, sample site, and related information for the geochemistry samples in and near the Lake Joy 7.5-minute quadrangle. Elements for all samples determined using XRF and ICP analytical methods (see Tables C2 and C3 for geochemical data). Samples are located in Figure C1. See Figure C3 for plots of the geochemical data. See abbreviations below. Geochemical sample powders and the remaining original samples are archived at the DNR, Division of Geology and Earth Resources.
Abbreviations: chem, geochemistry; kspar, potassium feldspar; SP, (ancient) Snoqualmie River basin provenance (Appendix F); OSL, Optically Stimulated Luminescence; IRSL, Infrared Stimulated Luminescence; XRF, X-ray fluorescence; ICP, inductively coupled plasma; LOI, loss on ignition; TCFZ, Tokul Creek Fault Zone; CF-1, Carnation fault no. 1; CCFZ, Cherry Creek fault zone; SVF-3, Snoqualmie Valley fault no. 3.

Site-sample no.	Geologic unit	General sample site notes	Digital photos (Appendix E)	Sample locations					OSL/IRSL age (Appendix B)	Radiocarbon age (Appendix A)	Rock sample geochemistry	Sand sample geochemistry	Thin-section, geochemistry and additional site notes										Sieve weights for sand geochemistry samples		
				Latitude	Longitude	Township	Range	Section					Petrography notes	hornblende	augite	hypersthene	plagioclase	quartz (free)	% kspar	% mica	other minerals	rock name thin section	Weight (g) on sieve no. 10 (pebbles)	Weight (g) on sieve no. 200; chem sample sent	Weight (g) below sieve no. 200 in pan (silt and/or clay)
11-1F	tz_h of Eva_p	Site 1F is at the top of the river canyon on the west side of the North Fork Tolt River in the Lake Joy 7.5-minute quadrangle. The outcrop is a massive andesite flow that is greenish-gray weathering to brown. Flow contains abundant phenocrysts, most of which are plagioclase, as well as some altered dark mafic minerals with lesser interstitial volcanic glass showing a light green cast due to hydrothermal alteration. Light greenish andesite sample collected for geochemical and petrographic analyses.	NONE	47.70601639	-121.7973911	T26N	R8E	27	NONE	NONE	X	NONE	Typical andesite with large block euhedral plagioclase to a few millimeters in a glass with golden color. Opaque and alteration products present. Glomeroporphyritic texture with blocky plagioclase and mafic minerals (likely pyroxene); mafic minerals converted to Fe-chlorite or chlorite + calcite. Rock is distinctly altered. Alteration could be late magmatic.		?		X		0			"altered" andesite flow			
11-1P	Eva_{pd}	Site 1P is located near the eastern edge of the Lake Joy 7.5-minute quadrangle directly north of the North Fork Tolt River. This fine grained volcanic flow rock may be interbedded with vitric tuff. This porphyritic rock with plagioclase phenocrysts was classified as a basaltic andesite in the field due to the dark color but is geochemically an andesite. A dark bluish-gray rock sample was collected for geochemical and petrographic analyses.	NONE	47.70130391	-121.7586146	T26N	R8E	34	NONE	NONE	X	NONE	Typical mafic flow rock. Plagioclase microlites are abundant and define a wavy flow alignment; scatted larger subhedral phenocrysts of plagioclase were also noted. Flow is also indicated by broken plagioclase and slightly folded or warped bands with slightly more glass. Possible quartz-filled vesicles and minor secondary calcite in clear glass. Disseminated small opaque minerals ubiquitous. Some volcanic glass between dense microlites locally replaced by green chlorite. Alteration is moderate. Sample lacks mafic minerals. Sample is essentially microlitic plagioclase and glass with opaque minerals and scattered, distinctly large plagioclase phenocrysts with albite twinning.				x		0			"altered" basaltic andesite			
11-1Q	Eva_{pd}	Site 1Q is located on the eastern edge of the Lake Joy 7.5-minute quadrangle directly north of the North Fork Tolt River. Very large outcrop of fine-grained, dark-gray andesite or basaltic andesite; massive with a light green hue and microlites. Flow texturally similar to flow rocks at site 1P. A dark-gray rock sample was collected for geochemical and petrographic analyses.	NONE	47.70060042	-121.7536416	T26N	R8E	35	NONE	NONE	X	NONE	Sample very similar to sample 1P and suspect this is the same flow. Flow banding is distinct microscopically. Same texture and mineralogy as 1P with much aligned plagioclase microlites (eutaxitic). Also contains disseminated fine opaque minerals and glass-rich bands with minor quartz and no mafic minerals. Very minor secondary potassium feldspar and few large plagioclase phenocrysts. Calcite, chlorite and potassium feldspar are common and the rock shows moderate alteration. The lighter bands with quartz may be secondary alteration fronts but unsure.				x		1			"altered" basaltic andesite			
11-4L	Eva_p	Site 4L is located along an old logging road in the southwestern corner of the Lake Joy 7.5-minute quadrangle. Outcrop of massive dark bluish-gray andesite flow overlain by till. Primary jointing strikes north-south and dips slightly west. Flow bedding could be mocking jointing and similarly dip slightly west. A fresh dark-gray andesite sample was collected for geochemical and petrographic analyses.	NONE	47.63901187	-121.8291131	T25N	R8E	19	NONE	NONE	X	NONE	Sample is massive volcanic flow; microscopically sample is homogeneous and has no flow textures such as mineral alignment or other distinct structure. Andesite with large blocky euhedral plagioclase up to 3 mm long with continuous size decrease to microlites. Plagioclase is surrounded by a clear golden glass containing fine opaque minerals. Also, contains subhedral phenocrysts of augite and possible hypersthene with books of probable biotite that is likely primary. Most pyroxene is moderate birefringent, but some pyroxene is low birefringent and might be hypersthene. Alteration is low. (Rock is similar to sample 4X and might be the same flow.)		x	?	x		0	x	biotite	andesite flow			
11-4X	Eva_p	Site 4X is located in the southwestern corner of the Lake Joy 7.5-minute quadrangle. The site is in a quarry with possibly the same dark andesite flow that was suggested to have made up the bedrock at 4J and 4L. Flow is at least 50 ft thick. Vesicles were apparent but lacked orientation. Andesite seems to form "columns" that suggest possible westerly dip. Joints and small faults were scatted throughout outcrop, but had no obvious pattern upon cursory examination. A dark greenish/bluish gray andesite sample was collected for geochemical and petrographic analyses.	NONE	47.6437277 (N 47°38'37.4")	-121.82767572 (W 121° 49'39.6")	T25N	R8E	19	NONE	NONE	X	NONE	Andesite, has a massive texture, also very similar texturally and mineralogically to nearby sample 4L, suggesting the same flow. Clean euhedral plagioclase phenocrysts to microlites in a clear glass with phenocrysts of moderate to moderately high birefringent pyroxene (augite). Glomeroporphyritic pyroxene and plagioclase locally noted. Sample has low alteration thus geochemical analyses should be representative of the original flows. No biotite, hypersthene, and scattered opaque minerals.		x		x		0			andesite flow			

Site-sample no.	Geologic unit	General sample site notes	Digital photos (Appendix E)	Sample locations					OSL/IRSL age (Appendix B)	Radiocarbon age (Appendix A)	Rock sample geochemistry	Sand sample geochemistry	Thin-section, geochemistry and additional site notes									Sieve weights for sand geochemistry samples		
				Latitude	Longitude	Township	Range	Section					Petrography notes	hornblende	augite	hypersthene	plagioclase	quartz (free)	% kspar	% mica	other minerals	rock name thin section	Weight (g) on sieve no. 10 (pebbles)	Weight (g) on sieve no. 200; chem sample sent	Weight (g) below sieve no. 200 in pan (silt and/or clay)
11-9A	Eva_p	Site 9A is located along the southeastern corner of the Tolt Regulating Basin in the middle of the Lake Joy 7.5-minute quadrangle; 5-m-high roadcut of black andesite flow. Possible planar flow features suggest steeply dipping south- and east-west-striking primary volcanic bedding. A dark greenish/bluish gray andesite sample was collected for geochemical and petrographic analyses.	NONE	47.7001022 (N 47°42'00.4")	-121.78294184 (W 121°46'58.6")	T26N	R8E	33	NONE	NONE	X	NONE	Regulating basin andesite. Plagioclase phenocryst–rich with few large plagioclase to 3 mm in cloudy glass. (Many phenocrysts are anhedral and appear to be resorbed.) Also contains subhedral smaller phenocrysts of augite and few decidedly pleochroic green hornblende grains. Glass has many fine grains of opaque minerals and small alteration products giving dirty appearance. Alteration is moderate and the glass is dirty suggesting caution with geochemistry. Biotite like mineral after pyroxene(?) may be secondary. (See sample 9C might be the same flow and has a similar texture and composition petrographically.)	x	x		x		1	x	biotite?	andesite or basaltic andesite flow			
11-9C	Eva_p	Site 9C is located next to a USGS steam gage along the west bank of the South Fork Tolt River, directly south of the Tolt Regulating Basin near the center of the Lake Joy 7.5-minute quadrangle. River bank outcrop of unweathered and massive dark gray andesite (similar to site 9A) with uniformly spaced fine jointing. A dark bluish-gray andesite sample was collected for geochemical and petrographic analyses.	NONE	47.6967481 (N 47°41'48.3)	-121.78743311 (W 121°47'14.7")	T26N	R8E	33	NONE	NONE	X	NONE	Very similar to 9A to north-northeast with subhedral phenocrysts of plagioclase and augite and generally smaller grains of distinct green pleochroic hornblende and may be the same flow. Both samples have the same cloudy glass with much scattered opaque minerals and other small grains in the light colored glass. As with many volcanic rocks of Mount Persis the plagioclase in the flow rocks is distinctly zoned and displays albite twinning. Massive texture and the slight alteration (local slightly chloritized hornblende) is noted for the geochemical interpretation otherwise relatively healthy.	x	x		x		0			altered "barely" dacite			
11-13U	Qgod	Site 13U is located in the southeastern most corner of the Lake Joy 7.5-minute quadrangle on the border with the Devils Slide 7.5-minute quadrangle. An excavation of a 2-m-high cutbank revealed poorly stratified, well-sorted, loose sand under stratified pebble to cobble gravel. Lack of compaction, geomorphic setting, and stratigraphic position imply ancient Vashon recessional delta deposits. A light brownish-gray fine sand sample was collected for geochemical and petrographic analyses.	NONE	Approx. N47 37'39.1"	Approx. W121 45'08.5"	T25N	R8E	26	NONE	NONE	NONE	X	Recessional sand deposits (likely glacial lake sands) in the southeastern part of the Lake Joy 7.5-minute quadrangle. Like nearby non-glacial Olympia beds the sands have a partial granitic source including some granitic lithic grains, appreciable potassium feldspar (~8%) but polymictic with variable monocrystalline quartz, plagioclase, volcanic lithics, hornblende, pyroxene, with some meta-sedimentary lithic grains. Distinct northeast provenance with mélange belt, volcanic and granitic provenance. Some polycrystalline quartz but compared to advance outwash the sample has a low percentage of both polycrystalline quartz and high-grade metamorphic lithic grains. For example, only observed one foliated quartz aggregate metamorphic lithic grain. See unit ~~M~~Oig granite body in the southeast part of the map area for source of granitic detritus including potassium feldspar east of the map area. (Also see Index batholith intrusive rocks and the metamorphosed arkoses in the western mélange belt noted by previous workers for sources of potassium feldspar.)	x	x		x		8			fine sand (recessional lake deposit)	0	66.66	0.84
11-14B	Qgod	Site 14B is located in a sand and gravel borrow pit near the northeast part of the Lake Joy 7.5-minute quadrangle directly north of the North Fork Tolt River. The pit wall reveals planar, thick (10+ m high) delta foreset beds dipping to the west. These deltaic deposits are moderately to well-stratified, loose, and consist of cobble gravel, pebble gravel, and coarse sand with localized cobbly sand. The deltaic deposits are capped by high-energy fluvial-outwash deposits consisting mostly of boulder and cobble gravel. A light gray coarse sand and gravel sample was collected for geochemical and petrographic analyses.	NONE	47.72158795	-121.7746779	T26N	R8E	22	NONE	NONE	NONE	X	Well sorted and rounded coarse sand from deltaic deposits; sampled from sand and gravel pit. Lithic sand is mostly western mélange belt meta-sandstone and meta-argillite and volcanic grains with lesser but distinct granitic lithics with green hornblende. Contains a few grains of metachert (polycrystalline quartz), greenstone, and minor mineral grains. This distinctly lithic rich sand contains a few grains of plagioclase and polycrystalline quartz including probable vein quartz. Some western mélange belt fragments in this section contain pumpellyite. Low potassium feldspar in coarse meta-sandstone grains suggest meta-arkoses noted in previous studies low in volume to east and northeast of the Lake Joy 7.5-minute quadrangle and thus the meta-sandstones from the source area for the lithics in this recessional glacial deposit were derived from western mélange belt meta-sedimentary rocks low in potassium feldspar.	x			x	x	1			deltaic coarse sand (recessional)	79.78	25.29	0.39
11-14M	Eva_{pd}	Site 14M is located in a quarry along an old logging road along a steep hillside directly north of the North Fork Tolt River in the northeast corner of the Lake Joy 7.5-minute quadrangle. The quarry walls exposed a massive, dark basaltic andesite flow as well as several minor faults with tightly spaced subparallel fractures. One fault had clay gouge up to 30 cm thick. Some carbonate veins were seen locally in fractures. A dark gray rock sample was collected for geochemical and petrographic analyses.	NONE	47.72540716 (N 47°43'31.5")	-121.76222295 (W 121°45'44.0")	T26N	R8E	22	NONE	NONE	X	NONE	Andesite contains a dense network of medium-sized plagioclase grains (~0.5 mm). These plagioclase microphenocrysts constitute over 60 percent of the sample giving the rock an almost hypabyssal intrusive appearance. Few scattered grains of euhedral augite. Minor glass between grains contains much disseminated opaque minerals and other small grains and material giving the rock a clouded or semi-opaque appearance. Most of the plagioclase grains also cloudy. Rock is altered (geochemistry) and likely has fine chlorite in the matrix and replacing some of the plagioclase. Some of this low-level alteration is likely related to the faulting and fracturing pervading the outcrop as noted in the field. For example, few veins with secondary quartz and chlorite noted in the sample and likely from fluids offered during fault dislocation.		x		x		0			"altered" andesite			
11-15W	tz of Eva_p	Site 15W is located is a rock quarry along the northern part of the Lake Joy 7.5-minute quadrangle. The bluish-gray andesite exposed in the pit walls has flow characteristics and high levels of hydrothermal alteration. The rock contains several millimeter-wide glomeroporphyritic texture pockets of augite and hypersthene between zones dominated by protomylonitized matrix predominately made of glass. The rock has a microcrystalline texture, is sparsely porphyritic, and has possible primary bedding dipping north to northwest. A light bluish-gray andesite sample was collected for geochemical and petrographic analyses.	NONE	approx. N47 44'15.7"	approx. W121 49'03.8"	T26N	R8E	17	NONE	NONE	X	NONE	Protomylonitized andesite with sheared mineral grains in a shear-reduced glassy matrix; strong structural alignment of plagioclase phenocrysts is the result of low temperature shear. Contains appreciable secondary calcite and chlorite and thus caution with geochemical interpretation. Contains opaque minerals. Mafic minerals have been completely chloritized. Shear could be from east-west-trending or northwest-southeast-trending faults near this quarry on a bedrock knob or hillock. Glomeroporphyritic texture noted in the field area, actual areas of calcite replacement seen.				x		0			"altered" + protomylonitized andesite flow			

Site-sample no.	Geologic unit	General sample site notes	Digital photos (Appendix E)	Sample locations					OSL/IRSL age (Appendix B)	Radiocarbon age (Appendix A)	Rock sample geochemistry	Sand sample geochemistry	Thin-section, geochemistry and additional site notes										Sieve weights for sand geochemistry samples		
				Latitude	Longitude	Township	Range	Section					Petrography notes	hornblende	augite	hypersthene	plagioclase	quartz (free)	% kspar	% mica	other minerals	rock name thin section	Weight (g) on sieve no. 10 (pebbles)	Weight (g) on sieve no. 200; chem sample sent	Weight (g) below sieve no. 200 in pan (silt and/or clay)
11-16A	Qc_{hmp}	Site 16A is a Tolt River erosional cutbank near the western edge of the Lake Joy 7.5-minute quadrangle. (Also see site 44B.) The stratigraphy is exposed in multiple debris slide erosional scars. (Lack of evidence of bedding rotation parallel to the slope suggests the stratigraphy is in place.) The site contains highly weathered moderately stratified gravely sand, cobble gravel, and coarse sand. Sand beds are lenticular and are commonly greenish-blue. Gravel clasts are strongly weathered and typically soft. Basalt gravel clasts have 3-3.5 mm weathering rinds. Sands are similarly weathered and "smear" when struck with a rock hammer or geopick. (See petrography.) Sand and gravel have a local eastern provenance (ancient Tolt River alluvium) with significant dark meta-argillite and volcanic grains. Most gravel beds are matrix supported except towards bottom of the outcrop, which is clast supported. Site is overlain by well-stratified sand, silt, and peat of unit Qc_{ws}. A pale yellow sand sample was collected for geochemical and petrographic analyses.	NONE	47.67814966 (N 47°40'42.3")	-121.85340045 (W 121°51'12.2")	T25N	R7E	1	X (see site 11-44B)	NONE	NONE	X	Sample of distinctly weathered sand with definitive clayification of the matrix and clasts. Sand sample is poorly sorted as a result of weathering and contains many small grains of clay weathering products. Fine material gives the section a poor quality. Polymictic with monocrystalline quartz, volcanic lithic grains, meta-sedimentary lithic grains, polycrystalline quartz, plagioclase, few granitic lithics, hornblende and pyroxene. Weathering of sand-sized material results in difficult interpretation of sample petrographically.	x			x	x	2				20.75	117.4	6.97
11-19A	Eva_{pd}	Site 19A is located north of Hull Lake between Griffin Creek and Canyon Creek in the Lake Joy 7.5-minute quadrangle. Rock quarry exposing dark basaltic andesite with either primary flow bedding or tight and persistent jointing. Weathered face suggests phenocryst alignment subparallel to the inferred bedding plane. This direction is subparallel to north-northeast-trending Tokul Creek fault zone. A dark gray rock sample was collected for geochemical and petrographic analyses.	NONE	47.67825745 (N 47°40'41.7")	-121.79698119 (W 121°47'49.1")	T25N	R8E	4	NONE	NONE	X	NONE	Contains microlites of plagioclase and small blades of hypersthene in a clear glassy matrix with disseminated opaque minerals and a few scattered phenocrysts of euhedral plagioclase to 2 mm. Small blades of hypersthene are abundant and have low birefringence and straight extinction. Few small but broad blades of anhedral pleochroic green hornblende observed. Rock is nearly holocrystalline as a result of the dense network of microlites. Few chlorite filled vesicles are apparent. Although there is some secondary chlorite as well as one calcite filled vein that is apparent, the alteration is moderate to low and thus geochemistry should be representative of these basalt or basaltic andesite flows.	x		x	x		1			basaltic andesite to basalt flow			
11-19P	Evb_p	Site 19P is a rock quarry near the eastern edge of the Lake Joy 7.5-minute quadrangle west of Tokul Creek and south of the South Fork Tolt River. The dark aphanitic basalt in the quarry walls has possible bedding planes related to flow features or a persistent joint spaced every 0.5 to 1 m. Definite northwest-trending minor faults with thin to thick gouge are also exposed in the quarry walls as well as locally observed northwest- and northeast-trending transtensional extensional veins. A dark-gray basalt sample was collected for geochemical and petrographic analyses.	NONE	47.69079644 (N 47°41'26.9")	-121.78050857 (W 121°46'49.8")	T26N	R8E	33	NONE	NONE	X	NONE	Homogeneous holocrystalline basalt with mostly aligned network on fine subhedral to euhedral plagioclase blades and small sugary grains of augite with scattered interstitial, anhedral masses of brownish pleochroic hornblende(?). Hornblende is replaced mostly by chlorite or biotite. Some of the pyroxene may be hypersthene as suggested by yellow birefringence and straight extinction. Few scattered opaque minerals. Brown masses have difficult optical properties (subtle pleochroism with difficult birefringence determination) thus correlation with hornblende is tentative. Alteration is moderate and thus the geochemistry should be representative of this flow. Sample 19T is similar texturally and mineralogically and thus may be the same flow.						0			basaltic andesite to basalt flow			
11-20A	Qc_{pf}	Site 20A (same as site 44D OSL site) is located off of Highway 203 in the Carnation 7.5-minute quadrangle and is an abandoned and re-vegetated sand and gravel pit. The steep pit wall exposes crossbedded and plane-bedded sand, gravel, and pebble gravel. Gravel deposits locally contain silt rip-up clasts and ripple marks. The pit also exposes meter-scale faults with up to 20 cm of apparent offset. Typical bedding is dipping south to southeast. Scattered detrital sticks and small dark pieces of charcoalized wood were disseminated throughout pit strata. There were no large deposits of wood, so multiple pieces were meticulously removed from different areas of the outcrop with a pocket knife. The samples were fragmented and microscopically cleaned to removed possible modern organic contaminants. The sample was then sent to Beta Analytic Inc. and analyzed as an AMS sample. An optically stimulated luminescence sample was taken 5 m from the top of the pit wall. Also, a greenish-gray coarse sand sample was collected for geochemical and petrographic analyses. (See Appendices A, B and E for further information on this sample.)	x (photo 63)	47.69238733 (approx. N47°41'34.3")	-121.96427149 (approx. W121°57'54.2")	T26N	R7E	31	X (see site 11-44D)	X (see site 11-44D)	NONE	X	Ancient Snoqualmie River alluvium in the Carnation 7.5-minute quadrangle. Medium to fine, well sorted alluvial sand from outcrop with faults along the SVF-3. (See Optically Stimulated Luminescence and radiocarbon ages.) Sand is polymictic with significant monocrystalline quartz, plagioclase and potassium feldspar and lesser but significant granitic lithics. Lithics are variable in composition and include volcanic and metamorphic clasts. Granitic lithic grains are commonly contain both quartz, potassium feldspar, and (or) plagioclase indicative of a true granite source (that is, parts of the Snoqualmie batholith). Other noted grains include phyllite, meta-argillite, pyroxene and serpentinite.	x			x	x	15			ancient Snoqualmie river provenance sand	5.15	99.95	0.79

Site-sample no.	Geologic unit	General sample site notes	Digital photos (Appendix E)	Sample locations					OSL/IRSL age (Appendix B)	Radiocarbon age (Appendix A)	Rock sample geochemistry	Sand sample geochemistry	Thin-section, geochemistry and additional site notes										Sieve weights for sand geochemistry samples		
				Latitude	Longitude	Township	Range	Section					Petrography notes	hornblende	augite	hypersthene	plagioclase	quartz (free)	% kspar	% mica	other minerals	rock name thin section	Weight (g) on sieve no. 10 (pebbles)	Weight (g) on sieve no. 200; chem sample sent	Weight (g) below sieve no. 200 in pan (silt and/or clay)
11-22E	Qc_{ws}	Site 22E is located in a private driveway roadcut northwest of the Tolt River near the western edge of the Lake Joy 7.5-minute quadrangle. The cutbank exposes very compact and distinctly tilted micaceous sand, silty sand, and thin- to medium-bedded peat. Some thin clay beds occur in the peat beds. The beds are well-stratified and represent ancient Snoqualmie River alluvium overbank deposits. Within peat beds, localized larger pieces of flattened charred bark were removed. The bark was fragmented and microscopically cleaned to remove any potential modern organics including rootlets before being sent to Beta Analytic Inc. for radiometric analyses. Also, a light yellowish brown coarse sand sample was collected for geochemical and petrographic analyses. (See Appendices A and B for further information on this site.)	NONE	47.67399332 (N47°40.440')	-121.86310158 (W 121°51.786)	T25N	R7E	1	X (see sites 11-44C-1 and 11-44C-2)	X	NONE	X	Typical ancient Snoqualmie River provenance sands with much monocrystalline quartz, plagioclase and potassium feldspar with some biotite and hornblende grains. Volcanic lithic grains dominate the lithic grain population. Mineral rich with some volcanic and granitic lithic grains as well as a few sedimentary or meta-sedimentary lithic grains. Weathering products in fine-grain fraction thus geochemistry should be interpreted with some caution. Monocrystalline quartz content is high and monocrystalline quartz distinctly greater than polycrystalline quartz consistent with ancient Snoqualmie River alluvium compositions observed regionally. Meta-argillite seems low suggesting contribution of clasts from the east along ancient Tolt River routes is limited or has been swamped by ancient Snoqualmie River provenance detritus.						15			ancient Snoqualmie river provenance sand	10.99	210.9	9.11
11-22J	Qc_{hmp}	Site 22J is located on the south side of the Tolt River near the western edge of the Lake Joy 7.5-minute quadrangle. The cutbank exposes very thickly bedded cobble gravel with beds of silt. Beds are very compact and mostly contain subrounded cobbles in a dark green sandy matrix. The gravels locally contain thick beds of laminated gray silt and silty fine sand. The gravel is volcanic-rich and contains ~40% andesite, ~10% basalt and basaltic andesite, and ~50% other clast types. Most basalt clasts have little to no rind, however, many andesitic clasts are rotten and some can even be cut in half with a geopick. Petrographic examination of the unit sands indicates significant weathering of this deposit overall. Unit Qoa boulder gravel unconformably overlies this ancient Tolt River alluvium. A coarse sand sample was collected for geochemical and petrographic analyses.	NONE	47.67631017	-121.8507462	T25N	R7E	1	NONE	NONE	NONE	X	This poorly sorted sand is weathered and has fine-grained weathering products. Clasts variable with volcanic, meta-sandstone and meta-argillite lithic clasts as well as granitic grains. Contains much hornblende, some pyroxene, monocrystalline quartz, plagioclase with some polycrystalline quartz, biotite, epidote and chlorite. Many of the fine-grains are likely weathering products for this sandy deposit. Hornblende and the biotite appear to be dominantly from the Mount Persis volcanic rocks and encased in volcanic lithics in a few cases. The degree of alteration of some of the volcanic rocks of Mount Persis observed petrographically might have contributed to the chlorite and epidote observed in these ancient alluvium sands.	x	x		x	x	2			ancient Tolt river alluvium	96.17	246.97	0.68
11-23D	Evt_p	Site 23D is located along a logging road along a steep slope directly east of Hull Lake in eastern portion of the Lake Joy 7.5-minute quadrangle. The roadcut exposed several lithologies but is dominated by semi-vesiculated vitric tuff that is light green in color. Also exposed is an aphanitic basalt flow with circular to ellipsoidal vesicles (up to 4-5 cm long). The vitric tuff is possibly bedded as defined by possible compositional bands several centimeters in thickness, as well as probably flow-aligned crystals. Some compositional bands contain pumice inclusions. A moderate bedding dip to the northeast is consistent with vesicle alignment in interbedded basalt. A light bluish-gray rock sample was collected for geochemical and petrographic analyses.	NONE	47.65906088 (N 47°39.544')	-121.7901745 (W 121°47.411)	T25N	R8E	9	NONE	NONE	X	NONE	Contains subhedral to euhedral plagioclase grains to 1 mm in a light greenish matrix of glass and small plagioclase crystals. No mafic minerals preserved. Calcite replacement of the plagioclase and matrix is locally strong with perhaps some fine chlorite thus geochemistry should be interpreted with caution. Contains many rounded to flattened vesicles filled with quartz or calcite. Flattening is likely subparallel to the bedding measured in the field. Some anhedral masses to few millimeters may be replaced felsic lithic grains (thus the sample may contain a small percentage of replaced pumice) but the masking by the replacement products is strong and thus these may be vesicles or replaced minerals. Protolith is felsic with no evidence of replaced mafic minerals.					x		0			"altered" crystal tuff			
11-23P	Eva_{pd}	Site 23P is located in the eastern part of the Lake Joy 7.5-minute quadrangle, northeast of Hull Lake but west of Tokul Creek. It is a cliff exposure of a dark-gray basaltic andesite or andesite flow. This flow contains a small percent of phenocrysts along with a few dark mafic minerals; the rock mostly consists of a dark gray glassy matrix. Possible friable or crumbly flow top texture suggests that the flow dips to the southeast. A dark-gray to reddish-black rock sample was collected for geochemical and petrographic analyses.	NONE	47.66824619	-121.7785185	T25N	R8E	10	NONE	NONE	X	NONE	Is homogeneous basaltic andesite to andesite flow with much carbonate and calcite replacement of the matrix and grains. Some grains partially replaced and recognizable as subhedral to euhedral phenocrysts of plagioclase or augite. Geochemical analyses of these rocks should be viewed with suspicion given the significant replacement of this volcanic rock. Subrounded carbonate and chlorite filled vesicles observed. Chlorite replaces probable mafic minerals as well as parts of the semi-opaque matrix. Some microlitic blades are observable in the dark-green and variable matrix. The inhomogeneous nature, alteration and vesicles suggests flow top sample.		?		x		0			"altered" andesite to basaltic andesite flow?			
11-25C	Qa	Site 25C is located on the Tolt River directly downstream from where the north and south forks merge to form the Tolt River. At this site we sampled well-sorted modern Tolt River alluvial sand from a channel deposit on a boulder cobble gravel point bar. A bluish-gray coarse sand sample was collected for geochemical and petrographic analyses.	NONE	47.68585766	-121.8374234	T25N	R8E	6	NONE	NONE	NONE	X	Tolt River alluvium from point bar. Well sorted coarse to very coarse lithic sand. Lithic rounded sand grains with granite, metachert, metasandstone, meta-argillite, and volcanic lithic grains. Some granitic lithic grains contain potassium feldspar grains with hornblende, plagioclase, and quartz. Radiolarians observed in the metachert grains. Although this very coarse sand is distinctly lithic grain rich, also observed a few grains of monocrystalline quartz, polycrystalline quartz, and plagioclase. Potassium feldspar noted in one granitic lithic with plagioclase and quartz. No high-grade metamorphic lithic grains or foliated aggregates observed and the sand has a strong local easterly provenance much like the recessional outwash deposits. Alteration is extremely low and geochemistry sample good for analyses.	X			X	X	1			Tolt River alluvial sand	21.51	188.14	2.39

Site-sample no.	Geologic unit	General sample site notes	Digital photos (Appendix E)	Sample locations					OSL/IRSL age (Appendix B)	Radiocarbon age (Appendix A)	Rock sample geochemistry	Sand sample geochemistry	Thin-section, geochemistry and additional site notes									Sieve weights for sand geochemistry samples		
				Latitude	Longitude	Township	Range	Section					Petrography notes	hornblende	augite	hypersthene	plagioclase	quartz (free)	% kspar	% mica	other minerals	rock name thin section	Weight (g) on sieve no. 10 (pebbles)	Weight (g) on sieve no. 200; chem sample sent	Weight (g) below sieve no. 200 in pan (silt and/or clay)
11-25F	Qa	Site 25F is located on a large gravel bar on the Tolt River in the western part of the Lake Joy 7.5-minute quadrangle. Samples at the site consisted of clean coarse sand from a modern alluvial gravel bar. A bluish-gray coarse sand sample was collected for geochemical and petrographic analyses.	NONE	47.68043457	-121.8455141	T25N	R7E	1	NONE	NONE	NONE	X	Tolt River coarse sand alluvium sample site. Sands here finer and decidedly more mineral rich and variable than sample 25C. Polymictic sand with volcanic, and meta-sedimentary lithics with some granitic lithics and metachert. Contains some monocrystalline quartz, polycrystalline quartz, and plagioclase with some potassium feldspar in the granitic lithics. Noted a few foliate high grade metamorphic lithics and greenstone. Also contain distinct metachert grains likely from the western mélange belt. Metasandstone, metasiltstone and volcanic clasts dominant the lithic grain population. Consistent with the Holocene age of this sand, no evidence of extensive weathering noted for the grains such as clayification of many mineral and lithic grains. (Compare with ancient Tolt River alluvial sand samples.)				x	x	2			alluvial sand Tolt River	14.39	202.34	0.048
11-27W	Evb_p	Site 27W is located near the eastern edge of the Lake Joy 7.5-minute quadrangle. Massive dark basalt in this quarry has multiple fault-gouge zones up to 1 m thick that define near vertical faults. Northwest-dipping joints were also present. A dark bluish-gray basalt sample was collected for geochemical and petrographic analyses.	NONE	47.68937529 (N 47°41'21.8")	-121.75593392 (W 121°45'21.4")	T26N	R8E	35	NONE	NONE	X	NONE	Flow on the eastern edge of the Lake Joy 7.5-minute quadrangle with the same holocrystalline texture as other basalts. Contains aligned elongate blades of plagioclase with sugary subhedral to anhedral grains and phenocrysts of augite. Most augite is interstitial. Rock contains little glass and disseminated small opaque mineral grains with interstitial grains or masses of green pleochroic hornblende. (The apparent moderate birefringence and pleochroism of these anhedral masses suggests chloritized equivalents in other basalts are likely hornblende as previously suggested.) Some of the hornblende occurs as small prismatic pleochroic brown green minerals. Some sugary grains of epidote after plagioclase. Brownish green small biotite also evident. Amount of alteration is relatively low and thus the geochemistry rocks are probably reflective of primary volcanic processes and not late alteration.	x	x		x		0	x	biotite?	"altered" basaltic andesite or basalt flow			
11-28C	Eva_{pd}	Site 28C is located on the south side of the Tolt River near the western edge of the Lake Joy 7.5-minute quadrangle. This basalt crops out directly north of the CF-1 mylonites on the Tolt River. This outcrop along the river exposes highly jointed, dark-gray basaltic andesite (outcrop in and above the water). It is aphanitic basaltic andesite. A dark greenish-gray rock sample was collected for geochemical and petrographic analyses.	NONE	47.67014444 (N 47°40'12.5")	-121.85736199 (W 121°51'26.5")	T25N	R7E	12	NONE	NONE	X	NONE	Typical crystal rich basalt with euhedral phenocrysts of plagioclase to 1 mm with microlitic plagioclase in the matrix. The glass matrix is clear. Also contains subhedral to euhedral phenocrysts of augite and hypersthene. Opaque minerals are disseminated through the sample. The glomerophyric texture of one plagioclase phenocrysts contains a long euhedral blade of light to dark green pleochroic hornblende. Some grains are replaced by brown low-birefringent mats that are likely chlorite, but mostly the rock has low alteration and is good for geochemistry. It is noteworthy here that the deformation of the basalt is low.	x	x	x	x		0			basaltic andesite or basalt flow north of CF no. 1			
11-32F	Eva_p	Site 32F is located in the northern most part of the Lake Joy 7.5-minute quadrangle near the Sultan 7.5-minute quadrangle. It is a well-exposed outcrop of blocky jointed andesite with scattered small plagioclase and mafic mineral phenocrysts in a gray glassy matrix. The outcrop is generally unsheared and has low weathering resulting in a good exposure and clean samples. A dark-gray andesite sample was collected for geochemical and petrographic analyses.	NONE	47.74414969	-121.8091708	T26N	R8E	17	NONE	NONE	X	NONE	Homogeneous andesite or basaltic andesite with euhedral blades of plagioclase as well as euhedral blades of augite in a clear glass with microlites of plagioclase. Few zoned plagioclase grains up to 3 mm. Good phenocrysts of hornblende have green pleochroism but have been mostly chloritized. Fine disseminated opaque minerals pervade the rock. Alteration is generally low (see geochemistry). Flow alignment of phenocrysts is distinct. Hypersthene grains not observed amongst pyroxene. Texturally the rocks similar to other volcanic flows observed in the field area. Pleochroism and crystal form indicates definitive hornblende in this flow and suggests other chloritized masses observed in previous petrography from the study area are also likely hornblende.	x	x		x		0			andesite or basaltic andesite			
11-32K	Ei andesite	Site 32K is located along an old logging road in the northeastern corner of the Lake Joy 7.5-minute quadrangle. The steep road cuts have created a 200 m long by 5 m high exposure of bedrock. The layered andesite, basaltic andesite or basalt and gabbro probably form an intrusive complex. The dark andesite or basaltic andesite contain small scattered plagioclase. Gabbro texture with centimeter thick compositional banding observed locally. A greenish/bluish-gray andesite sample was collected for geochemical and petrographic analyses.	NONE	47.73800701	-121.7984005	T26N	R8E	16	NONE	NONE	X	NONE	This aphanite has strong alignment of the plagioclase microlites and small phenocryst grains probably as a result of intrusive emplacement within the complex. Very thin shear zone bands with mylonites being parallel to the mineral alignment. Opal, chlorite, and some epidote are the result of definitive secondary alteration (see geochemistry) possibly by magmatic fluids. Mafic minerals are largely chloritized or replaced by epidote(?) although one remaining pyroxene maybe augite or hypersthene. The planar shearing and variable grain reduction along with the variable alteration gives the rock an unorganized appearance.	?	?	?	x		5			"altered" Ei basaltic andesite			
11-32L	Ei gabbro	Site 32L is located along an old logging road in the northeastern part of the Lake Joy 7.5-minute quadrangle. This 200 m long by 5 m high roadcut exposure locally contains gabbro. Definite banding foliation or layering on a centimeter to many centimeters scale was observed in the gabbro. There were many variable textures along the outcrop; contact with basalt from site 32K appears to be intrusive, with layers of fine-grained aphanite to localized pockets or layers of gabbro. This is a probable intrusive complex believed to be at least 100 ft thick. A light greenish-gray rock sample was collected for geochemical and petrographic analyses.	NONE	47.73841278 (N 47°44'18.3")	-121.79912813 (W 121°47'56.9")	T26N	R8E	16	NONE	NONE	X	NONE	Rock has been almost completely altered to chlorite, potassium feldspar, zeolites, opaline like masses, or secondary quartz. Outlines of plagioclase blades cloudy and altered. The rock is likely altered during magmatic intrusion within magmatic fluids. Geochemical analyses should be interpreted with distinct caution. Few original grains remain and the rock is strongly replaced.				?		2			gabbro (completed altered)			

Site-sample no.	Geologic unit	General sample site notes	Digital photos (Appendix E)	Sample locations					OSL/IRSL age (Appendix B)	Radiocarbon age (Appendix A)	Rock sample geochemistry	Sand sample geochemistry	Thin-section, geochemistry and additional site notes									Sieve weights for sand geochemistry samples		
				Latitude	Longitude	Township	Range	Section					Petrography notes	hornblende	augite	hypersthene	plagioclase	quartz (free)	% kspar	% mica	other minerals	rock name thin section	Weight (g) on sieve no. 10 (pebbles)	Weight (g) on sieve no. 200; chem sample sent	Weight (g) below sieve no. 200 in pan (silt and/or clay)
11-34N	Eva_p	Site 34N is located in the south central part of the Lake Joy 7.5-minute quadrangle directly east of Griffin Creek. Aphanitic volcanic outcrop with no plagioclase or microcrystalline minerals observable in hand-sample. Rock is massive with box jointing. Nearby sites suggest a dip slope to the west. A dark bluish gray andesite sample was collected for geochemical and petrographic analyses.	NONE	approx. N47 38'57.5"	approx. W121 49'12.9"	T25N	R8E	17	NONE	NONE	X	NONE	Homogeneous, nearly holocrystalline flow with euhedral to subhedral phenocrysts of plagioclase, hypersthene, and hornblende in a clear, organized glassy matrix with many microlites of plagioclase. Few small euhedral to subhedral augite grains. Fine opaque disseminated in the rock. Hornblende occurs as chloritized blades that also may be converted to biotite. Slight green pleochroism and lines of chlorite replacement common in the hornblende. Overall alteration is low for geochemical analyses. Grains somewhat aligned as a result of flow.	x	x	x	x		0			andesite flow			
11-35U	Qgof	Site 35U is located in a sand and gravel borrow pit along the south central edge of the Lake Joy 7.5-minute quadrangle. The pit walls expose bedded Vashon recessional (fluvial) outwash with distinct subhorizontal bedding and consists mostly of coarse sand, pebble gravel, and cobble pebble gravel. This fluvial outwash is locally deposited as high energy deposits (glacial outwash floods?) due to the boulders (up to ~1 m) in the highest portion of the exposed strata. A dark olive brown fine sand sample was collected for geochemical and petrographic analyses.	NONE	47.62842528	-121.7927707	T25N	R8E	28	NONE	NONE	NONE	X	Lithic rich (~60%) recessional outwash sand. Lithic sand compositions are variable. Lithic types from the northeast evident including mélange belt lithic types. The distinct occurrence of monocrystalline quartz, potassium feldspar, hornblende, pyroxene and granitic lithics is also consistent with a local Cascade derivation and clasts from the Grotto and Index batholiths to the northeast. The most distinctive lithic grains are foliate meta-argillite and meta-sandstone from the western mélange belt as well as few serpentinite grains. The granitic lithics also contain potassium feldspar and mafic minerals such as hornblende. Pleochroic green hornblende is distinct in the population and most likely primarily from the Tertiary intrusive rocks to the northeast. The dark color noted in the field is likely from the significant amount of meta-argillite from the western mélange belt observed petrographically in these sands. Western mélange belt sources and granitic lithics and grains are greater than the local Mount Persis volcanic lithic grains which is somewhat surprising given the volume of Persis unit exposed near the sand sample site.	x			x	x	4			recessional outwash sands	3.06	147.97	0.15
11-37R	Ei gabbro	Site 37R is located along an old logging road toward the northeastern portion of the Lake Joy 7.5-minute quadrangle. This outcrop was part of the intrusive complex observed at site 32K. It consisted of gabbro with mafic dikes and sills. There were also thin faults with reddish-orange alteration, some appear pegmatitic or compositionally banded. The gabbro has variable textures with mafic knots or similar, measuring 1-4 cm thick in some places. A greenish-gray rock sample was collected for geochemical and petrographic analyses.	NONE	47.73818705	-121.7866199	T26N	R8E	16	NONE	NONE	X	NONE	Rock is altered like other gabbro thin section sample but this rock contains distinct phenocryst ghost grains, but all are completely to almost completely altered to chlorite, calcite or locally epidote. Geochemical analyses should be interpreted with high caution because of the high degree of alteration of this sample. Some epidote grains are subhedral and relatively large. Some phenocrysts are completely altered to a mat of alternating calcite, chlorite and epidote. Grains and masses of opaque minerals are scattered around the slide and likely include sulphide minerals.						0			"altered" gabbro (strong altered or metasomatized) and tzh zone			
11-38AH	Qc_{hmp}	Site 38AH is located at the top of a very steep forested slope directly south of where the Tolt River south and north forks meet in the Lake Joy 7.5-minute quadrangle. Landslide scars along this steep slope expose mostly clast-supported, compact cobble gravel. The gravel has a sandy matrix that was sampled for petrography and geochemistry. The gravel is dominated by volcanic rock types and contains ~90% basalt, andesite, and basaltic andesite clast types. Weathering is low for the gravel component of the deposits but this is likely due to the stratigraphic position (high elevation on a steep slope) and location below an impermeable till layer. Volcanic-rich clast composition, compaction, and weathering of the coarse sand matrix observed petrographically indicate that this is likely a fluvial deposit of ancient Tolt River alluvium.	NONE	47.69201199	-121.816882	T26N	R8E	32	NONE	NONE	NONE	X	Medium to very coarse lithic sand containing mostly volcanic lithic grains (~75% by volume). Other clasts include several grains of pyroxene; also contains few granitic lithic grains (with potassium feldspar and hornblende in a few grains), meta-argillite, plagioclase, monocrystalline quartz, metachert, hornblende, opaque minerals, grains of weathering products, and epidote. This fluvial channel deposit and contains mostly lithic grains with some mineral fragments. Distinct ancient Tolt River provenance dominated by local volcanic rocks of Mount Persis with some western mélange belt and granitic detritus. Ancient alluvium sand here is less weathered because of position at the steep slope apex and occurrence under impermeable till. Thus weathering is lower than most ancient Tolt River alluvium and the geochemical signature should be relatively good.	x	x	x	x	x	3			sand matrix to cobble gravel	67.2	22.19	0.03
11-39D	Qc_{ws}	Site 39D is located in the hills directly south of the Tolt River on the western edge of the Lake Joy 7.5-minute quadrangle. This 3-m-high cutbank exposes thickly bedded micaceous ancient Snoqualmie River basin provenance silt, silty fine sand, fine sand, and medium sand. A light yellowish-brown coarse to fine sand sample was collected for geochemical and petrographic analyses.	NONE	47.67265691	-121.8446624	T25N	R7E	1	X (see site 11-44A-1 and 11-44A-2)	NONE	NONE	X	Definitive ancient Snoqualmie River provenance. Ancient Snoqualmie River alluvium medium sand with some fine sand grains. Mostly monocrystalline quartz, plagioclase with lesser potassium feldspar, hornblende, biotite and much pyroxene. Volcanic lithic rich with few but distinct granitic lithics (with internal potassium feldspar). Only a few other polycrystalline quartz and other lithic types are minor thus distinct ancient Snoqualmie River provenance. Grain size (sands, silts, peats) and composition consistent with ancient Snoqualmie River provenance. Volcanic lithic volume suggests contribution to ancient Snoqualmie River provenance in this area by the ancient Tolt River system, but the general lack of western mélange belt lithic grain types (meta-argillite, etc., very low %) suggests the contribution was muted by ancient Snoqualmie River sedimentation. Some alteration products around grains but generally clay weathering products are low for this ancient alluvium sample.	x			x	x	12			sand	0.41	527.65	3.65

Site-sample no.	Geologic unit	General sample site notes	Digital photos (Appendix E)	Sample locations					OSL/IRSL age (Appendix B)	Radiocarbon age (Appendix A)	Rock sample geochemistry	Sand sample geochemistry	Thin-section, geochemistry and additional site notes										Sieve weights for sand geochemistry samples		
				Latitude	Longitude	Township	Range	Section					Petrography notes	hornblende	augite	hypersthene	plagioclase	quartz (free)	% kspar	% mica	other minerals	rock name thin section	Weight (g) on sieve no. 10 (pebbles)	Weight (g) on sieve no. 200; chem sample sent	Weight (g) below sieve no. 200 in pan (silt and/or clay)
11-41D	Mzoig	Site 41D is located in the southeast portion of the Lake Joy 7.5-minute quadrangle directly east of Tokul Creek. An outcrop along an old logging road exposes medium-grained felsic intrusive rock. The rock is holocrystalline, olive green, and contains chloritized mafic minerals with dark inclusions. An outcrop directly south of the intrusive rock is 10 m high and contains millimeter-sized grains of plagioclase, as well as mafic minerals with chloritic alteration, and may be Western mélange belt wall rocks near the intrusive rocks. A dark-gray rock sample was collected for geochemical and petrographic analyses.	NONE	47.64407949	-121.7590874	T25N	R8E	15	NONE	NONE	X	NONE	Definitive medium grained granite with much plagioclase (35%), potassium feldspar (25%), and quartz (25%) with lesser hypersthene with some grains of reddish brown biotite (5%) and possible few grains of white mica (1%). Some plagioclase replaced by grains of epidote (mostly xenomorphic). Few green pleochroic grains within quartz may be anhedral grains of hornblende but unsure, and mostly chloritized plus minor in volume. (These small amphiboles might be secondary and likely not part of intrusive assemblage.) Some white mica contains dark bands suggestive of sedimentary lithic grains but likely fine opaque grains intergrown with white mica. Few small opaque grains. Overall rock is low in mafic mineral and quartzofeldspathic in composition. Alteration is generally low and the geochemistry should be indicative of the intrusive composition. Grains generally euhedral and equidimensional and overall is hypidiomorphic granular intrusive texture.	?			x	x	25		biotite and white mica	"altered" granite to granodiorite			
11-42E	Qga_v	Site 42E is a debris-flow landslide scar on a forested steep slope directly northwest of the Tolt River on the western edge of the Lake Joy 7.5-minute quadrangle. This landslide scar exposes moderately compact, coarse sand and pebble gravel with a few cobbles and interbedded thick to thin beds of silty sand and fine sand. Roughly 30% of clasts are andesite, basaltic andesite, or andesite with 60% exotic clasts, such as granite, meta-argillite, and other Western mélange belt provenance clasts. The clast composition implies significant local, but variable provenance. Gravel clasts had rinds as thick as 1.5 mm. Stratigraphic position and stratigraphic and sedimentologic information from nearby sites, as well as the overall provenance, suggest Vashon advance outwash at this site with a contribution of detritus from older nonglacial units. (See petrographic notes for example.) A very pale brown gravely sand sample was collected for geochemical and petrographic analyses.	NONE	47.67032918	-121.8692875	T25N	R7E	11	NONE	NONE	NONE	X	Probable advance outwash for samples 42E and 42F along western edge of the Lake Joy 7.5-minute quadrangle. This medium grained sand is polymictic with variety of lithic grain including granitic, metamorphic, sedimentary, and volcanic clast types. Monocrystalline quartz, polycrystalline quartz and plagioclase are distinct with some potassium feldspar included in granitic clasts. Volcanic lithics dominant and monocrystalline quartz and polycrystalline quartz roughly equal in abundance. Some pyroxene and hornblende grains. Some characteristics of older non-glacial deposits like slightly elevated potassium feldspar content but could be the result of deposition atop definitive ancient Snoqualmie River alluvium (unit Qc_{ws}). (Scouring of older non-glacial unit.)	x	x		x	x	4			gravelly sand	92.22	135.47	1.86
11-42F	Qga_v	Site 42F is located in the hills directly northwest of the Tolt River on the western edge of the Lake Joy 7.5-minute quadrangle. It is a small landslide scarp exposure of compact coarse sand with gravel to gravely sand. Clasts were variable and polymictic with low apparent weathering, which suggests advanced outwash. There was no apparent rind on basalt gravel clasts. An olive-yellow coarse sand sample was collected for geochemical and petrographic analyses.	NONE	47.67075095	-121.8691539	T25N	R7E	11	NONE	NONE	NONE	X	Probable advance outwash for 42E and 42F along western edge of the 7.5-minute quadrangle. Some characteristics of older non-glacial deposits, such as slightly elevated potassium feldspar content but could be the result of deposition atop definitive ancient Snoqualmie River alluvium (unit Qc_{ws}). Polymictic sand much like 42E with variable clasts, monocrystalline quartz, polycrystalline quartz, potassium feldspar and plagioclase. Like 42E contains more lithic grains than minerals. Some granitic clasts with potassium feldspar.						3			sand	1.95	213.14	3.55
11-43C	Eva_{pd}	Site 43C is located in the hills directly east of the Tolt River in the Lake Joy 7.5-minute quadrangle. At the bottom of a steep hillside, an accumulation of talus (along with possible in-place bedrock) consisted of basaltic andesite composed dominantly of dark-gray glass with scattered small yellow phenocrysts of plagioclase and small mafic grains. The outcrop was generally unweathered and massive. A dark bluish-gray rock sample was collected for geochemical and petrographic analyses.	NONE	47.66683292 (N 47°40'00.6")	-121.85082176 (W 121°51'03")	T25N	R7E	12	NONE	NONE	X	NONE	Homogeneous basaltic andesite with phenocrysts of euhedral plagioclase, smaller subhedral phenocrysts, and grains of augite and hypersthene (straight extinction from several sections) in a clear and unaltered glass with many microlites of plagioclase and disseminated grains of opaque minerals. No flow features or vesicles and very organized with no alteration indicating the rock is adequate for geochemical interpretation. (No secondary minerals observed petrographically.) The lack of any mylonitization or shear indicates the mylonites associated with CF-1 is north of these small flow outcrops. Dark color of these flows in the field suggested basaltic andesite but geochemistry of the samples suggests andesite.		x	x	x		0			basaltic andesite flow			
11-44A-2	Qc_{ws}	Site 44A-2 is east of site 44A-1. This 3 x 3 m exposure was excavated out of the 4-m high logging road cut. The exposure revealed thickly bedded silt, silty fine sand, fine sand, and medium sand. The exposure contains distinct beds of medium sand that are micaceous and have an ancient Snoqualmie River basin provenance. The OSL sample was collected at 217 cm below the soil surface. A brown fine sand sample was collected from site 39D for geochemical and petrographic analyses.(See sample 39D sand geochemical analyses for this site.)	NONE	47.67265264	-121.8442831	T25N	R7E	1	X	NONE	NONE	X	Definitive ancient Snoqualmie River provenance. Ancient Snoqualmie River alluvium medium sand with some fine sand grains. Mostly monocrystalline quartz, plagioclase with lesser potassium feldspar, hornblende, biotite and much pyroxene. Volcanic lithic rich with few but distinct granitic lithics (with internal potassium feldspar). Only a few other polycrystalline quartz and other lithic types are minor thus distinct ancient Snoqualmie River provenance. Grain size (sands, silts, peats) and composition consistent with ancient Snoqualmie River provenance. Volcanic lithic volume suggests contribution to ancient Snoqualmie River provenance in this area by the ancient Tolt River system, but the general lack of western mélange belt lithic grain types (meta-argillite, etc., very low %) suggests the contribution was muted by ancient Snoqualmie River sedimentation. Some alteration products around grains but generally clay weathering products are low for this ancient alluvium sample.	x			x	x	12				0.865	346.15	26.89
11-108C	Qc_{hmp}	Site 108C is located on the west bank of the South Fork Tolt River south of the Tolt Regulating Basin in the Lake Joy 7.5-minute quadrangle. The compact green silty sand sample was collected from a Tolt River bank erosion outcrop. Due to the high percentage of volcanic gravel clasts, it was inferred that this outcrop had local eastern provenance similar to other unit Qc_{hmp} outcrops. A light greenish-gray sample was collected for geochemical and petrographic analyses.	NONE	47.69304866	-121.7942641	T26N	R8E	33	NONE	NONE	NONE	X	Probable Qc_{hmp} volcanic rich old alluvium. Petrographically silty sand with strong local volcanic provenance and significant weathering of grains with weathering products part of fine-grained fraction. Weathering a problem for geochemical interpretation (see 9% LOI). Much silty or clayey material and volcanic alteration products with angular monocrystalline quartz, epidote and fragments that are likely volcanic lithic grains with chlorite. Difficult to separate alteration of the volcanic source area or clayification due to weathering of this ancient Tolt River alluvium as the source of the fines observed petrographically. Definitive weathering of unit Qc_{hmp} observed in the field with clayification of the sandy matrix of the fluvial sand and gravel units as well as distinct weathering rinds on basaltic clasts.						1			sand	142.54	130.68	9.57

Site-sample no.	Geologic unit	General sample site notes	Digital photos (Appendix E)	Sample locations					OSL/IRSL age (Appendix B)	Radiocarbon age (Appendix A)	Rock sample geochemistry	Sand sample geochemistry	Thin-section, geochemistry and additional site notes										Sieve weights for sand geochemistry samples		
				Latitude	Longitude	Township	Range	Section					Petrography notes	hornblende	augite	hypersthene	plagioclase	quartz (free)	% kspar	% mica	other minerals	rock name thin section	Weight (g) on sieve no. 10 (pebbles)	Weight (g) on sieve no. 200; chem sample sent	Weight (g) below sieve no. 200 in pan (silt and/or clay)
11-203E	Qgof	Site 203E is located on the north bank of the North Fork Tolt River directly south of Pipeline Rd in the Lake Joy 7.5-minute quadrangle. The site is a small landslide scar (1-2 m high) revealing a sequence of recessional outwash; this outwash fines upwards and is dipping slightly northeast. On the bottom is a very thickly bedded clast-supported cobble boulder gravel; the clasts are well rounded with some subrounded clasts. On top of the cobble boulder bed is a sandy gravel bed with subrounded to subangular pebbles. On top of this bed is a thick bed of coarsening upward silty sand to coarse sand with gravel. A light yellowish-brown sand sample was collected for geochemical and petrographic analyses.	NONE	47.70365202	-121.7991478	T26N	R8E	28	NONE	NONE	NONE	X	Well sorted recessional sand sample from a sand bed within unit Qgof. Polymictic sand with variable lithic grains from volcanic, granitic types with some metachert and metasedimentary lithic grains with a distinct easterly mélange belt provenance. Few high-grade metamorphic lithics. Some monocrystalline quartz, polycrystalline quartz, plagioclase and potassium feldspar including potassium feldspar in granitic lithic grains. Some pyroxene, pumpellyite, and epidote crystals. Here there is an extrabasinal component suggesting derivation from the Index batholith as a result ice-marginal melt water erosion. This provenance with a true granite component similar to other recessional outwash deposits derived from the northeast is consistently observed petrographically.		x		x	x	5			sand	0.049	103.18	2.75

Table C2. Geochemistry of selected samples from the Lake Joy quadrangle. All data listed below are not normalized. Please see Table C3 for the data that has been normalized on a LOI-free basis.

Sample	Unit	SiO_2	TiO_2	Al_2O_3	FeO^{T}*	MnO	MgO	CaO	Na_2O	K_2O	P_2O_5	LOI**	Total‡	Ni#	Cr#	Sc#	V#	La	Ce	Pr	Nd	Sm	Eu	Gd	Tb	Dy	Ho	Er	Tm	Yb	Lu	Ba	Th	Nb	Y	Hf	Ta	U	Pb	Rb	Cs	Sr	Sc	Zr	Zn#	Sample	Unit
11-1F	Eva_p	60.38	0.67	15.90	5.69	0.10	3.41	4.58	3.55	0.81	0.11	4.87	100.05	43	33	13	112	14.24	29.05	3.55	14.34	3.31	1.01	3.32	0.56	3.38	0.67	1.81	0.26	1.66	0.26	263	2.78	7.04	18	3.82	0.56	0.89	1.82	14	0.09	231	13.98	147	58	11-1F	Eva_p
11-1P†	Eva_{pd}	57.23	0.84	15.93	6.27	0.11	2.73	7.17	3.42	1.05	0.21	4.60	99.55	35	54	19	123	20.49	41.83	5.27	21.09	4.62	1.39	4.51	0.75	4.59	0.93	2.51	0.37	2.30	0.36	389	3.27	10.95	24	4.22	0.74	1.05	4.36	17	0.16	351	18.08	165	66	11-1P†	Eva_{pd}
11-1Q	Eva_{pd}	55.70	0.89	15.50	6.60	0.13	4.24	7.76	3.00	0.64	0.15	4.75	99.35	110	279	21	150	14.79	32.44	4.30	17.79	4.16	1.45	4.09	0.68	4.22	0.84	2.29	0.34	2.16	0.34	239	2.04	9.96	22	4.25	0.73	0.74	2.06	7	0.44	394	20.81	170	72	11-1Q	Eva_{pd}
11-4L	Eva_p	61.79	0.88	16.21	5.70	0.11	2.69	6.05	3.85	1.10	0.15	1.03	99.56	45	38	16	133	15.45	32.99	4.33	18.10	4.37	1.18	4.45	0.75	4.54	0.92	2.53	0.37	2.24	0.36	218	2.81	9.08	26	4.85	0.68	0.94	2.46	21	0.27	288	15.76	185	64	11-4L	Eva_p
11-4X	Eva_p	61.86	0.87	16.38	5.52	0.07	2.57	6.17	3.92	1.10	0.15	1.08	99.69	42	41	15	130	15.40	33.33	4.34	18.20	4.17	1.23	4.29	0.70	4.17	0.81	2.15	0.31	1.91	0.29	222	2.82	9.18	21	4.86	0.69	0.93	2.30	21	0.25	292	15.97	187	63	11-4X	Eva_p
11-9A	Eva_p	59.47	0.66	17.51	5.16	0.09	3.11	6.57	3.64	0.71	0.13	2.53	99.57	54	59	13	111	10.41	22.10	2.84	11.72	2.64	0.91	2.63	0.42	2.52	0.49	1.34	0.19	1.17	0.18	150	1.57	5.49	13	3.01	0.40	0.50	1.56	8	0.13	410	14.10	116	58	11-9A	Eva_p
11-9C	Eva_p	61.11	0.65	17.09	4.92	0.07	2.97	5.54	3.43	0.60	0.12	3.10	99.60	49	58	13	109	10.67	22.43	2.95	12.22	2.78	0.91	2.73	0.43	2.58	0.49	1.33	0.18	1.18	0.18	212	1.53	5.43	13	2.95	0.40	0.49	1.61	5	0.49	434	13.47	115	52	11-9C	Eva_p
11-13U	Qgod	68.64	0.58	14.04	4.34	0.08	2.19	2.29	2.68	1.24	0.09	3.73	99.92	46	96	13	100	11.70	26.05	2.82	11.15	2.52	0.81	2.43	0.43	2.61	0.54	1.49	0.22	1.40	0.22	443	2.97	5.54	13	2.75	0.42	1.01	5.79	32	1.33	227	12.92	102	57	11-13U	Qgod
11-14B	Qgod	62.71	0.78	15.44	6.36	0.11	3.13	3.68	2.78	1.21	0.14	3.53	99.86	75	212	19	140	13.95	29.55	3.88	15.97	3.84	1.15	3.92	0.66	3.96	0.81	2.18	0.32	2.04	0.33	370	3.31	7.18	21	3.54	0.52	1.16	6.93	32	1.72	244	18.64	131	79	11-14B	Qgod
11-14M	Eva_{pd}	58.79	0.86	15.09	6.09	0.09	2.82	4.86	4.16	0.98	0.22	5.57	99.56	64	82	15	97	13.29	28.85	3.73	15.35	3.53	1.19	3.48	0.58	3.48	0.69	1.85	0.26	1.66	0.26	238	1.17	10.12	18	3.29	0.67	0.35	1.18	15	0.41	436	15.00	136	69	11-14M	Eva_{pd}
11-15W	Eva_p	55.54	0.97	16.09	5.99	0.15	4.36	6.16	2.96	0.58	0.14	5.36	98.30	42	57	21	190	9.76	20.88	2.73	11.63	2.93	1.00	3.06	0.53	3.21	0.64	1.69	0.25	1.52	0.25	157	1.68	6.12	17	2.71	0.45	0.52	1.10	8	0.19	281	19.64	103	70	11-15W	Eva_p
11-16A	Qc_{hmp}	67.74	0.79	14.52	5.07	0.08	1.72	1.83	0.87	1.34	0.02	5.34	99.33	30	82	23	125	14.80	29.36	3.74	14.79	3.41	1.01	3.42	0.59	3.66	0.77	2.14	0.32	2.04	0.34	400	4.01	6.81	19	3.71	0.52	1.50	14.64	41	2.80	99	23.39	133	110	11-16A	Qc_{hmp}
11-19A	Eva_{pd}	52.85	0.96	17.26	7.68	0.13	4.86	7.41	2.79	0.29	0.21	4.85	99.29	94	164	19	152	11.84	26.51	3.55	15.13	3.71	1.32	3.96	0.67	4.08	0.82	2.23	0.32	2.01	0.31	106	1.31	9.36	21	3.45	0.63	0.46	0.62	3	0.70	251	19.40	136	68	11-19A	Eva_{pd}
11-19P	Evb_p	50.47	1.11	16.02	8.49	0.14	7.70	8.91	2.70	0.39	0.19	3.20	99.33	181	410	27	200	9.90	22.25	3.03	13.29	3.45	1.22	3.72	0.65	3.91	0.81	2.14	0.30	1.88	0.30	123	1.03	8.20	20	2.64	0.52	0.31	1.17	5	0.12	303	25.69	104	78	11-19P	Evb_p
11-20A	Qc_{pf}	73.58	0.45	11.48	3.40	0.07	2.09	2.57	2.81	1.04	0.10	2.15	99.75	65	128	11	77	9.48	19.15	2.49	10.41	2.41	0.79	2.46	0.42	2.57	0.55	1.52	0.22	1.40	0.23	409	2.03	3.67	14	2.21	0.27	0.90	5.06	24	0.80	247	10.44	81	44	11-20A	Qc_{ws}
11-22E	Qc_{ws}	70.84	0.54	14.38	2.66	0.04	0.74	1.74	2.19	1.96	0.04	4.24	99.36	10	25	12	70	15.77	31.26	3.77	14.33	3.18	1.00	3.07	0.53	3.25	0.67	1.92	0.28	1.85	0.29	559	5.55	6.48	17	3.90	0.53	1.86	8.96	56	2.43	166	11.85	141	60	11-22E	Qc_{ws}
11-22J	Qc_{hmp}	67.00	0.99	14.32	3.88	0.10	1.92	2.12	1.20	1.22	0.03	6.19	98.96	28	101	23	141	17.92	36.72	4.52	18.22	4.03	1.11	4.04	0.68	4.22	0.88	2.47	0.36	2.32	0.37	360	4.39	7.91	22	4.46	0.59	1.76	17.95	37	2.50	124	23.91	161	94	11-22J	Qc_{hmp}
11-23D	Evt_p	52.14	0.76	15.39	5.21	0.08	4.64	7.20	2.35	0.43	0.11	10.44	98.74	92	156	20	129	9.84	20.60	2.61	10.62	2.57	0.90	2.69	0.46	2.79	0.56	1.46	0.20	1.23	0.19	69	1.16	6.49	14	2.59	0.44	0.38	1.11	11	1.01	242	19.77	104	52	11-23D	Evt_p
11-23P	Eva_{pd}	55.20	1.04	16.61	7.34	0.09	6.10	3.57	4.50	0.61	0.28	4.63	99.97	122	113	20	149	15.30	33.77	4.47	18.67	4.23	1.40	4.04	0.65	3.87	0.75	2.00	0.28	1.72	0.26	201	1.43	10.87	19	3.78	0.69	0.45	1.86	11	2.18	374	19.57	154	80	11-23P	Eva_{pd}
11-25C	Qa	66.08	0.74	14.57	5.46	0.09	2.41	2.76	2.63	1.16	0.12	3.89	99.90	46	64	15	117	14.50	29.14	3.74	14.86	3.40	1.00	3.33	0.56	3.40	0.69	1.94	0.28	1.79	0.29	335	3.25	7.83	18	3.74	0.61	1.07	7.14	29	1.20	222	14.54	139	84	11-25C	Qa
11-25F	Qa	66.53	0.72	14.18	5.42	0.09	2.38	2.81	2.73	1.16	0.12	3.37	99.50	44	55	13	114	14.06	28.40	3.59	14.37	3.24	0.99	3.28	0.56	3.46	0.72	1.97	0.29	1.80	0.28	332	3.20	7.54	18	3.71	0.59	1.06	6.26	28	1.14	225	14.39	140	82	11-25F	Qa
11-27W	Evb_p	52.92	0.94	15.25	7.02	0.12	3.29	9.40	2.98	0.65	0.14	6.59	99.29	110	265	22	162	13.25	29.39	3.88	16.38	3.83	1.35	3.96	0.68	4.21	0.85	2.35	0.35	2.23	0.37	184	1.87	9.18	22	3.97	0.67	0.69	1.14	8	0.17	437	21.31	157	71	11-27W	Evb_p
11-28C	Eva_{pd}	59.65	0.73	17.33	6.22	0.08	2.60	6.19	3.86	0.72	0.14	1.86	99.38	65	52	14	117	11.41	22.79	3.06	12.44	2.94	1.05	2.88	0.47	2.78	0.54	1.43	0.19	1.17	0.18	170	1.80	6.47	13	3.22	0.47	0.57	1.35	11	0.21	357	14.38	123	73	11-28C	Eva_{pd}
11-32F	Eva_p	60.02	0.776	16.69	6.11	0.101	3.73	6.86	3.47	0.49	0.162	1.56	99.97	54	91	17	124	11.70	25.56	3.32	13.85	3.32	1.05	3.41	0.56	3.42	0.68	1.82	0.26	1.63	0.26	157	1.75	7.82	17	3.34	0.54	0.59	1.88	8	0.10	301	15.56	130	72	11-32F	Eva_p
11-32K†	Ei	56.42	0.92	17.55	7.44	0.12	3.87	6.80	2.42	0.08	0.12	3.46	99.20	42	36	19	176	10.33	21.96	2.87	12.22	3.15	1.13	3.25	0.53	3.30	0.66	1.79	0.26	1.61	0.24	50	1.53	5.94	17	2.95	0.44	0.58	12.30	1	0.05	270	18.75	111	75	11-32K†	Ei
11-32L	Ei	54.12	1.01	20.25	5.81	0.15	2.43	6.05	3.32	1.59	0.13	4.41	99.27	37	50	20	151	15.54	31.66	4.14	17.85	4.75	1.60	5.44	0.90	5.31	1.07	2.90	0.41	2.55	0.39	429	2.36	8.11	30	3.76	0.57	0.79	19.65	33	0.30	306	20.94	144	110	11-32L	Ei
11-34N	Eva_p	60.66	0.73	17.79	4.89	0.10	2.41	6.31	3.86	0.92	0.14	1.55	99.36	21	17	13	116	12.44	24.47	3.05	12.39	2.74	0.97	2.64	0.42	2.48	0.47	1.25	0.18	1.17	0.18	223	1.88	6.47	12	2.91	0.47	0.62	1.96	14	0.13	476	13.02	115	69	11-34N	Eva_p
11-35U	Qgof	61.70	0.75	14.55	6.80	0.11	3.97	2.76	2.06	1.23	0.12	4.93	98.98	111	376	22	153	15.78	29.13	4.58	19.62	4.82	1.46	4.76	0.76	4.57	0.91	2.38	0.33	2.09	0.32	381	3.53	6.72	24	2.97	0.48	1.25	6.14	37	1.64	182	22.28	111	82	11-35U	Qgof
11-37R	Ei	55.15	0.95	16.18	8.25	0.10	4.35	5.64	2.52	0.36	0.13	5.92	99.54	60	72	18	164	12.13	25.16	3.22	13.14	3.16	1.26	3.21	0.53	3.18	0.62	1.68	0.24	1.52	0.23	99	1.88	6.17	16	2.96	0.47	0.60	2.51	8	0.75	240	17.53	112	27	11-37R	Ei
11-38AH	Qc_{hmp}	55.05	1.07	18.26	7.93	0.14	2.95	2.92	1.95	0.85	0.18	8.04	99.33	78	170	21	156	20.70	49.15	5.51	22.28	4.69	1.38	4.19	0.66	3.88	0.76	2.03	0.29	1.88	0.28	304	3.20	12.76	19	4.13	0.85	0.99	4.93	20	1.44	263	21.04	160	88	11-38AH	Qc_{hmp}
11-39D	Qc_{ws}	62.11	0.81	14.52	6.18	0.13	5.13	4.68	2.96	1.16	0.16	1.78	99.62	32	73	21	121	15.09	30.35	4.30	17.61	3.96	1.14	3.60	0.58	3.46	0.67	1.86	0.27	1.73	0.26	439	3.10	4.71	17	3.08	0.32	1.18	7.11	23	0.77	445	20.84	113	89	11-39D	Qc_{ws}
11-41D	~~M~~Øig	67.89	0.45	14.47	3.26	0.06	1.42	2.27	3.79	2.18	0.11	3.52	99.41	14	37	8	74	24.34	44.44	5.20	19.15	3.66	1.01	3.03	0.46	2.71	0.53	1.43	0.21	1.35	0.21	867	7.41	8.88	14	3.62	0.72	2.19	11.28	58	1.12	343	8.90	135	58	11-41D	~~M~~Øig
11-42E	Qga_v	64.88	0.73	14.54	5.57	0.11	2.39	3.30	2.83	1.20	0.14	3.66	99.35	40	87	18	127	16.57	31.31	4.31	17.46	4.10	1.22	4.11	0.67	4.11	0.82	2.23	0.32	2.02	0.33	351	3.47	7.10	22	3.27	0.54	1.15	6.68	31	1.38	240	16.91	123	75	11-42E	Qga_v
11-42F	Qga_v	65.48	0.73	14.08	5.35	0.10	2.09	3.00	2.70	1.16	0.12	3.77	98.59	38	94	16	122	15.79	30.02	4.09	16.33	3.66	1.09	3.67	0.62	3.77	0.75	2.07	0.30	1.91	0.28	356	3.55	7.16	20	3.25	0.55	1.20	6.50	31	1.34	232	16.08	122	70	11-42F	Qga_v
11-43C	Eva_{pd}	59.93	0.76	17.63	5.52	0.10	3.22	6.66	3.79	0.88	0.12	0.97	99.60	50	49	16	128	10.68	21.92	2.78	11.62	2.77	0.92	2.87	0.48	2.88	0.57	1.54	0.23	1.41	0.22	224	1.92	6.29	14	2.95	0.46	0.99	1.67	15	0.11	379	15.50	111	64	11-43C	Eva_{pd}
11-44A-2	Qc_{ws}	59.82	1.03	14.50	7.98	0.16	5.94	4.94	2.83	1.00	0.16	1.67	100.04	33	99	23	171	14.47	29.46	4.17	17.14	3.91	1.14	3.58	0.57	3.43	0.67	1.84	0.27	1.74	0.27	379	2.82	5.26	18	3.75	0.35	1.06	6.68	20	0.75	457	23.66	143	109	11-44A-2	Qc_{ws}
11-108C	Qc_{hmp}	62.94	1.10	16.45	5.06	0.04	1.27	1.34	0.44	1.15	0.03	9.09	98.91	43	111	17	134	23.46	41.74	5.55	20.96	4.42	1.20	4.02	0.66	3.90	0.77	2.13	0.32	2.00	0.32	274	4.36	12.54	20	4.76	0.92	1.30	9.06	39	2.61	107	16.81	182	80	11-108C	Qc_{hmp}
11-203E	Qgof	64.08	0.82	15.24	5.84	0.10	2.64	2.86	2.60	1.32	0.09	4.21	99.81	47	141	18	142	14.40	30.91	3.60	14.30	3.22	0.97	3.30	0.55	3.43	0.69	1.87	0.29	1.83	0.28	397	3.44	7.44	18	3.72	0.55	1.26	8.52	36	1.86	222	17.60	141	91	11-203E	Qgof

* All Fe reported as Fe^{2+}

**LOI = loss on ignition

‡Total is the sum of all major elements and LOI.

†X-ray fluorescence and inductively coupled plasma mass spectrometry is the average of two analytical runs for samples 1P and 32K.

#Ni, Cr, Sc, Zn are from X-ray fluorescence. All other trace elements were measured by inductively coupled plasma mass spectrometry.

Table C3. Normalized geochemistry of selected samples from the Lake Joy quadrangle. All data listed below have been normalized to 100% on a LOI-free basis. Please see Table C2 for the raw data and LOI values.

Sample	Unit	SiO_2	TiO_2	Al_2O_3	FeO^T*	MnO	MgO	CaO	Na_2O	K_2O	P_2O_5	CIA**	Ba	Rb	Sr	Y	Zr	Nb	Th	Pb	$Zn^{\#}$	Cu	$Ni^{\#}$	$V^{\#}$	$Cr^{\#}$	Hf	Cs	Sc	Ta	U	La	Ce	Pr	Nd	Sm	Eu	Gd	Tb	Dy	Ho	Er	Tm	Yb	Lu	Sample	Unit
11-1F	Eva_p	63.43	0.71	16.70	5.98	0.11	3.58	4.81	3.72	0.85	0.11	51.41	276	15	242	19	154	7.39	2.92	1.91	61	98	45	118	35	4.01	0.10	14.69	0.59	0.93	14.96	30.52	3.73	15.07	3.47	1.06	3.48	0.59	3.56	0.70	1.90	0.28	1.75	0.27	11-1F	Eva_p
11-1P†	Eva_{pd}	60.28	0.88	16.77	6.60	0.12	2.88	7.55	3.60	1.11	0.22	44.58	409	18	370	25	174	11.53	3.44	4.60	69	43	37	130	57	4.44	0.17	19.04	0.78	1.11	21.58	44.06	5.55	22.21	4.86	1.47	4.75	0.79	4.84	0.98	2.64	0.39	2.42	0.38	11-1P†	Eva_{pd}
11-1Q	Eva_{pd}	58.88	0.94	16.39	6.98	0.14	4.48	8.20	3.17	0.67	0.16	44.01	253	7	417	23	180	10.53	2.16	2.18	76	54	116	158	295	4.49	0.47	22.00	0.77	0.78	15.64	34.29	4.54	18.81	4.40	1.53	4.32	0.72	4.46	0.89	2.42	0.36	2.28	0.36	11-1Q	Eva_{pd}
11-4L	Eva_p	62.71	0.89	16.45	5.79	0.11	2.73	6.14	3.91	1.12	0.16	46.66	221	21	293	27	187	9.22	2.85	2.49	65	71	46	135	39	4.92	0.27	15.99	0.69	0.95	15.68	33.48	4.40	18.37	4.44	1.20	4.52	0.76	4.60	0.94	2.57	0.37	2.27	0.37	11-4L	Eva_p
11-4X	Eva_p	62.73	0.88	16.61	5.60	0.07	2.61	6.26	3.97	1.12	0.16	46.48	225	21	296	21	190	9.31	2.86	2.33	64	73	42	132	42	4.93	0.25	16.19	0.70	0.95	15.61	33.80	4.40	18.46	4.23	1.25	4.35	0.71	4.23	0.83	2.18	0.31	1.94	0.30	11-4X	Eva_p
11-9A	Eva_p	61.28	0.68	18.05	5.32	0.09	3.20	6.77	3.75	0.73	0.13	48.37	155	8	423	13	119	5.66	1.61	1.60	60	52	56	115	61	3.10	0.13	14.53	0.41	0.51	10.72	22.78	2.93	12.08	2.72	0.94	2.71	0.43	2.60	0.51	1.38	0.20	1.20	0.19	11-9A	Eva_p
11-9C	Eva_p	63.33	0.67	17.71	5.10	0.07	3.08	5.74	3.56	0.62	0.13	51.08	219	6	450	13	119	5.63	1.59	1.67	54	53	51	113	60	3.05	0.50	13.95	0.41	0.51	11.06	23.24	3.06	12.66	2.88	0.95	2.83	0.45	2.67	0.51	1.38	0.19	1.22	0.19	11-9C	Eva_p
11-13U	Qgod	71.36	0.61	14.60	4.51	0.08	2.28	2.38	2.79	1.29	0.10	58.60	460	33	236	14	106	5.76	3.09	6.02	60	43	48	104	100	2.86	1.38	13.44	0.44	1.05	12.17	27.09	2.93	11.59	2.62	0.84	2.53	0.45	2.72	0.56	1.55	0.23	1.46	0.23	11-13U	Qgod
11-14B	Qgod	65.10	0.81	16.03	6.60	0.11	3.25	3.82	2.88	1.25	0.15	55.15	384	34	253	22	136	7.46	3.44	7.19	83	84	78	145	221	3.68	1.78	19.35	0.54	1.20	14.48	30.67	4.03	16.58	3.99	1.20	4.07	0.69	4.11	0.84	2.26	0.33	2.12	0.34	11-14B	Qgod
11-14M	Eva_{pd}	62.56	0.91	16.06	6.48	0.10	3.00	5.17	4.43	1.04	0.24	47.41	253	16	464	19	145	10.77	1.25	1.25	74	170	68	103	87	3.50	0.43	15.96	0.71	0.38	14.14	30.69	3.97	16.34	3.76	1.27	3.70	0.62	3.71	0.74	1.97	0.28	1.76	0.28	11-14M	Eva_{pd}
11-15W	Eva_p	59.76	1.04	17.31	6.45	0.16	4.69	6.63	3.19	0.63	0.15	49.05	169	9	303	18	110	6.58	1.81	1.18	76	73	45	205	62	2.92	0.20	21.13	0.48	0.56	10.50	22.47	2.94	12.51	3.15	1.08	3.29	0.57	3.46	0.69	1.82	0.27	1.64	0.27	11-15W	Eva_p
11-16A	Qc_{hmp}	72.08	0.85	15.45	5.40	0.08	1.83	1.94	0.92	1.42	0.02	70.14	426	43	105	21	142	7.24	4.27	15.57	117	54	32	133	87	3.95	2.98	24.89	0.55	1.60	15.75	31.23	3.97	15.74	3.62	1.07	3.64	0.63	3.89	0.82	2.28	0.34	2.17	0.36	11-16A	Qc_{hmp}
11-19A	Eva_{pd}	55.97	1.02	18.28	8.13	0.13	5.15	7.84	2.95	0.30	0.22	48.47	113	3	266	22	144	9.91	1.39	0.66	71	37	100	161	174	3.65	0.74	20.54	0.67	0.49	12.54	28.08	3.76	16.02	3.93	1.40	4.19	0.71	4.32	0.87	2.37	0.34	2.13	0.33	11-19A	Eva_{pd}
11-19P	Evb_p	52.50	1.16	16.66	8.83	0.15	8.01	9.27	2.81	0.40	0.20	43.19	128	5	315	21	108	8.53	1.08	1.22	81	37	188	208	426	2.75	0.12	26.72	0.54	0.33	10.30	23.14	3.15	13.82	3.59	1.27	3.87	0.67	4.07	0.84	2.22	0.32	1.95	0.32	11-19P	Evb_p
11-20A	Qc_{pf}	75.39	0.46	11.76	3.49	0.07	2.14	2.63	2.88	1.07	0.10	52.41	420	25	253	14	83	3.76	2.08	5.19	45	20	67	79	131	2.27	0.82	10.69	0.28	0.92	9.71	19.62	2.55	10.67	2.47	0.81	2.52	0.43	2.63	0.56	1.56	0.22	1.43	0.24	11-20A	Qc_{ws}
11-22E	Qc_{ws}	74.48	0.57	15.12	2.79	0.04	0.77	1.83	2.31	2.06	0.04	61.77	587	59	175	18	148	6.82	5.84	9.42	63	25	10	73	26	4.10	2.56	12.46	0.55	1.95	16.58	32.86	3.96	15.06	3.35	1.06	3.22	0.56	3.41	0.70	2.02	0.30	1.95	0.30	11-22E	Qc_{ws}
11-22J	Qc_{hmp}	72.22	1.07	15.44	4.18	0.10	2.07	2.28	1.29	1.32	0.03	66.74	388	40	133	24	173	8.53	4.73	19.35	102	47	30	152	108	4.80	2.69	25.78	0.64	1.90	19.32	39.59	4.87	19.64	4.34	1.19	4.36	0.74	4.55	0.95	2.66	0.39	2.51	0.40	11-22J	Qc_{hmp}
11-23D	Evt_p	59.04	0.86	17.43	5.90	0.09	5.26	8.15	2.66	0.49	0.12	46.91	78	12	274	16	118	7.35	1.31	1.26	59	94	104	146	176	2.94	1.14	22.39	0.50	0.43	11.15	23.33	2.95	12.03	2.91	1.02	3.05	0.52	3.16	0.63	1.65	0.23	1.39	0.21	11-23D	Evt_p
11-23P	Eva_{pd}	57.90	1.09	17.42	7.70	0.10	6.40	3.75	4.72	0.64	0.29	53.28	211	11	392	20	162	11.40	1.51	1.95	83	58	128	156	118	3.96	2.29	20.52	0.72	0.48	16.04	35.42	4.69	19.58	4.44	1.47	4.24	0.68	4.06	0.78	2.10	0.29	1.80	0.27	11-23P	Eva_{pd}
11-25C	Qa	68.83	0.77	15.18	5.68	0.09	2.51	2.87	2.74	1.21	0.13	57.91	349	30	231	18	145	8.15	3.38	7.44	88	61	48	121	66	3.89	1.25	15.14	0.63	1.11	15.11	30.35	3.90	15.47	3.55	1.04	3.47	0.58	3.54	0.72	2.02	0.30	1.87	0.30	11-25C	Qa
11-25F	Qa	69.21	0.75	14.75	5.64	0.09	2.48	2.92	2.84	1.21	0.12	56.64	345	30	234	19	145	7.85	3.33	6.51	85	60	46	119	57	3.86	1.18	14.97	0.61	1.10	14.63	29.54	3.73	14.95	3.37	1.03	3.41	0.59	3.60	0.74	2.05	0.30	1.88	0.30	11-25F	Qa
11-27W	Evb_p	57.09	1.01	16.45	7.57	0.13	3.55	10.14	3.21	0.70	0.15	40.20	198	9	472	24	169	9.91	2.02	1.23	76	21	119	175	286	4.28	0.19	22.99	0.72	0.74	14.30	31.71	4.19	17.67	4.13	1.46	4.27	0.73	4.55	0.91	2.54	0.37	2.40	0.40	11-27W	Evb_p
11-28C	Eva_{pd}	61.16	0.75	17.77	6.38	0.08	2.67	6.35	3.96	0.74	0.14	48.51	174	12	366	13	126	6.63	1.84	1.39	74	79	67	120	53	3.31	0.21	14.74	0.48	0.59	11.70	23.37	3.14	12.75	3.02	1.08	2.96	0.48	2.86	0.56	1.47	0.20	1.20	0.18	11-28C	Eva_{pd}
11-32F	Eva_p	60.98	0.79	16.95	6.20	0.10	3.79	6.97	3.53	0.50	0.16	47.13	159	8	306	18	132	7.95	1.78	1.91	76	68	55	126	92	3.40	0.10	15.81	0.55	0.60	11.88	25.97	3.38	14.07	3.37	1.06	3.47	0.57	3.47	0.69	1.85	0.26	1.65	0.26	11-32F	Eva_p
11-32K†	Ei	58.93	0.96	18.33	7.77	0.13	4.05	7.10	2.52	0.08	0.13	51.68	52	1	282	18	116	6.20	1.60	12.85	78	84	44	183	37	3.08	0.05	19.59	0.45	0.60	10.79	22.94	3.00	12.76	3.29	1.18	3.39	0.56	3.45	0.69	1.87	0.27	1.68	0.25	11-32K†	Ei
11-32L	Ei	57.06	1.06	21.34	6.12	0.16	2.57	6.38	3.50	1.67	0.14	52.69	452	35	322	31	152	8.55	2.49	20.72	116	207	39	159	53	3.97	0.32	22.08	0.60	0.84	16.38	33.38	4.37	18.82	5.01	1.69	5.73	0.95	5.60	1.13	3.06	0.43	2.68	0.41	11-32L	Ei
11-34N	Eva_p	62.02	0.75	18.19	5.00	0.10	2.47	6.45	3.95	0.94	0.14	48.59	228	14	486	12	118	6.61	1.92	2.00	70	39	21	119	18	2.97	0.14	13.31	0.48	0.63	12.72	25.02	3.11	12.67	2.80	0.99	2.70	0.43	2.53	0.48	1.28	0.19	1.19	0.18	11-34N	Eva_p
11-35U	Qgof	65.60	0.79	15.47	7.23	0.12	4.22	2.94	2.19	1.31	0.13	59.88	405	40	193	26	118	7.14	3.76	6.53	87	69	119	162	400	3.16	1.75	23.68	0.51	1.33	16.78	30.97	4.87	20.86	5.12	1.56	5.06	0.81	4.86	0.97	2.54	0.35	2.22	0.34	11-35U	Qgof
11-37R	Ei	58.91	1.01	17.29	8.81	0.10	4.64	6.02	2.69	0.39	0.13	52.26	106	8	257	17	119	6.59	2.01	2.68	28	182	64	175	76	3.16	0.80	18.73	0.50	0.65	12.96	26.88	3.44	14.03	3.37	1.34	3.43	0.57	3.40	0.67	1.79	0.26	1.63	0.25	11-37R	Ei
11-38AH	Qc_{hmp}	60.30	1.17	20.00	8.68	0.15	3.23	3.20	2.13	0.93	0.20	65.94	333	22	288	21	175	13.98	3.51	5.40	96	193	85	171	186	4.52	1.57	23.05	0.93	1.08	22.68	53.84	6.03	24.40	5.14	1.51	4.59	0.72	4.25	0.83	2.22	0.32	2.05	0.31	11-38AH	Qc_{hmp}
11-39D	Qc_{ws}	63.48	0.83	14.84	6.31	0.13	5.24	4.78	3.02	1.18	0.17	49.84	448	23	455	18	116	4.81	3.17	7.26	91	15	32	123	75	3.15	0.79	21.29	0.33	1.21	15.42	31.02	4.40	17.99	4.05	1.16	3.68	0.60	3.53	0.69	1.90	0.28	1.76	0.26	11-39D	Qc_{ws}
11-41D	Moig	70.80	0.47	15.09	3.40	0.06	1.48	2.36	3.95	2.27	0.12	53.25	904	60	358	15	141	9.26	7.73	11.77	60	13	15	77	38	3.77	1.17	9.28	0.75	2.28	25.39	46.34	5.42	19.97	3.82	1.05	3.16	0.48	2.83	0.55	1.49	0.22	1.40	0.22	11-41D	Moig
11-42E	Qga_v	67.81	0.76	15.20	5.82	0.11	2.50	3.45	2.96	1.25	0.14	54.88	367	32	251	23	129	7.42	3.62	6.98	78	71	42	133	90	3.42	1.44	17.67	0.56	1.20	17.32	32.72	4.50	18.24	4.29	1.27	4.30	0.70	4.29	0.86	2.33	0.34	2.11	0.34	11-42E	Qga_v
11-42F	Qga_v	69.06	0.77	14.85	5.64	0.10	2.20	3.17	2.85	1.23	0.13	55.76	375	33	245	21	129	7.55	3.74	6.85	74	56	40	128	99	3.43	1.42	16.96	0.58	1.26	16.66	31.66	4.32	17.22	3.86	1.15	3.87	0.65	3.97	0.79	2.18	0.31	2.01	0.30	11-42F	Qga_v
11-43C	Eva_{pd}	60.77	0.77	17.87	5.60	0.11	3.27	6.76	3.85	0.89	0.12	47.71	227	15	384	15	113	6.38	1.95	1.69	65	54	51	130	49	2.99	0.11	15.72	0.47	1.01	10.83	22.23	2.82	11.78	2.81	0.93	2.91	0.48	2.92	0.58	1.56	0.23	1.43	0.22	11-43C	Eva_{pd}
11-44A-2	Qc_{ws}	60.82	1.05	14.74	8.11	0.16	6.04	5.02	2.88	1.02	0.17	49.62	386	20	465	18	145	5.34	2.87	6.80	111	15	34	174	101	3.81	0.76	24.05	0.36	1.08	14.71	29.96	4.24	17.42	3.97	1.16	3.64	0.58	3.49	0.69	1.87	0.28	1.77	0.27	11-44A-2	Qc_{ws}
11-108C	Qc_{hmp}	70.07	1.23	18.31	5.63	0.05	1.42	1.49	0.49	1.28	0.03	78.89	305	44	119	22	202	13.96	4.86	10.08	89	68	48	150	124	5.29	2.90	18.71	1.03	1.45	26.12	46.46	6.18	23.34	4.92	1.34	4.48	0.73	4.34	0.85	2.37	0.35	2.23	0.36	11-108C	Qc_{hmp}
11-203E	Qgof	67.03	0.86	15.95	6.11	0.11	2.76	2.99	2.72	1.38	0.10	58.31	416	38	233	19	147	7.78	3.60	8.91	95	62	49	149	148	3.90	1.95	18.42	0.58	1.31	15.07	32.33	3.77	14.96	3.37	1.02	3.45	0.58	3.59	0.73	1.96	0.30	1.92	0.30	11-203E	Qgof

* All Fe reported as Fe^{2+}

**CIA = chemical index of alteration $[(Al_2O_3/101.96)/(Al_2O_3/101.96)+(CaO/56.08)+(Na_2O/61.98)+(K_2O/94.20)]*100$. Typically, an "unaltered" sample will have a CIA of 50 or lower.

#Ni, Cr, Sc, Zn are from X-ray fluorescence. All other trace elements were measured by inductively coupled plasma mass spectrometry.

†X-ray fluorescence and inductively coupled plasma mass spectrometry is the average of two analytical runs for samples 1P and 32K.

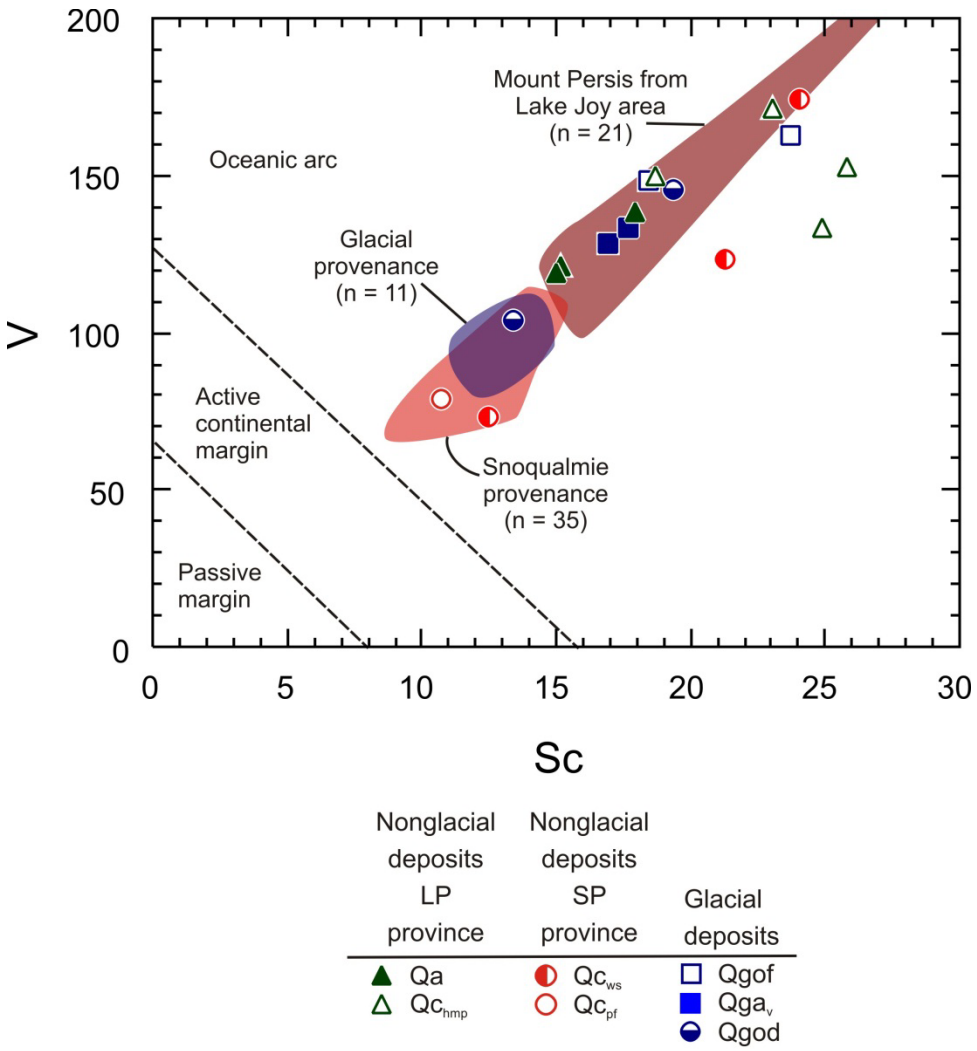

Figure C3. Sc vs. V tectonic discrimination diagram of Bhatia and Crook (1986). Fields for glacial and Snoqualmie provenance are from Dragovich (2007) and Dragovich and others (2009b,c; 2010a,b; 2011a,b). The volcanic rocks of Mount Persis of Tabor and others (1993) from the Lake Joy quadrangle are plotted as the "Mount Persis from Lake Joy area" field. Data normalized LOI-free before being plotted.

Vashon advance outwash (unit Qga$_v$)—Two advance outwash sands plot in the arc field on the Sc vs. V diagram of Bhatia and Crook (1986)(Fig. C3). They both plot transitionally between intermediate and felsic arc sources on the La/Th vs. Hf diagram of Floyd and Leveridge (1987)(Fig. C4). These samples have chondrite-normalized La/Lu ratios between 5.22 and 5.76 and Pb/Yb ratios from 3.30 to 3.41 (Fig. C5).

Pleistocene Nonglacial Deposits

Whidbey Formation, Snoqualmie River facies (unit Qc$_{ws}$)—Three sands from this unit plot in the arc field on the Sc vs. V diagram of Bhatia and Crook (1986)(Fig. C3). Samples 11-39D and 11-44A-2 plot between the intermediate and felsic arc sources on the La/Th vs. Hf diagram of Floyd and Leveridge (1987), while sample 11-22E plots in the felsic arc source field (Fig. C4). These samples have chondrite-normalized La/Lu ratios between 5.55 and 6.08 and Pb/Yb ratios from 3.83 to 4.84 (Fig. C5).

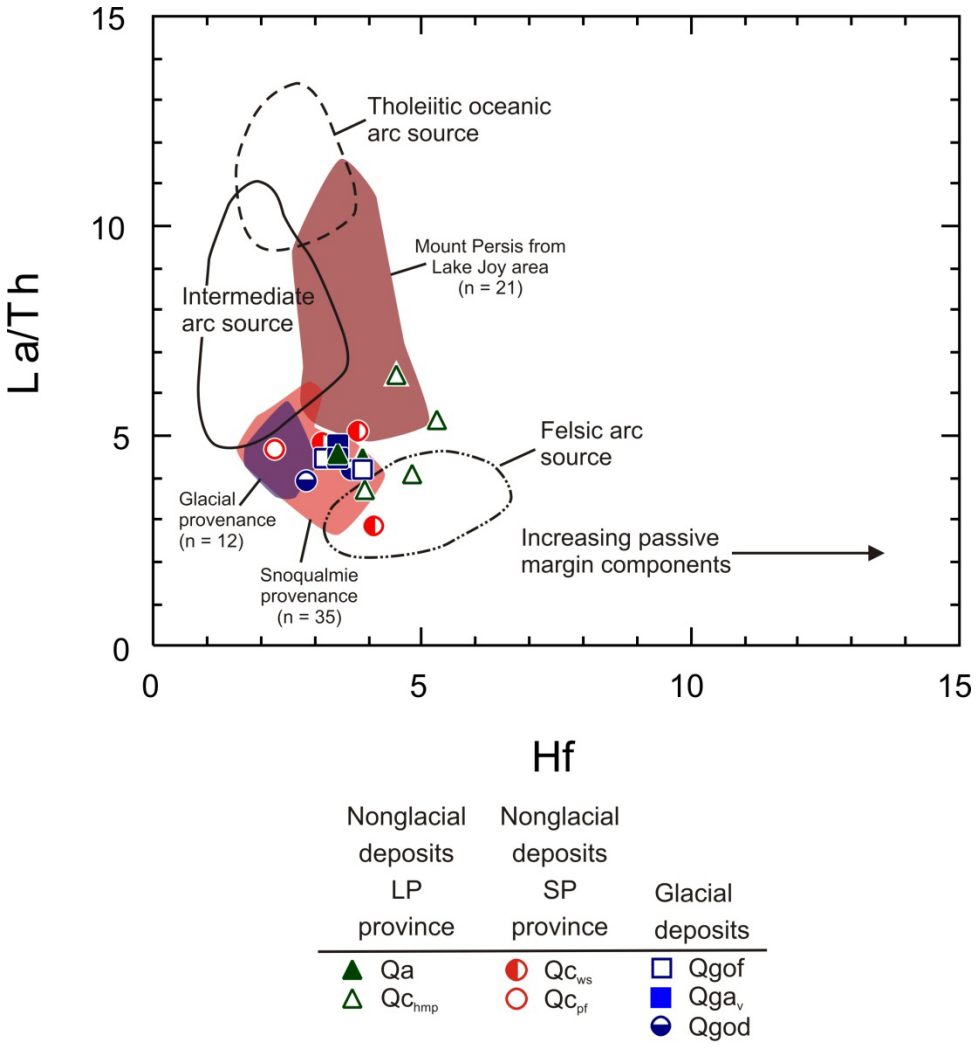

Figure C4. La/Th-Hf source and compositional discrimination diagram of Floyd and Leveridge (1987). Fields for glacial and Snoqualmie provenance are from Dragovich (2007) and Dragovich and others (2009b,c; 2010a,b; 2011a,b). The volcanic rocks of Mount Persis of Tabor and others (1993) from the Lake Joy quadrangle are plotted as the "Mount Persis from Lake Joy area" field. Data normalized LOI-free before being plotted.

Pre-Fraser continental nonglacial deposits, Snoqualmie River facies (unit Qc$_{pf}$)—One sand from this unit, sample 11-20A, plots in the arc field on the Sc vs. V diagram of Bhatia and Crook (1986)(Fig. C3). This sand plots close to the intermediate arc source filed on the La/Th vs. Hf diagram of Floyd and Leveridge (1987)(Fig. C4). The chondrite-normalized La/Lu ratio for this sample is 4.26, and the Pb/Yb ratio is 3.63 (Fig. C5).

Hamm Creek unit, Mount Persis volcanic facies (unit Qc$_{hmp}$)—Four sands from unit Qc$_{hmp}$ plot in the arc field on the Sc vs. V diagram of Bhatia and Crook (1986)(Fig. C3). Samples 11-16A and 11-22J plot in the felsic arc source field on the La/Th vs. Hf diagram of Floyd and Leveridge (1987)(Fig. C4). Samples 11-38AH and 11-108C have elevated La/Th ratios when compared to the other Hamm Creek unit sands (Fig. C4). The chondrite-normalized La/Lu ratios for these samples range from 4.50 to 7.60, and their Pb/Yb ratio range from 2.62 to 7.72 (Fig. C5).

Nonglacial Sand Provenance

Geochemistry of the nonglacial sands suggests that they had an arc source with minor passive or continental margin input (Figs. C3 and C4). This is supported by their petrography (Table C1 and Appendix F, Table F1). The high Sc, V, Pb/Yb, low Hf, and moderate La/Th, as well as the chondrite-normalized La/Lu, of these samples suggest that this arc source was intermediate in composition (Bhatia and Crook, 1986; Floyd and Leveridge, 1987; Floyd and others,

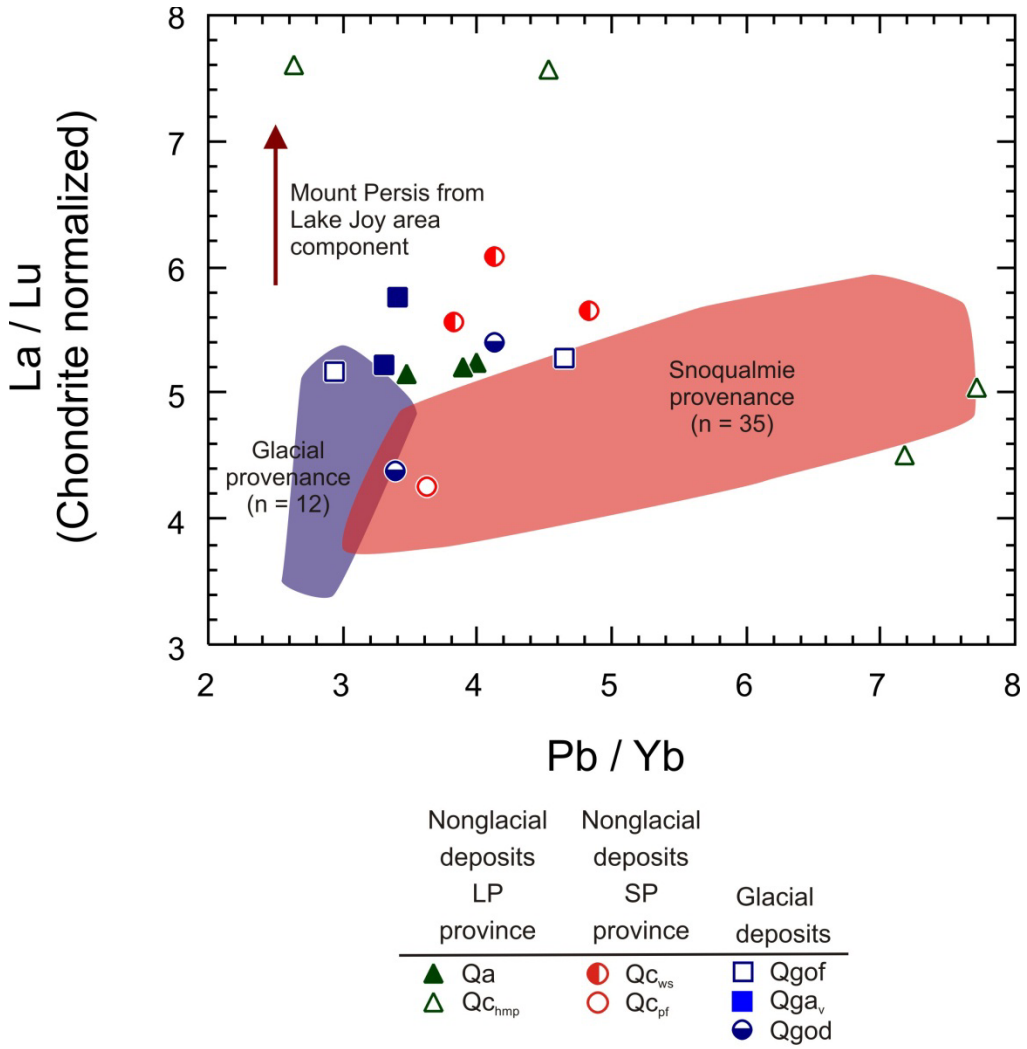

Figure C5. Chondrite-normalized La/Lu vs. Pb/Yb diagram for sands from the Lake Joy area. Normalization values are from McDonough and Sun (1995). Fields for glacial and Snoqualmie provenance are from Dragovich (2007) and Dragovich and others (2010a,b; 2011a,b). The red arrow defines the geochemical trend that would be caused by increasing contributions from the volcanic rocks of Mount Persis of Tabor and others (1993) from the Lake Joy quadrangle. Data normalized LOI-free before being plotted.

1991; McLennan and others, 1990, 1993; McDonough and Sun, 1995; McLennan, 2001). A field defined by the compositions of the volcanic rocks of Mount Persis from the Lake Joy quadrangle is indicated on Figures C3, C4, and C5. This volcanic unit is widely exposed in the study area, underlies the sampled Quaternary sands at depth, and dominates the local basin. This geochemical field for the volcanic rocks of Mount Persis from the Lake Joy quadrangle is labeled "Mount Persis from the Lake Joy area" on Figures C3, C4, and C5 (see local provenance, LP, discussed in Appendix F). Tolt River alluvium (unit Qa) and Hamm Creek unit (unit Qc$_{hmp}$), Mount Persis provenance sands plot in or around the field defined by the Lake Joy-area volcanic rocks of Mount Persis on Figure C3. Samples 11-38AH and 11-108C from unit Qc$_{hmp}$ have La/Th, chondrite-normalized La/Lu and Pb/Yb ratios that are consistent with the Lake Joy-area Mount Persis source (Figs. C4 and C5). This geochemistry supports the petrographic observation that the Tolt River alluvium and Hamm Creek unit have a local provenance that is predominantly derived from the volcanic rocks of Mount Persis (Table C1 and Table F1). Hamm Creek unit samples 11-16A and 11-22J also have a strong felsic plutonic geochemical signature. This is indicated by these samples plotting in the felsic arc source field on Figure C4 and their high Pb/Yb ratio (Fig. C5). Both of these samples contain granitic lithic and monocrystalline quartz clasts that corroborate this geochemical observation (Table C1; Appendix F).

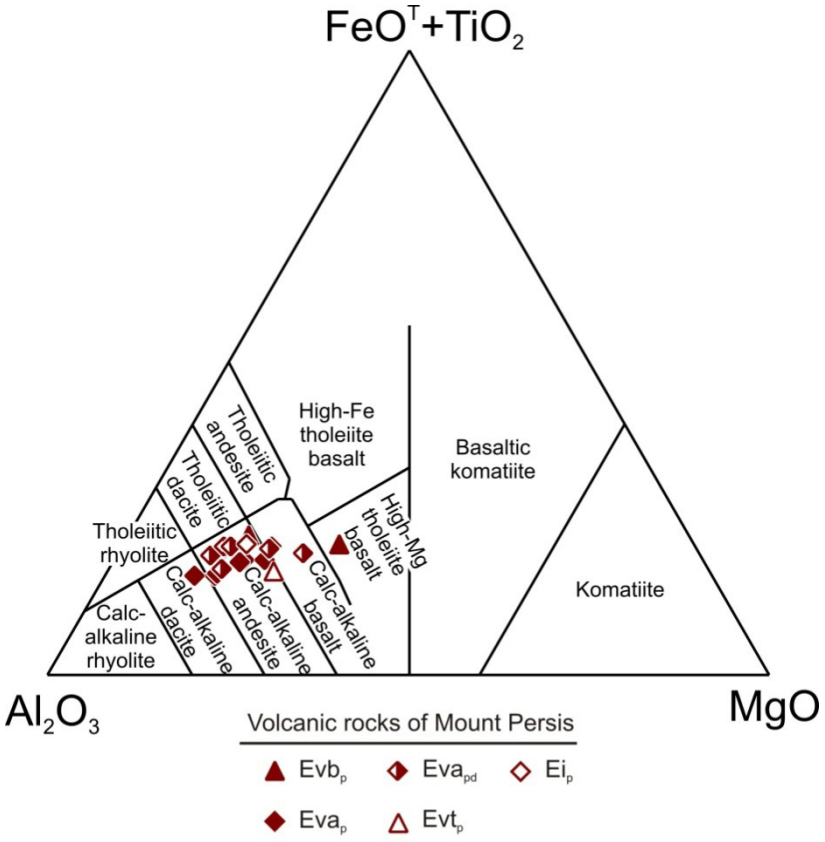

Figure C6. Classification of volcanic rocks of Mount Persis of Tabor and others (1993) according to their cation percentages of Al, Fe-total + Ti, and Mg. Diagram from Jensen (1976) with fields modified from Rickwood (1989). Data normalized LOI-free before being plotted.

A field for all nonglacial Snoqualmie River basin provenance sands from previous studies is shown on Figures C3, C4, and C5 (Dragovich, 2007; Dragovich and others, 2010a,b, 2011a,b). Sands 11-20A (unit Qcpf) and 11-23E (unit Qcws) plot in or near the Snoqualmie River basin provenance field on these three figures (Dragovich, 2007; Dragovich and others, 2009a,b,c, 2010a,b, 2011a,b). This suggests that the geochemistry of these two samples supports their petrography (Tables C1 and F1). However, samples 11-39D and 11-44A-2 (unit Qcws) plot in or near the field defined by Lake Joy area volcanic rocks of Mount Persis on Figures C3 and C4, and they have elevated chondrite-normalized La/Lu ratios (Fig. C5). The high percentage of volcanic lithic grains in both these samples suggests a contribution to ancient Snoqualmie River basin provenance in this area by the ancient Tolt River system; however, the general lack of Western mélange belt lithic grain types (for example meta-argillite lithic grains) suggests the contribution was muted by ancient Snoqualmie River sedimentation (Table C1). This suggests that these two samples were receiving components from the local basin prior to their deposition, perhaps indicating a mixed local Tolt River and ancient Snoqualmie River source or that the ancient Tolt River basin contained less exposed basement at that time (Appendix F).

Glacial Sand Provenance

Geochemistry of glacial sands suggests that they had an arc source with minor passive or continental margin input (Figs. C3, C4). The lack of a "continental" geochemical signature differs from the petrography of these glacial sands that supports the arc source of these sands (Tables C1 and F1). The high Sc, V, Pb/Yb, low Hf, and moderate La/Th, as well as chondrite-normalized La/Lu ratios, of these samples suggest that this arc source was intermediate in composition (Bhatia and Crook, 1986; Floyd and Leveridge, 1987; Floyd and others, 1991; McLennan and others, 1990, 1993; McDonough and Sun, 1995; McLennan, 2001). A field for glacial sands from previous studies is plotted on Figures C3, C4, and C5 (Dragovich, 2007; Dragovich and others, 2010a,b, 2011a,b). Glacial sands, such as 11-13U, plot within the field defined by Lake Joy-area volcanic rocks of Mount Persis on Figure C3. Sample 11-13U

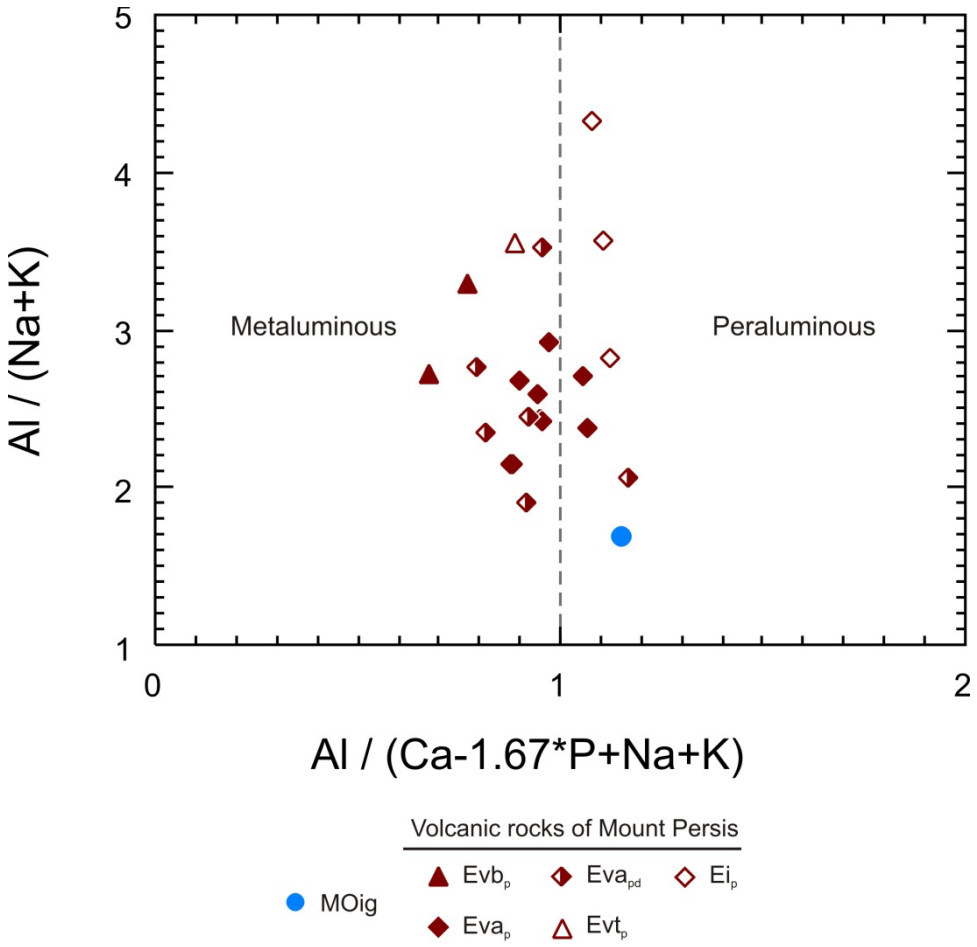

Figure C7. Aluminum saturation index vs. molecular Al/(Na+K) diagram for volcanic rocks of Mount Persis of Tabor and others (1993). Aluminum saturation index calculated using the method of Frost and others (2001). Data normalized LOI-free before being plotted.

(unit Qgod) plots in the overlap between glacial and Snoqualmie River basin provenances (Fig. C3). These samples do not have strongly elevated La/Th or chondrite-normalized La/Lu ratios; however, Figures C4 and C5 suggest that the volcanic rocks of Mount Persis in the Lake Joy area are contributing minor amounts of detritus to these deposits. Petrographically, sample 11-13U has a partial granitic source, including some granitic lithic grains and appreciable potassium feldspar (~8%), but is polymictic with monocrystalline quartz, plagioclase, volcanic lithic grains, hornblende, pyroxene, and some metasedimentary lithic grains. Consistent with the transitional geochemistry, these glacial meltwater sands have northeast provenance with mélange belt, volcanic, and granitic provenances.

Geochemical Discrimination of Glacial vs. Nonglacial Sand Deposits

In previous studies, Dragovich and others (2010a,b, 2011a,b) used chondrite-normalized La/Lu ratios vs. Pb/Yb or Sr + Ba diagrams to discriminate glacial from nonglacial sands (Fig. C5). However, the degrees of weathering of some of the Pleistocene nonglacial sands from this study (Fig. C2) do not allow for the use of Sr and Ba due to their geochemical mobility. Also, the addition of the volcanic rocks of Mount Persis to these samples is elevating the chondrite-normalized La/Lu ratios of glacial and nonglacial samples (Fig. C5). Yet, the Pb/Yb ratio of these samples is still a strong discriminator between glacial and nonglacial sands because a higher Pb/Yb ratio can be a result of a plutonic arc source (McDonough and Sun, 1995; McLennan, 2001). Outwash sample 11-203E (Qgof) has a Pb/Yb ratio that is elevated when compared to all other glacial sands and plots in the field defined by Snoqualmie River basin provenance sands (Fig. C5). This high Pb/Yb ratio suggests that this glacial sample has a strong geochemical arc signature. Petrography of this sample also indicates that it has a significant plutonic component (Table C1),

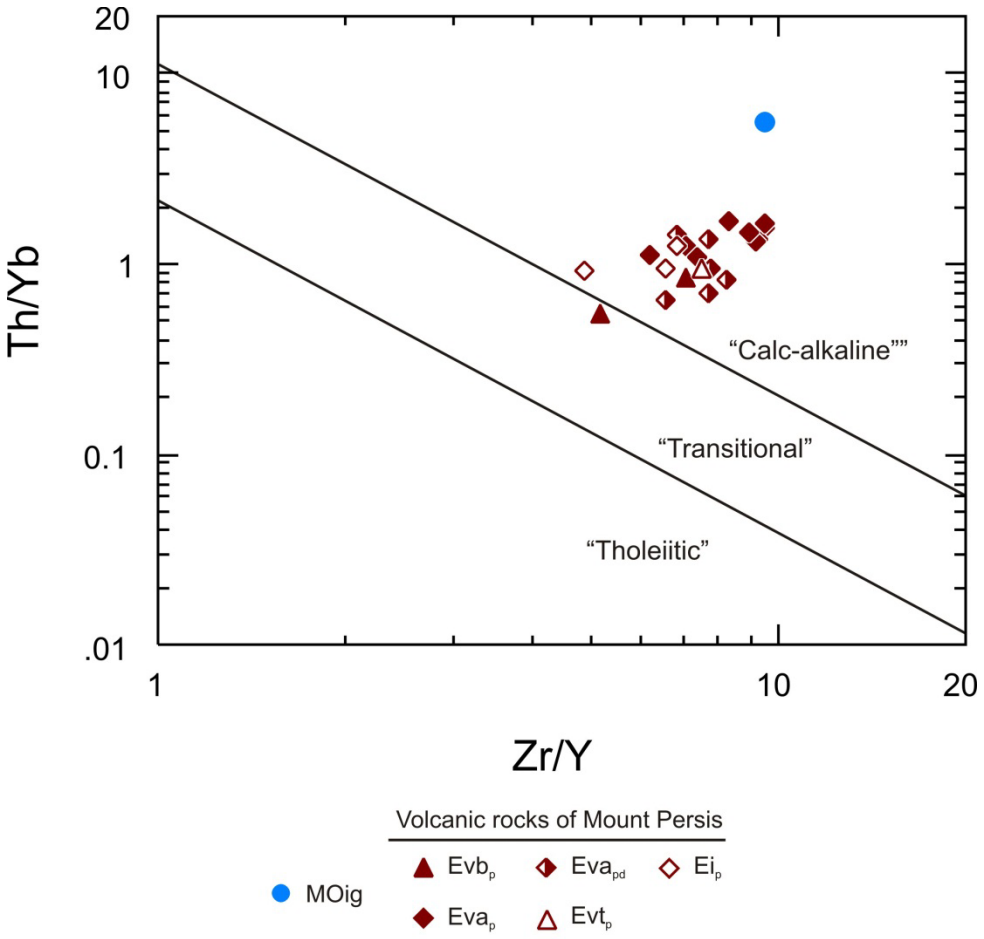

Figure C8. Th/Yb vs. Zr/Y diagram for discrimination of magmatic affinities. Diagram modified from Ross and Bédard (2009). Data normalized LOI-free before being plotted.

possibly originating from the Index batholith, and contains mostly volcanic and granitic lithic grain types with some metachert and metasedimentary lithic grains. Here there is an extrabasinal component, suggesting it is derived from the Index batholith as a result of ice-marginal meltwater erosion with a distinct secondary easterly mélange belt source.

Igneous Rock Geochemistry

Petrography and geochemistry indicate that the volcanic rocks of Mount Persis of Tabor and others (1993) and sample 11-41D from unit MOig, have undergone extensive hydrothermal alteration (Table C1 and C3; Fig. C2). Harper and others (1988) demonstrated that hydrothermal alteration can enrich Si by as much as 60% while also causing mobility of Na and K. For this reason, the total alkali-silica diagram of Le Maitre and others (2002) cannot be used to chemically classify the extrusive igneous rocks from this study. Instead, the cation classification diagram of Jensen (1976)(Fig. C6), with fields modified by Rickwood (1989), is used to chemically classify the extrusive igneous rocks from this study because this diagram utilizes elements that are resistant to hydrothermal alteration (Pearce, 1996). The classification of these extrusive igneous rocks on Figure C6 is in agreement with their field and petrographic name determinations (Table C1).

MIOCENE TO OLIGOCENE INTRUSIVE ROCKS

Granite to granodiorite (unit MOig)—One intrusive sample from this unit, 11-41D, has quartz-plagioclase feldspar-potassium feldspar ratios that suggest it is a granite (Table C1); however, it has molecular normative anorthite-albite-orthoclase ratios (O'Connor, 1965; Barker, 1979) that suggest it is a granodiorite (diagrams not

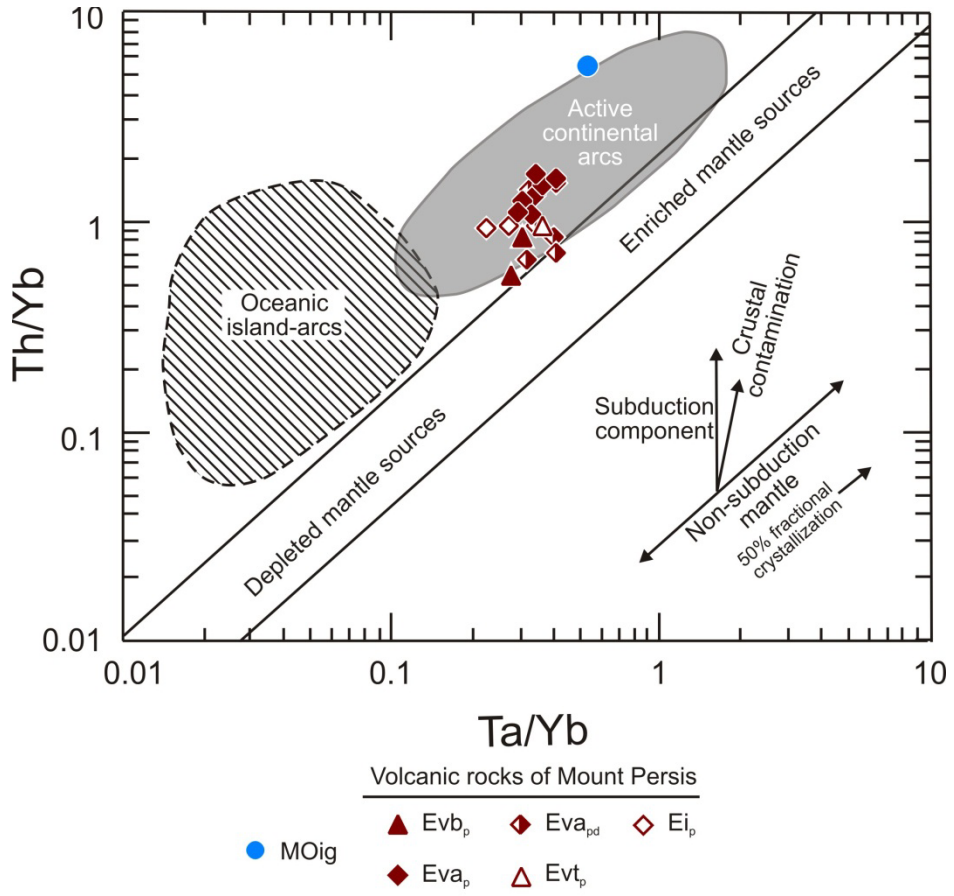

Figure C9. Th/Yb vs. Ta/Yb discrimination diagram for volcanic rocks of Mount Persis of Tabor and others (1993) and unit „…ig. Diagram after Pearce (1982, 1983). Data normalized LOI-free before being plotted.

displayed). This sample has an aluminum saturation index (ASI) of 1.15 and a molecular Al/(Na+K) ratio of 1.69 (Fig. C7). This indicates that this sample is peraluminous (Frost and others, 2001). On the Th/Yb-Zr/Y magmatic affinity diagram of Ross and Bédard (2009), sample 11-41D plots in the calc-alkaline field (Fig. C8). Sample 11-41D plots in the field defined by modern active continental arcs on the Th/Yb-Ta/Yb tectonic discrimination diagram of Pearce (1982, 1983, Fig. C9).

Volcanic rocks of Mount Persis of Tabor and others (1993)

Andesite flows (unit Eva$_p$)—Seven of the flows from this unit plot in the calc-alkaline andesite field on Figure C6. However, flow 11-34N plots in the calc-alkaline dacite field (Fig. C6). These flows have an ASI that ranges from 0.87 to 1.07, with samples 11-1F and 11-9C having an ASI greater than 1 (Fig. C7). The molecular Al/(Na+K) ratios of the flows range from 2.14 to 2.92 (Fig. C7). This indicates that these flows are metaluminous, while 11-1F and 11-9C are peraluminous (Frost and others, 2001). These flows plot in the calc-alkaline field on the Th/Yb-Zr/Y magmatic affinity diagram of Ross and Bédard (2009, Fig. C8). All eight of these flows plot in the field defined by modern active continental arcs on the Th/Yb-Ta/Yb tectonic discrimination diagram of Pearce (1982, 1983, Fig. C9).

Dark basaltic andesite flows (unit Eva$_{pd}$)—Three of the flows from this unit plot in the calc-alkaline basalt field on Figure C6, while four more flows plot in the calc-alkaline andesite field. These flows have an ASI that ranges from 0.79 to 0.96, and sample 11-23P has an ASI of 1.17 (Fig. C7). The molecular Al/(Na+K) ratios of the flows range from 1.90 to 3.53 (Fig. C7). This indicates that these flows are metaluminous, while 11-23P is peraluminous (Frost and others, 2001). These flows plot in the calc-alkaline field on the Th/Yb-Zr/Y magmatic affinity diagram of Ross and Bédard (2009, Fig. C8). Seven of these flows plot in the field defined by modern active continental arcs on

the Th/Yb-Ta/Yb tectonic discrimination diagram of Pearce (1982, 1983) (Fig. C9), while sample 11-14M plots in the mantle array near enriched mantle sources.

Basalt flows (unit Evb_p)—The basalt flow sample 11-19P plots in the high-Mg tholeiite basalt field on Figure C6, while flow 11-27W plots in the calc-alkaline andesite field. These flows have an ASI that ranges from 0.67 to 0.77 (Fig. C7). The molecular Al/(Na+K) ratios of the flows range from 2.72 to 3.30 (Fig. C7). This indicates that these flows are metaluminous (Frost and others, 2001). Flow sample 11-19P plots in the transitional field, while 11-27W plots in the calc-alkaline field on the Th/Yb-Zr/Y magmatic affinity diagram of Ross and Bédard (2009, Fig. C8). Both of these flows plot in the field defined by modern active continental arcs on the Th/Yb-Ta/Yb tectonic discrimination diagram of Pearce (1982, 1983, Fig. C9).

Crystal vitric tuff (unit Evt_p)—One crystal vitric tuff from this unit plots in the calc-alkaline andesite field on Fig. C6. The ASI of this tuff is 0.89, and its molecular Al/(Na+K) ratio is 3.55 (Fig. C7). This indicates that the tuff is metaluminous (Frost and others, 2001). This tuff plots in the calc-alkaline field on the Th/Yb-Zr/Y magmatic affinity diagram of Ross and Bédard (2009, Fig. C8). This tuff also plots in the field defined by modern active continental arcs on the Th/Yb-Ta/Yb tectonic discrimination diagram of Pearce (1982, 1983, Fig. C9).

North Fork Creek intrusive complex (unit Ei_p)—Samples 11-32L and 11-37R have been petrographically identified as gabbro (Table C1); sample 11-32K plots in the calc-alkaline andesite field on Figure C6. The ASI of these samples are 1.08 and 1.12 (Fig. C7). The molecular Al/(Na+K) ratios of these two samples are 2.82 and 4.33 (Fig. C7). This indicates that these samples are peraluminous (Frost and others, 2001). These igneous rocks plot in the calc-alkaline field on the Th/Yb-Zr/Y magmatic affinity diagram of Ross and Bédard (2009, Fig. C8). All three of these rocks plot in the field defined by modern active continental arcs on the Th/Yb-Ta/Yb tectonic discrimination diagram of Pearce (1982, 1983, Fig. C9).

Volcanic Rocks of Mount Persis Interpretations

Geophysical modeling along Cross Section A indicates that a shallow intrusive body, possibly the Index batholith, is present in the eastern part of the Lake Joy quadrangle (Plate 1, Figs. 1 and 2). This shallow intrusive body could have been the source of the extensive hydrothermal alteration of igneous rocks in the Lake Joy area (Tables C1 and C3; Fig. C2). The volcanic rocks of Mount Persis from previous studies (Dragovich and others, 2009b,c, 2010a,b, 2011a,b) are medium-K calc-alkaline with minor samples that are transitional to tholeiitic. The Mount Persis volcanic rock samples from the Lake Joy area are predominantly calc-alkaline (Figs. C6 and C8). However, basalt flow sample 11-19P is transitional between tholeiitic and calc-alkaline (Figs. C6 and C8).The K-content of these samples cannot be accurately determined due to their alteration.

The ASI of the Mount Persis unit from previous studies is metaluminous at lower SiO_2 values, but peraluminous at higher SiO_2 values (Dragovich and others, 2009b,c, 2010a,b, 2011a,b). The Mount Persis samples from the Lake Joy area are also predominantly metaluminous with minor peraluminous samples (Fig. C7). The peraluminous samples have higher Ti and lower Cr, Ni, and Sc contents (Table C3). This, along with previous results, indicates that assimilation of continental crust increased as the Mount Persis magma evolved along fractionation trends. The Ta/Yb ratios, along with amphibole mafic phase of these samples, indicate that they evolved from partial melting and hydration of an enriched mafic mantle source (Fig. C9, Pearce, 1982, 1983). This unit's predominantly metaluminous, calc-alkaline composition, with elevated Th/Yb and Ta/Yb ratios, suggests that the volcanic rocks of Mount Persis formed in a "Cordilleran-type" continental arc (Pearce, 1983; Frost and others, 2001).

The volcanic rocks of Mount Persis differs from published ancestral Cascades arc rocks that span the same time frame (36–45 Ma) as studied by du Bray and John (2011). They indicate that the ancestral Cascades arc volcanic rocks from 36–45 Ma are predominantly basalt to basaltic andesite, whereas the Mount Persis unit rocks are predominantly basaltic andesite to andesite (Fig. C6, Dragovich and others, 2009a,b, 2010a,b, 2011a, b). The ancestral Cascades arc rocks from 36 to 45 Ma are transitional between tholeiitic and calc-alkaline—with a near equal number of tholeiitic and calc-alkaline samples (du Bray and John, 2011). Conversely, the Mount Persis unit is predominantly calc-alkaline with fewer tholeiitic samples (Figs. C6 and C8). The petrological differences between the ancestral Cascades arc and the volcanic rocks of Mount Persis could be attributed to the higher degree of assimilation for the Mount Persis unit parent magma.

Unit MOig Interpretations

Because only one intrusive rock sample was analyzed (11-41D), only rudimentary interpretations can be forwarded. This sample is slightly hydrothermally altered (Table C1; Fig. C2), calc-alkaline and peraluminous granite to granodiorite (Figs. C7 and C8) resulting from magmatic activity in a continental arc setting (Fig. C9). The rock contains plagioclase (~40%), potassium feldspar (~30%), and quartz (~30%), thus is modally near the boundary between granite and granodiorite, consistent with the geochemical discrimination diagram classifications (not shown) of this evolved rock that contains low mafic mineral content.

Appendix D. Isostatic Gravity and Aeromagnetic Data

Aeromagnetic data are from a survey flown in 1997, contracted by the U.S. Geological Survey (Blakely and others, 1999). North-south flight lines predominate in the survey, spaced 250 m (820 ft) apart, with more widely spaced east-west tie lines. We interpret a reduced-to-pole version of the magnetic map, in which magnetic anomalies are directly above the magnetic source units. For interpretation purposes, we upward continue the reduced-to-pole magnetic grid to 50 m (164 ft) above the flight altitude and then subtract this from our original magnetic grid. The result is a map that isolates the anomalies produced by near-surface magnetic rocks (see aeromagnetic map on Plate 1, Fig. 1). We do not present the original reduced-to-pole magnetic map because anomalies represented on the high-resolution map simply reflect positions of anomalies on the original map, although magnetic intensity of these anomalies is different. Recent data constrain the gravity anomalies for this region (Anderson and others, 2006; Dragovich and others, 2007, 2009a,c, 2010a,b, 2011a,b). In addition, a new survey added data to the Lake Joy quadrangle in particular, especially along Cross Section B (Plate 1, Figs. 1 and 2). Establishment and use of a local base station with multiple ties to regional base stations connect these new data to the World Gravity Relative Reference Network, thus allowing for comparison to existing data for the region. Villenueve (2012) described additional details about data collection and reduction (including spatial control and terrain corrections) of the new survey. Villenueve (2012) applied standard formulas and reduction procedures of Blakely (1995), as well as a reduction density of 2670 kg/m^3 for the crust, to compute the isostatic gravity anomaly contours from the Complete Bouguer Anomaly grid.

GEOPHYSICAL MODELS

We use GM-SYS Geophysical Modeling software (NGA, Inc.) to test cross section stratigraphic models developed with geologic mapping data against the isostatic gravity and aeromagnetic data (called "geophysical models" hereafter). Therefore, our modeling procedure honors both mapped lithologic boundaries and any known thicknesses of Quaternary sediments across the profiles in addition to the geophysical data. We are careful to assure that the dip of beds measured at the surface is consistent with folded materials below as we develop and test the geophysical models. Spacing for the magnetic data sampled from the map is 0.5 km (0.31 mi), somewhat sparser than the actual survey data, because we wanted both gravity and magnetic data to have similar spacing along the model. Radar altimetry collected during the survey constrains altitudes for the aeromagnetic data above the land surface (Plate 1, Fig. 2). Isostatic gravity data points represented on the geophysical models lie within 1.5 km (0.93 mi) of each model line. While Model B has fairly consistent 0.5 km (0.31 mi)-spacing for gravity data points, Model A has much more sparse data; therefore, the size of rock bodies that we can constrain in the subsurface with the data is much smaller for Model B than Model A. We discuss the details of certainty in specific regions of the models below, but in general, details of the models that are less than 1 km width, though based on geologic mapping, are not well constrained by the geophysical data.

Hand-sample and outcrop magnetic susceptibility measurements, as well as hand-sample density measurements for samples gathered within the Lake Joy quadrangle and throughout the eastern Puget Lowland region (Table D1 below), support density and magnetic properties of the rock units used in the map interpretation and two-dimensional geophysical modeling. Magnetic susceptibilities are measured via a SatisGeo Model KT-6 Kappameter. We use a method involving weight ratios of saturated and immersed samples to calculate saturated density (SBD) utilizing the following formula:

$$SBD = \frac{Was}{Was - Ww}$$

where Ww = sample weight saturated underwater and Was = sample weight saturated in air.

Where density and magnetic susceptibility measurements are not available, we apply reasonable densities from past geophysical modeling in the region (Dragovich and others, 2007, 2009a,c, 2010a,b, 2011a,b). Physical properties of units used during the modeling process may be different from hand-sample values to allow better data fit of the models to geophysical anomalies in this region, recognizing the natural variability of rock compositions throughout a region. In particular, where there is a large variability in property measurements for the unit, we allow more latitude in density and magnetic properties used in the modeling process. There is also a consistent relationship

between depth of burial and physical properties. Rock density is greater with deeper burial, due to lithification and metamorphism resulting in compaction and recrystallization of the rocks, especially in clastic rocks of any type. Magnetic susceptibility is greater at depth due to lack of weathering, which can alter magnetic characteristics of the rock (generally making the rocks less magnetic). We assume most of our hand samples have been somewhat weathered by virtue of being at the surface of the Earth.

INTERPRETATION—GEOPHYSICAL MAP AND CROSS SECTIONS

A gradual gravity gradient from low values in the west to high in the east dominates the isostatic gravity map (Fig. 1 on Plate 1). There are two factors governing this trend: (1) thicker Tertiary volcanic rocks (and thus deeper pre-Tertiary basement) to the west and, conversely, shallower basement to the east, and (2) a large body of Index batholith (unit Mzig) within the Western mélange belt basement to the east. The Index batholith is granodiorite on average and thus likely to have a density of as much as 2.79 g/cm^3 (Telford and others, 1990), substantially higher than the average Western mélange belt density of 2.70 g/cm^3 indicated by our measurements and modeling (Table D1). The existence of the Index batholith is supported by outcrops of the batholith east of the quadrangle (Tabor and others, 1993), unit Mzig exposures in the study area, and regional modeling of gravity data requiring a denser basement rock under the far eastern part of the Puget Lowland (Anderson and others, 2011). By far the most magnetic rocks in the region are the basalts and basaltic andesites in the volcanic rocks of Mount Persis (Mount Persis; Table D1). On the basis of our measurements of these units, they are nearly indistinguishable from each other via either magnetic or density properties, though the basaltic andesite is overall slightly less dense. Therefore, we interpret most of the magnetic highs within the quadrangle as either basalt or basaltic andesite. There is a relation between high magnetic anomalies (for instance **PH1** and **PH2** in Fig. 1 on Plate 1) and the low gravity anomalies within the map that leads to the interpretation of highly magnetic basaltic andesite and basaltic flows filling low-lying areas at the time of their eruption. This is similar to interpretations in the Monroe 7.5-minute quadrangle to the northwest (Dragovich and others, 2011a,b). This finding is also consistent with the general interpretation of high-magnetization basalt-flow-dominated packages within the unit originating as more fluid, farther-travelled volcanic flows (potential source generally to the north of the Lake Joy quadrangle). There is a converse relation of an area with generally higher gravity and very low magnetism just to the north of the Carnation fault no. 1 (**KJ** in Fig. 1 on Plate 1). We believe this represents nonmagnetic Western mélange belt basement rocks north of the fault, very close to the surface, supporting reverse faulting along Carnation fault no. 1. In this and other areas of the map, locations of faults mapped in the field commonly coincide with mathematically determined maximum gradients computed for both the isostatic gravity and reduced-to-pole aeromagnetic anomaly data; therefore we use these relations to extend faults into regions of poor exposure.

Model A—(Plate 1, Fig. 2) has relatively sparse gravity data support and thus features less than 2 km wide along this line are not well supported by the gravity modeling (see gravity station location density in Fig. 1 on Plate 1). Only the general trend from lower gravity values in the west to higher values in the east is clear, but smaller localized gradients in the middle of the line are poorly constrained. It is likely that the far west end of the line has more complex stratigraphy than depicted (and as represented at the north end of Model B; Plate 1, Fig. 2), but because of the lack of constraint, all units are merged into a general Mount Persis unit with average properties similar to the basaltic andesite (unit Evapd). However, because of the magnitude of the magnetic high associated with this region, it is likely that the volcanic units are dominated by the more magnetic basaltic variants.

Model B—supports Carnation fault no. 1 as a major and long-lived tectonic feature of the region. The geophysical model strongly supports substantial offset of both the Western mélange belt basement/Mount Persis contact and the Mount Persis/Quaternary sediment contact across this fault; therefore, it has likely been active as far back as the Eocene and as recently as the Pleistocene and perhaps the Holocene (Appendices G and H). Its reverse sense of offset is corroborated by mapping of micro- and mesoscale structures within and to the north of the fault (Appendix H) and a significant number of reverse or thrust focal mechanisms for earthquakes spatially correlated with the fault trace (Appendix G). The southern end of Model B is similar to Model A in that it depicts a simple stratigraphy within the Mount Persis volcanic rocks; the Mount Persis unit is likely more complex in this subsurface area, but with the lack of surface constraint, we know only that on average, these rocks are quite magnetic and there is a large proportion of basalt and basaltic andesite within the stratigraphy. Though the details are uncertain, the bulk properties are not, because fitting both the magnetic high and the gravity low in this region requires a delicate balance between magnetic susceptibility and density of the rocks, which only fits with the more basaltic rocks of the region. Volcanic rocks filling lows on the basement surface along Model B also attests to the syn- or post-tectonic

nature of the volcanism, similar to our interpretations in the Monroe quadrangle (Dragovich and others, 2011a,b). Carnation fault no. 2 is also useful for fitting the magnetic data, but the interpretation is more tenuous, given uncertainties produced by poorly constrained regional trends in thickness of various Mount Persis volcanic units. The Griffin Creek fault north of Carnation fault no. 1 on Model B is also well constrained by the geophysics; a substantial thickness of less dense volcaniclastic rocks in the subsurface north of the fault is needed to fit the gravity data. The Western mélange belt metagabbro ($KJigb_w$) body at depth in the center of Model B is quite speculative. This dense body is necessary to offset the gravity low created by the overlying thick Quaternary stratigraphic section that is constrained by well data in the Tolt River valley. Also more speculative are the positions and properties of cataclasites (unit tz) along faults; they typically have low densities and are less magnetically susceptible than surrounding rocks, but their presence is largely not needed for modeling the gravity data. They are included on the basis of observed: (1) cataclasite or highly fractured rocks along faults within the present map area and along other faults in the region (Dragovich and others, 2007, 2009a,b,c, 2010a,b, 2011a,b), and (2) our contention that some of the faults are major and long-lived structures that have accumulated much permanent strain.

GENERAL MODEL UNCERTAINTIES

Due to the complexity of the subsurface geology, there are many possible subsurface rock geometries that will fit our geophysical data. Subunits of the volcanic rocks of Mount Persis (for example, geologic units Eva_p and Evc_p) could have numerous configurations that would fit the geophysical data; however, the basaltic units, andesite, and volcaniclastic rocks have physical properties fairly distinguishable from each other (Table D1 below); therefore, their general distribution across the models is quite well constrained.

Table D1. Physical property values for geologic units used in the geophysical models for the Lake Joy 7.5-minute quadrangle. SBD, saturated bulk density in g/cm^3 from hand sample; 95%, 95% confidence interval; SH, susceptibility from hand sample in SI units x 10^3; NH, number of hand samples; SO, susceptibility from outcrop measurements in SI x 103; NO, number of outcrop measurements; Mount Persis, volcanic rocks of Mount Persis of Tabor and others (1993). We have no physical property measurements for unit ~~M~~Φigd; therefore, it is not discussed here. This table includes data from 24 samples within the Lake Joy quadrangle in addition to other samples from the immediate region gathered from prior mapping efforts (Dragovich and others, 2007, 2009a,b,c, 2010a,b, 2011a,b).

Geologic unit	SBD	95%	SH	95%	NH	SO	95%	NO
Mount Persis (undivided), unit Evs_p	2.55	0.04	8.0	21.9	44	9.9	0.8	331
Mount Persis andesite, unit Eva_p	2.61	0.03	10.5	2.9	17	11.2	1.3	131
Mount Persis basalt, unit Evb_p	2.73	0.04	10.5	7.8	4	–	–	–
Mount Persis basaltic andesite, unit Eva_{pd}	2.65	0.06	11.9	3.6	7	17.3	1.3	71
Mount Persis breccia, unit $Evbx_p$	2.44	0.05	3.6	2.8	7	6.1	0.8	62
Mount Persis volcanic sedimentary rocks, unit Evc_p	2.38	0.10	2.7	1.6	7	7.4	1.1	8
Mount Persis tuff, unit Evt_p	2.15	–	1.8	–	1	2.1	0.5	59
Western mélange belt (undivided), unit KJm	2.70	0.05	4.0	6.0	30	6.4	1.4	242
Western mélange belt metagabbro, unit $KJigb_w$	2.78	0.17	23.2	38.7	4	20.6	12.8	14
Quaternary units (undivided), all units beginning in Q	2.01	0.16	5.2	6.8	6	2.6	0.1	575

Appendix E. Photographs of geologic features

Many of these photograph sites are significant or age sites located on Plate 1 or are discussed in other appendices.

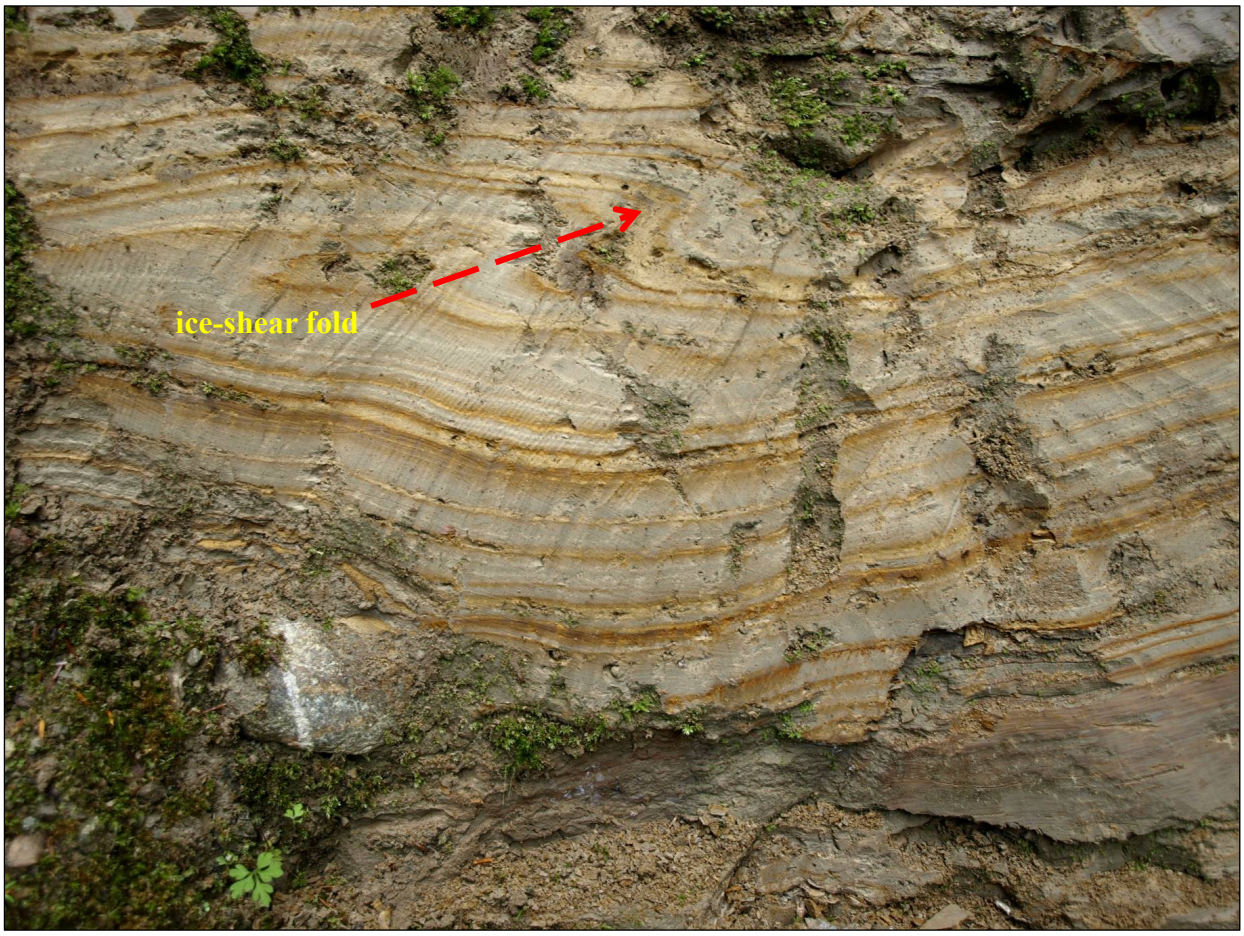

Figure E1. Site 202F, photo 10, shows a 3-m exposure of Vashon advanced glaciolacustrine deposits (unit Qgl_v). This cutbank exposure along an unnamed creek in the southwestern part of Lake Joy 7.5-minute quadrangle (sec.14, T25N R7E; N 47.64983819º, W -121.87180057º) is about 5 ft wide. Strata consist of well-sorted and compact silt and clay forming alternating laminae or thin beds. Some strata of silts contain scattered dropstones. Beds vary from light grayish-blue to rusty orange. Some of the beds are shear-folded into recumbent folds, likely as a result of Vashon Stade ice shear to the east-southeast (red arrow in the photo). See Figure E8 (site 204T, photo 288) just up river for sand dikes. Similar ice-shear features were observed to the southwest within a Tolt River cutbank (Fig. E2, site 28N, photo 160).

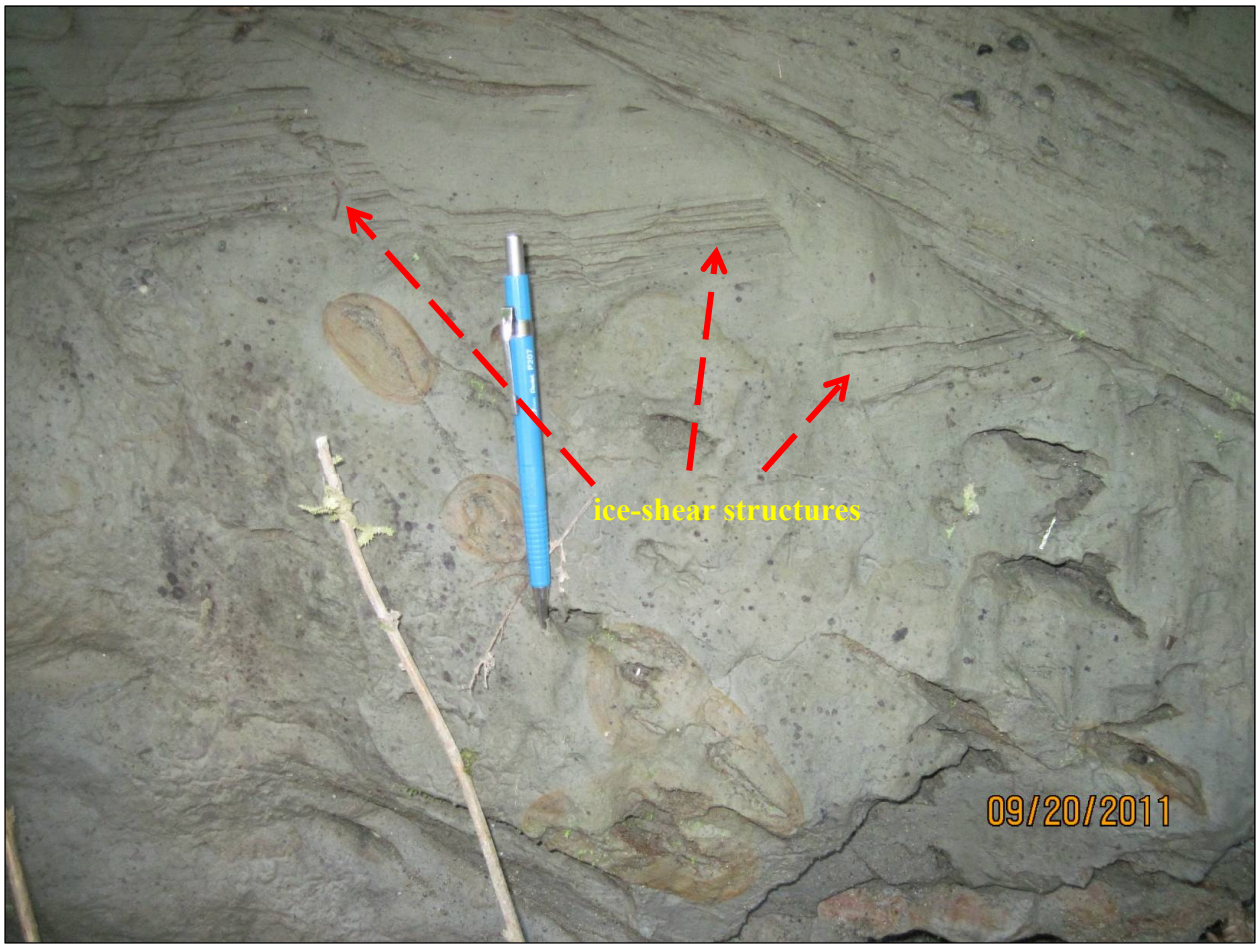

Figure E2. Site 28N, photo 160, a 2-m-high exposure in an unnamed creek flowing into the Tolt River in the southwestern part of the Lake Joy quadrangle (sec. 14, T25N, R7E; N 47.64883479º, W -121.8713746 º). Strata are composed of thickly bedded clay and silt and are overlain by laminated clay and silt typical of unit Qgl_V (Vashon Stade advance glaciolacustrine deposits). The laminated clays and silts are offset vertically along small faults (at red arrows). Deformation elsewhere near the site includes ductile overturned ice-shear folds of laminated silts and clays, suggesting the faulting here is also the result of ice-shear deformation.

Figure E3. Site 20A, photo 63, an abandoned quarry just off State Highway 203 in the central eastern edge of the Carnation 7.5-minute quadrangle (Fig. C1, site 20A; sec. 31, T26N R7E; N 47.69238733º, W -121.96427149º). The quarry consists of well-sorted, crossbedded, and planar-bedded sands and gravels that have inclusions of detrital peat and charcoal. The sand is moderately compacted and typically light gray to gray. Radiocarbon dating of wood from this outcrop yielded a date of >43,500 yr BP (Appendix A, sample 11-44D). We also obtained an OSL date of >250 ka for this nonglacial deposit (Table B1, sample 11-44D). Geochemical (Table C1, unit Qcpf; Fig. C1) and petrographic analysis of sands show that this deposit is ancient Snoqualmie River alluvium containing significant monocrystalline quartz, plagioclase, and potassium feldspar and lesser but significant hornblende, granitic lithic grains, and mica. Bedding strike varies around northeast, and the dip is dominantly ~20º southeast. The faults strike north-northeast to northeast and dip both northwest and southeast. These extensional faults have vertical offsets of up to 0.5 m. The north-northwest-trending Snoqualmie valley fault no. 3 (SVF-3) of Dragovich and others (2010a) is mapped very near this site. We suspect that these faults are extensional conjugate faults and (or) extensional splays within or adjacent to the right-lateral SVF-3. The probability that these faults are of tectonic origin supports the contention of Dragovich and others (2009a,b) that SVR-3 is a potentially active structure.

Figure E4. Site 28D, photo 143, significant site 28D (Plate 1), a cutbank on the Tolt River in the southwestern part of the Lake Joy 7.5-minute quadrangle (sec. 12, T25N R7E; N 47.67022298º, W -121.85790564º) where Carnation fault no. 1 crosses the Tolt River. The outcrop consists of protomylonitic to cataclastic andesite of the volcanic rocks of Mount Persis (mapped as unit tz). The occurrence of mylonitic fabrics in this location is consistent with other geologic evidence of an east-trending reverse fault we map as Carnation fault no. 1 through this area as discussed below (also see Plate 1 and Appendix H). The subtle fabric within the outcrop on the left side of the photo directly below the trees is the mylonitic to cataclastic fabric of the fault zone. See Figure E5, site 28D, photos 147 and 149 below, for detailed pictures and descriptions of the mylonites.

Site 28D, Photo 147

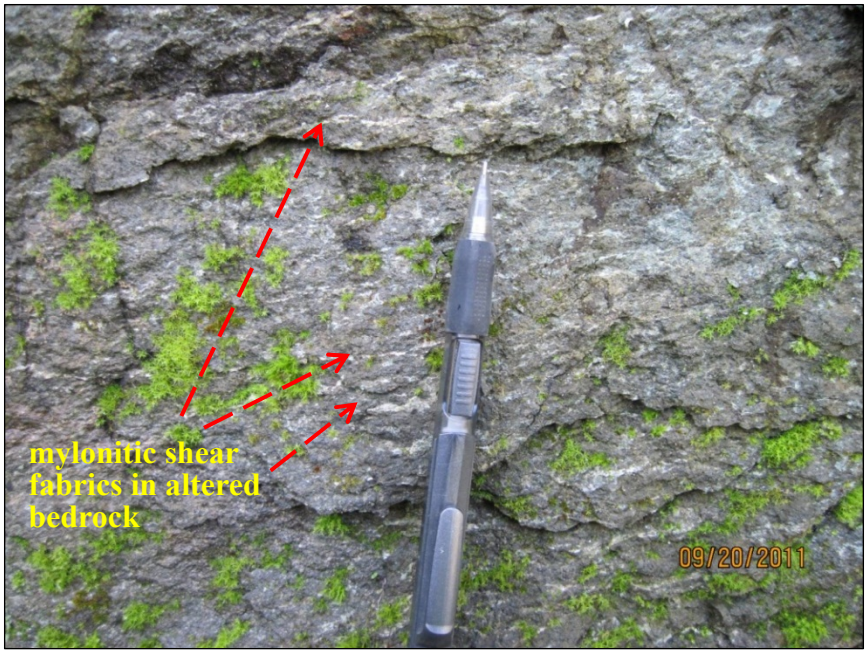

Site 28D, Photo 149

Figure E5. Site 28D, photos 147 & 149, close-ups of mylonites at significant site 28D (Plate 1), a large outcrop along the Tolt River in the southwestern part of the Lake Joy quadrangle. See photo143 (Fig. E4) above for an overview of the large river bank outcrop. Andesites at the site are protomylonitic and have a strong moderately south-dipping shear fabric. The mylonitic fabric is defined by planar alignment zones of intense, low-temperature shear producing the white "streaks" in photo 147 (see Appendix H). These planar streaks are zones of intense grain reduction. Photo 149 shows the east-striking and northerly dipping mylonitic fabric parallel to the trend of Carnation fault no. 1. Hydrothermal alteration is associated with this shear and has resulted in alteration of the andesite or basaltic andesite along this east-striking reverse fault.

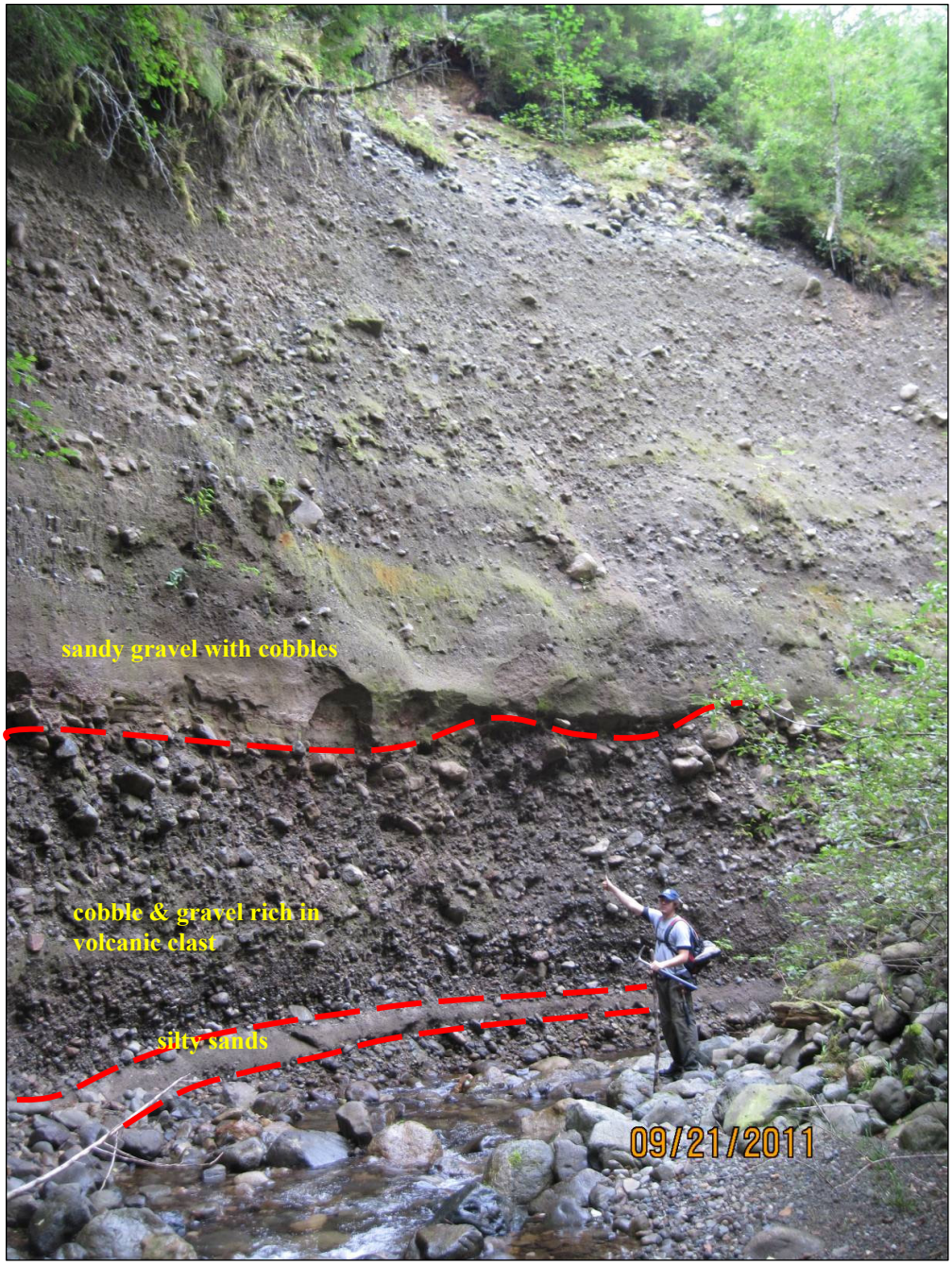

Figure E6. Site 29J, photo 169. Site 29J, ancient Tolt River deposits (unit Qc_{ol}) along Yellow Creek in the northeastern part of the Lake Joy 7.5-minute quadrangle (sec. 23, T26N R8E; N 47.72471541°, W -121.75699566°). A local easterly provenance is indicated for these fluvial deposits by the dominance of local clast types, such as basalt, andesite, and basaltic andesite from the volcanic rocks of Mount Persis. Strata here consist of alternating thickly bedded cobble gravel, sandy gravel, and silty sand beds. Boulders are scattered throughout the entire outcrop. Foreset-bedded bar deposits imply paleoflow directions generally to the southwest to northeast, similar to the modern Tolt River. A radiocarbon sample of plant material from nearby site 111C (N 47.72023503º, W -121.75452392º) yielded a date of 30,550 ±190 yr BP (Plate 1; Appendix A, Site 11-111C).

Figure E7. Site 37Q, photo 246, a gabbro rich in plagioclase and mafic minerals (unit Ei_p) in the northwest corner of the Lake Joy 7.5-minute quadrangle (sec. 16, T26N R8E; N 47.7377807º, W -121.78578297º). This outcrop is part of the Tolt intrusive complex consisting of dikes and sills of gabbro, basalt, and andesite (Plate 1). Some areas of the intrusive complex have a banded foliation that strikes northeast and dips ~45–60º NW and is likely a submagmatic to magmatic flow foliation.

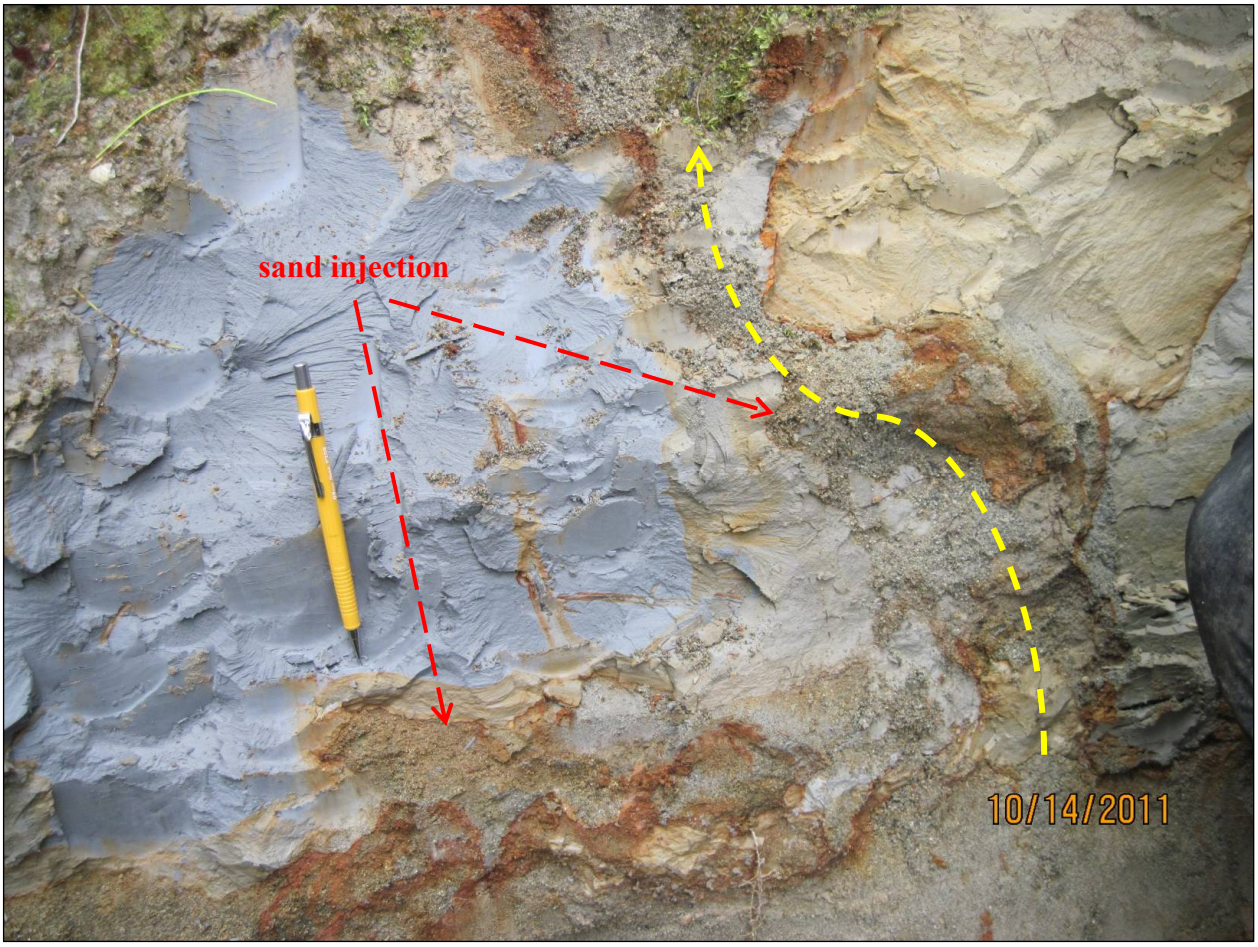

Figure E8. Site 204T, photo 288, Vashon Stade advance glaciolacustrine deposits (unit Qgl_V) at the top of a steep slope east of the Tolt River in the southwestern part of the Lake Joy 7.5-minute quadrangle (Plate 1; sec. 11, T25N R7E; N 47.66278479°, W -121.86382737°). The site is just south of Carnation fault no. 1 (Appendix H). Exposed here are thick beds of silt alternating with beds of sand that strike southwest and dip 8º NW. The silt beds are interrupted by subvertical sand dikes (yellow arrow) emanating from the lower sandy strata. These injection features could be the result of liquefaction due to seismic shaking.

Figure E9. Site 109H, photo 1257, dark grayish-blue, very stiff silt and clayey silt on the eastern bank of the Tolt River near the western edge of the Lake Joy 7.5-minute quadrangle (sec. 11, T25N R7E; N 47.66338217°, W -121.86581631°). The laminations in these Vashon Stade advance glaciolacustrine deposits (unit Qgl_v) have been complexly folded as a result of ice shear. The high density of the deposit suggests ice flow as the source of the deformation, not downslope creep of the beds towards the river. (Slumping or flow during mass wasting of beds tends to reduce the density of the beds, resulting in an overall soft deposit.)

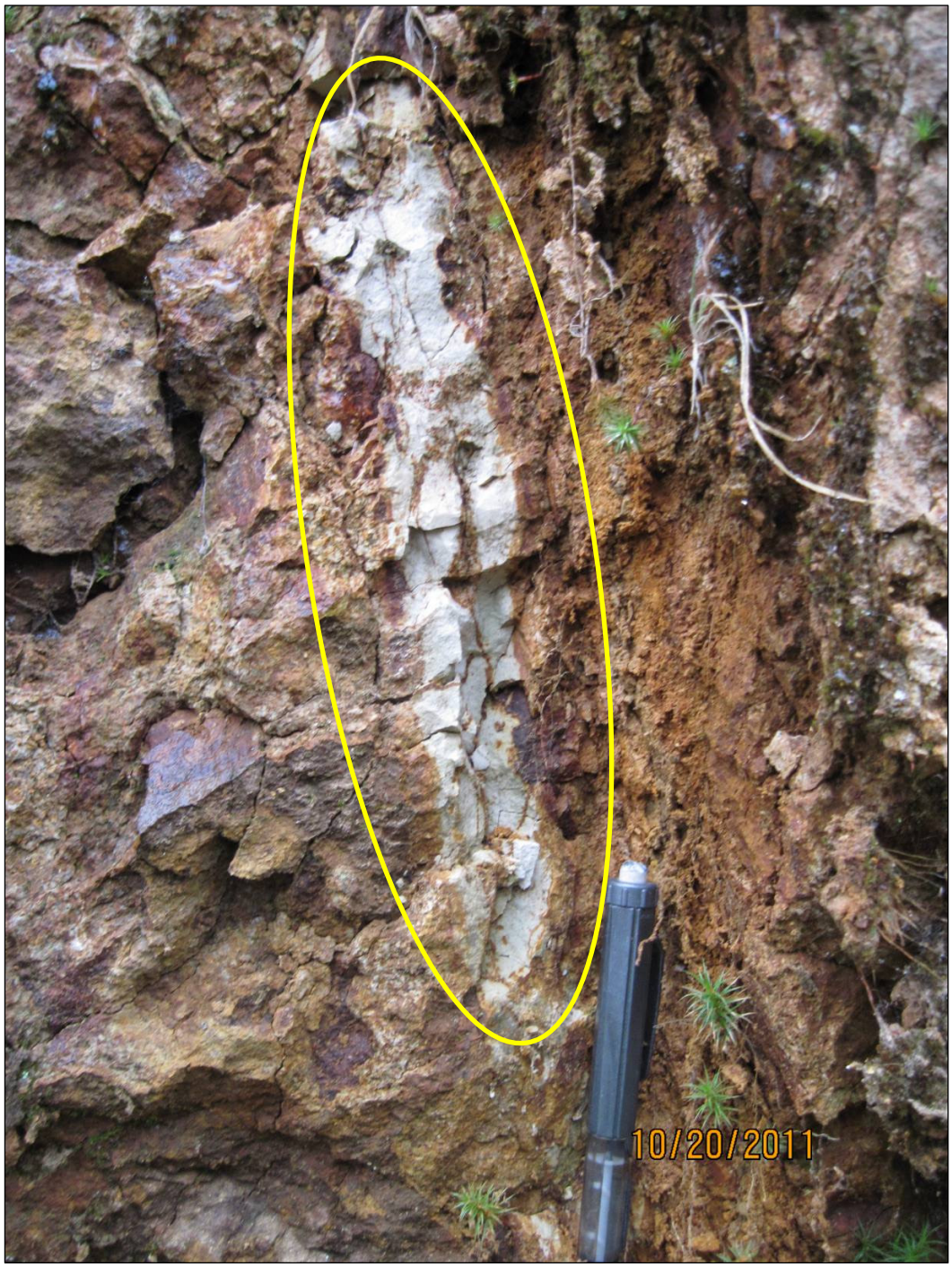

Figure E10. Site 205A, photo 301, a typical fractured reddish-tan to light tan porphyritic andesite (unit Eva_p, within the yellow circle) along a subvertical minor fault that strikes north just east of the Cherry Creek fault zone (CCFZ; Appendix H) in the northwest corner of the Lake Joy 7.5-minute quadrangle (sec. 19, T26N R8E; N 47.724544°, W -121.84082273°). Fault zones in the volcanic rocks of Mount Persis in the study area are common and display mild to complete propylitic alteration resulting in red, scarlet, to white ("bleached") rock exposures. In some areas, these hydrothermal zones are broad and mappable. (See unit Tz_h.)

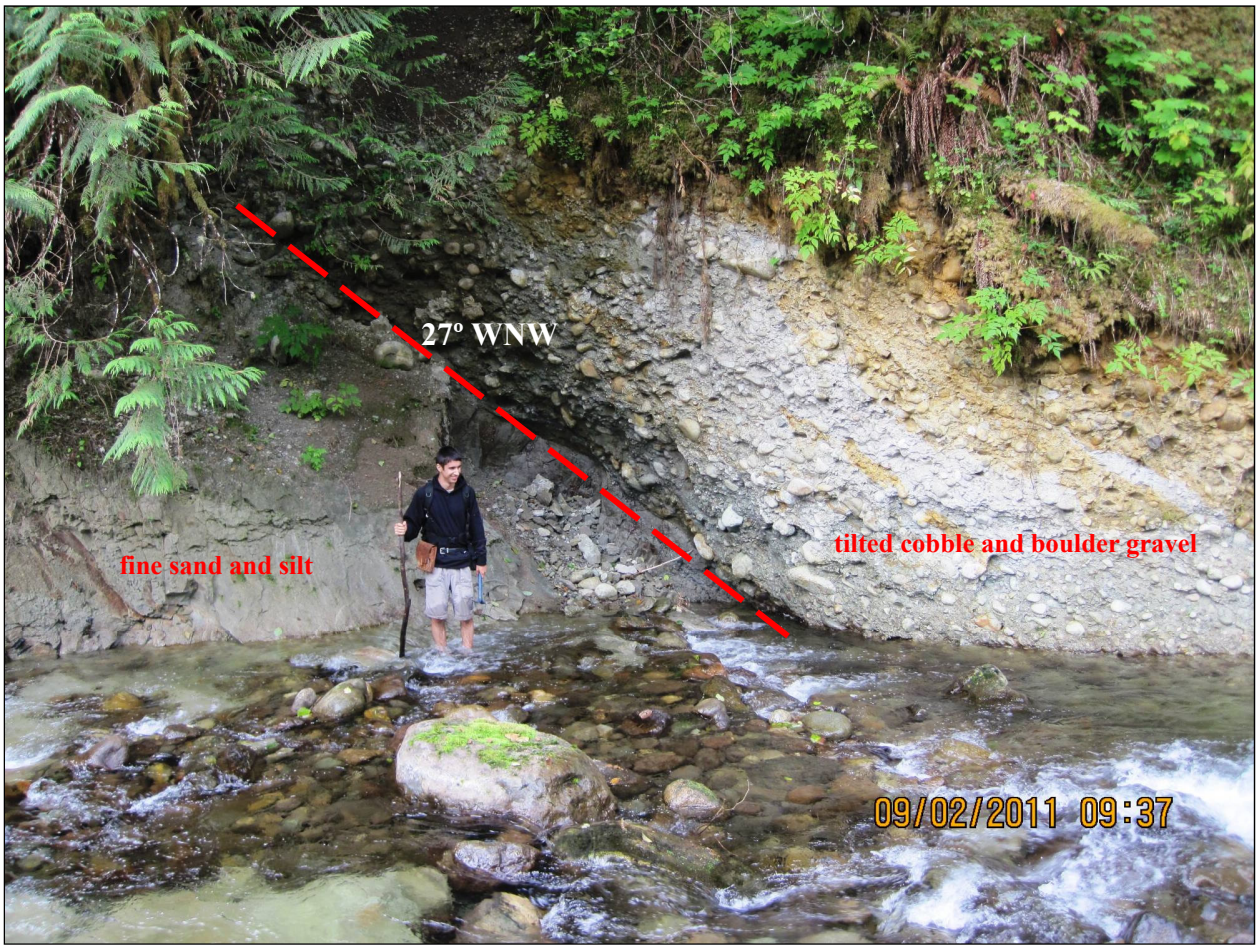

Figure E11. Site 108A, photo 937, ancient Tolt River alluvium on the south bank of the South Fork Tolt River in the northeastern part of the Lake Joy 7.5-minute quadrangle (Plate 1, sec. 33, T26N R8E; N47.69310088°, W -121.79326071°). Ancient Tolt River alluvium here consists of thick to very thickly bedded compact beds of alternating cobble gravel and boulder gravel with interbedded sand lenses; the lower beds here are of fine sand and silt (unit Qc_{hmp}). Clasts are dominated by basalt, andesite, and basaltic andesite, suggesting a local provenance. The sand and gravel clasts are strongly weathered and display distinct rinds of clay. The tilted bedding in the photo is striking SSW and dipping 27° WNW. (See Fig. E12 for radiocarbon age analyses at this site.)

Figure E12. Site 108A, photo 1029, a log within ancient Tolt River alluvium (unit Qc_{hmp}) along the South Fork Tolt River in the Lake Joy 7.5-minute quadrangle (sec. 33, T26N R8E; N 47.69310088°, W -121.79326071°) at the same site as photo 937 above. Part of this log was collected for radiocarbon dating. The sample yielded an age of >43,500 yr BP (Appendix A, sample 11-108A). The outcrop consists primarily of cobble and boulder gravel with interbedded sands. Weathering characteristics suggest that these ancient fluvial deposits are older than the Double Bluff glaciation. (See OSL data for unit Qc_{hmp} in the Lake Joy 7.5-minute quadrangle in Table B1.)

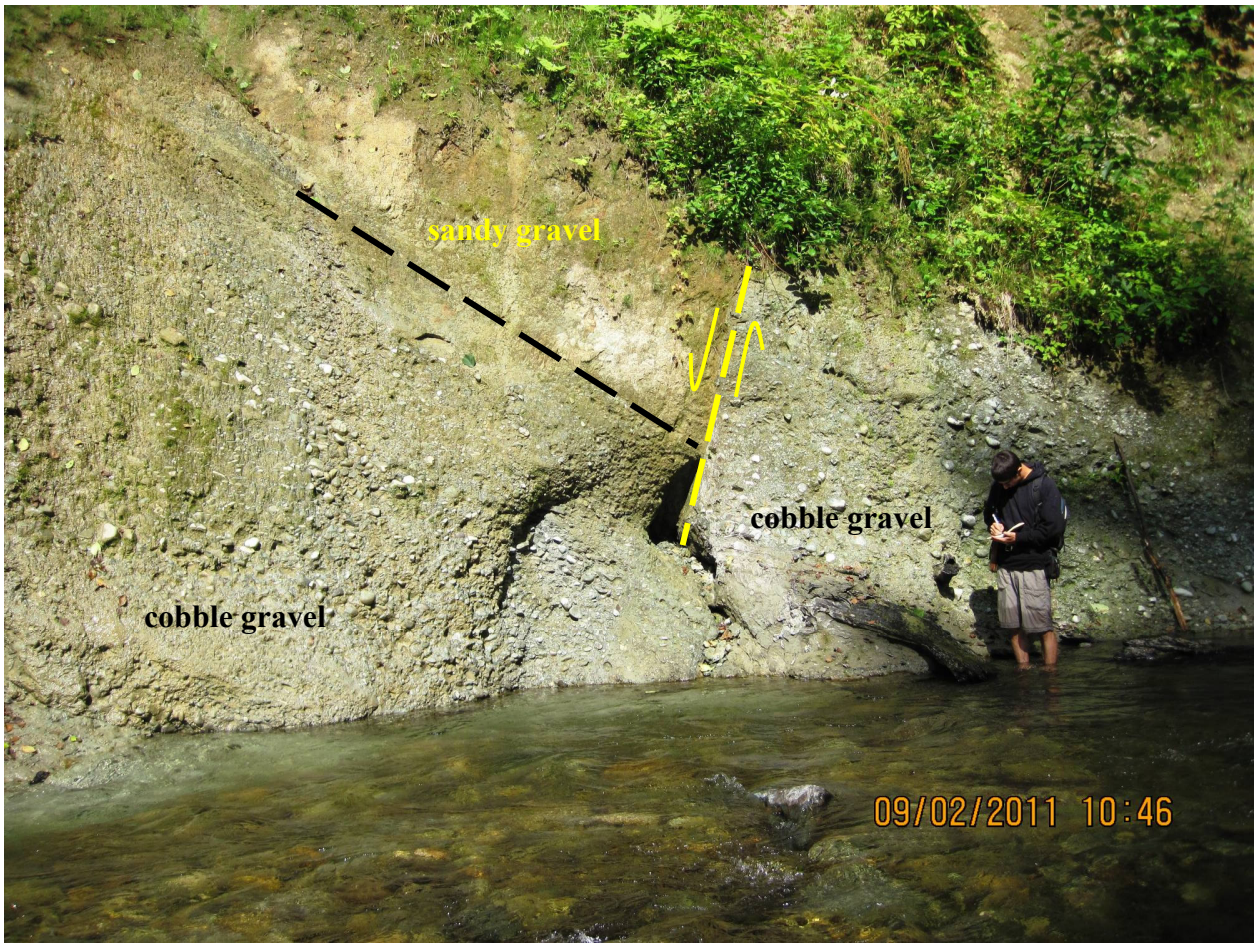

Figure E13. Site 108D, photo 1046, an outcrop of mostly weathered, thickly to very thickly bedded cobble gravel and pebbly sand on the north bank of the South Fork Tolt River in the east-central part of the Lake Joy 7.5-minute quadrangle (Plate 1; sec. 33, T26N R8E; N 47.69304866°, W -121.79426411°). The strata are similar to site 108A (photos above). A steeply dipping fault (yellow dashed line) has an offset of ~2 m and displaces the unit Qc_{hmp}. The fault strikes southwest, dips 75º NW, and is subparallel to nearby Tokul Creek fault no. 4 (Appendix H). The orientation and style of the fault and tilted bedding suggest that this ancient alluvial unit has been tectonically deformed, that is, the sense of offset of the fault suggests the fault is not related to landsliding. (Geochemical data for unit Qc_{hmp} are in Appendix C; Table C1, site 108C.)

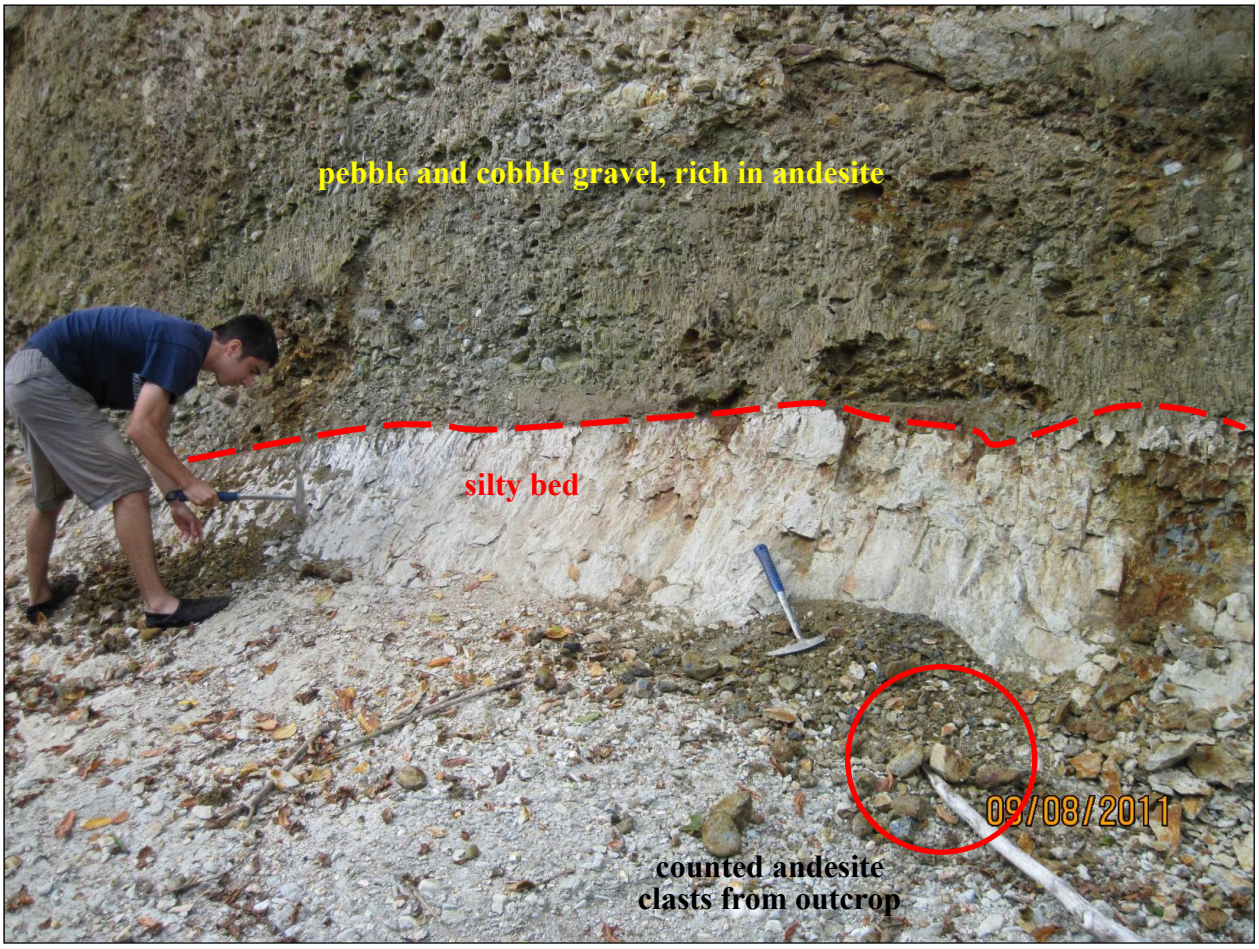

Figure E14. Site 26F, photo 130, ancient Tolt River alluvium (unit Qc_{hmp}) on the north bank of the North Fork Tolt River in the middle of the Lake Joy 7.5-minute quadrangle (Plate 1; sec. 32, T26N R8E; N 47.69298806°, W -121.81301485°). Similar to other exposures of the ancient Tolt River alluvium, this exposure is dominated by very thickly bedded pebble and cobble gravel with thick beds of gray silt containing detrital organic fragments including flattened logs. Gravel clasts are dominated by andesite, basaltic andesite, and basalt (~70%) derived from the volcanic rocks of Mount Persis. An infinite radiocarbon age of >43,500 yr BP was obtained from a log at this site. (See Plate 1, Fig. E15 [age site 26F, photo 134] or Appendix A for additional radiocarbon sample details.)

Figure E15. Site 26F, photo 134, an in-place log in unit Qc_{hmp} on the South Fork Tolt River in the middle of the Lake Joy 7.5-minute quadrangle (Plate 1; age site 26F; sec. 32, T26N R8E; N 47.69298806°, W -121.81301485°). This log is just out of sight and directly to the left in the outcrop shown in photo 130 (Fig. E14) above. This deposit is ancient Tolt River alluvium dominated by thick beds of pebble or cobble gravel. The ~2-kg log contained no microscopic evidence for contamination (for example, rootlets) and yielded a radiocarbon age of >43,500 yr BP (Appendix A, sample 11-26F).

Appendix F. Sedimentary provenances and basin inversion for Quaternary deposits in and around the Lake Joy 7.5-minute quadrangle

Dragovich (2007) and Dragovich and others (2009a,b,c, 2010a,b, 2011a,b) supply sand point-count data for various Quaternary geologic units, including Holocene Snoqualmie, Skykomish, and Tolt River alluvium, Vashon glacial units, sediments of the Olympia nonglacial interval, Whidbey Formation, Hamm Creek unit, and Possession glacial outwash for the Fall City, Snoqualmie, North Bend, Carnation, and Monroe quadrangles, respectively. Provenances are defined by compositional data derived from sand point-count data, general petrographic observations, and sand geochemistry, as well as field data and observations. We supplemented Quaternary provenance information for these quadrangles with the petrographic study of 21 mounted sand thin-sections, as well the geochemistry of 16 sand samples (Appendix C) obtained from the study area. As shown in Table F1 below, Quaternary strata in the Snoqualmie valley and Monroe/Lake Joy areas are assigned to four major sedimentary provenances: (1) nonglacial Snoqualmie River basin southeastern source (SP), (2) nonglacial local eastern source (LP), including ancient fluvial deposits with a distinct local volcanic rocks of Mount Persis source, (3) nonglacial Puget Group northern source (PG), and (4) glacial mixed northern source (GP). Modern Snoqualmie River alluvium (unit Qa) is modally similar to ancient Snoqualmie River alluvium, such as that in the Whidbey Formation (unit Qc_{ws}), and these units have a distinct Snoqualmie River basin (SP) provenance. Additionally, Dragovich and others (2011a,b) correlated some ancient SP with the Hamm Creek unit. They also surmised in the field and confirmed petrographically, geochemically, and geochronologically that most Pleistocene nonglacial units in the western part of the Monroe quadrangle are ancient Skykomish River alluvium. These nonglacial units have a provenance very similar to the ancient and modern Snoqualmie alluvium because the Skykomish River has a source area similar to that of the Snoqualmie River basin. SP strata for the Snoqualmie basin have a distinct granodiorite to granite batholith provenance that has significant monocrystalline quartz (~10–20%), plagioclase, lesser but significant granitic lithic clasts, potassium feldspar, hornblende, and mica. The ratio of monocrystalline quartz to polycrystalline quartz is distinctly high and comparable to SP nonglacial (for example, unit Qc_{ws}) and modern Skykomish and Snoqualmie River alluvium west and north of the map area. Geochemically, SP is very similar to modern alluvium and can be distinguished from glacially derived samples (Appendix C).

We suspect uplift or tilting of ancient alluvium within the Lake Joy quadrangle along the Carnation fault no. 1 and other reverse faults. (See discussion of 'pop-up' structures in Dragovich and others, 2011a,b, as well as for Carnation fault no. 1 and the Tolt River anticline in Appendices G and H.) Distinct SP sands are anomalously high (uplifted?) directly south of the Carnation fault no. 1 and appear to be folded around the Tolt River anticline (Cross Section B). In this scenario, ancient alluvium is deposited in a structural basin and uplifted by later faulting. This is indicated by (1) anomalous thickness, (2) tilting, (3) folding, and (or) (4) anomalously high elevation of the SP and LP strata. These thick SP stratigraphic sections represent 'inverted basins' and are the result of strike-slip or reverse faulting within the southern Whidbey Island fault zone (Dragovich and others, 2009a,b, 2010a,b). In this model, we hypothesize that the thick SP alluvium west of the study area formed in a transtensional basin within a broad active fault zone. The basin was inverted when the SP sediments underwent uplift and folding during transpressional deformation.

Table F1. Major Quaternary sedimentary provenances in the Lake Joy, Monroe, Carnation, North Bend, Fall City, and Snoqualmie 7.5-minute quadrangles. Ancient nonglacial provenances for primary Quaternary geologic units are mostly fluvial deposits of major or minor rivers. RMFZ, Rattlesnake Mountain fault zone; SWIF, southern Whidbey Island fault zone; TCFZ, Tokul Creek fault zone; CF, Carnation faults no.1 and no. 2.

Group	Geologic unit(s)	Provenance	Notes
SP (Snoqualmie or Skykomish River basin Provenance)	Qa (Snoqualmie and Skykomish Rivers), Qc_o, Qc_{ws}, Qc_h, Qc_{pf}	Snoqualmie basin provenance with generally southeastern fluvial sources; rivers flowing generally northwest along RMFZ–SWIF over time (Dragovich and others, 2010a,b). Ancient and modern Skykomish River alluvium is petrographically similar to ancient and modern Snoqualmie River alluvium.	Nonglacial units that contain abundant mono-crystalline quartz and significant potassium feldspar and plagioclase and minor but distinct granitic lithic grains, biotite, and (or) hornblende; the major bedrock source is the Snoqualmie batholith that covers much of the headwaters of the Snoqualmie River. Rivers were trapped among strands of the RMFZ–SWIF during nonglacial or interglacial intervals (Dragovich and others, 2010a,b). Thick deposits of ancient and modern Snoqualmie River alluvium are found in postulated transpressional basins controlled by the Carnation fault no. 1 and the Tolt River fault.
LP (local provenance)	Qa (Tolt River), Qc_{ol}, Qc_{hmp}	Local provenance is within 40 to 100 mi^2 of its Tolt River basin origin with generally eastern sources; rivers flow to the west from the Cascade foothills. Deposited in alluvial, alluvial fan, and swamp settings and likely represent small ancient tributary basin deposits of limited extent. Modern Tolt River alluvium is compositionally similar to ancient Tolt River alluvium in the Lake Joy quadrangle. Unit Qc_{hmp} (originally mapped during this Lake Joy geologic map study) is ancient alluvium with a distinct local Mount Persis volcanic provenance. (See volcanic rocks of Mount Persis.) Also see unit Qc_{ol} in Dragovich and others (2010a,b, 2011a,b).	Nonglacial units that contain significant local lithic grains including meta-argillite, volcanic lithic grains, and metasandstone. The primary sources of LP clasts are the volcanic rocks of Mount Persis and the Western mélange belt. Sands are typically lithic rich (as seen in the eastern part of the Carnation quadrangle; Dragovich and others, 2010a,b). Sands along the Tolt River in the Lake Joy quadrangle have a similar composition due to the reworking of older glacial and nonglacial deposits. Ancient Tolt River alluvium may interfinger with ancient Snoqualmie River alluvium locally and may include alluvium fan deposits comparable to the modern Tolt River fan at Carnation.
PG (Puget Group provenance)	Qc_{wp}	Puget Group provenance with fluvial sources to the south and southwest originating from the Seattle uplift (for example, Tiger Mountain). Similar lithologically to LP. Primarily found toward the ancient Snoqualmie River west of the current map area.	Whidbey Formation (nonglacial) strata in the southwestern portion of the Carnation quadrangle (Dragovich and others, 2010a,b) are sourced by the Puget Group and contain significant andesite detritus, as well as some arkosic (feldspathic) sandstone, siltstone from the Tukwila, Renton, and Tiger Mountain Formations. Sands are lithic rich. (See Appendices 2–4 in Dragovich and others, 2010a, for more information.)
GP (Glacial provenance)	Qgl_r, Qgos, Qgod, Qgof, Qgic, Qgog, Qgt_v, Qga_v, Qgl_v, Qgt_p, Qgo_p, Qgl_p, Qgd_d, Qgd_{pd}	Glacial northern provenance locally mixed with some eastern and northeastern Cascade provenance (particularly for some Vashon Stade recessional deposits sourced by ice-marginal meltwater).	Glacial units contain various lithic clast types, including high-grade metamorphic clasts, and have a high polycrystalline/monocrystalline quartz ratio and less potassium feldspar when compared to local Cascade sources. Sand grain types tend to be polymictic or varied.

Appendix G. Earthquake epicenters, hypocenters, and focal mechanisms in and near in the Lake Joy 7.5-minute quadrangle

To better understand the relations among faults mapped using our geologic/geophysical interpretations and sense of fault movement at depth, we analyzed earthquake data for the Lake Joy quadrangle general area. Plate 2 shows about 350 hypocenters and 45 focal mechanisms obtained from the Advanced National Seismic System (ANSS) website (at http://quake.geo.berkeley.edu/anss/catalog-search.html) and Pacific Northwest Seismic Network (PNSN) ftp site (ftp://ftp.ess.washington.edu/pub/seis_net/focal.AMcards), respectively, for the Lake Joy 7.5-minute quadrangle area. The hypocenter depths are less than 40 km and are interpreted as crustal, nonsubduction events. Note that seven of the 45 focal mechanisms have two solutions (S. Malone and T. Yelin, PNSN, written commun., 2011). The P and T axes determined from these data constrain focal mechanism plots on stereonets and are used to calculate rakes (Lees, 1999, 2007, 2008). The focal mechanism data are listed in Tables G1 and G2 (below) for the Lake Joy 7.5-minute quadrangle and surrounding area; the reported focal mechanism solutions are derived from pick files provided by PNSN (T. Yelin, PNSN, written commun., 2011). The preferable fault plane solutions are denoted as black arrows on beach ball plots on Plate 2, as well as by bold data in Tables G1 and G2. Also shown are the fault kinematics of our preferred fault plane solutions in Table G1 (right column). We plotted the hypocenters using ZMAP as a tool for visualizing the seismicity patterns (Wiemer, 2001; Wyss and others, 2001). The hypocenter cross sections shown on Figures G1 and G2 project local seismic events onto cross section planes A–A′ and B–B′. These are the same cross section planes as the lithologic and geophysical cross sections shown on Plates 1 (also see Plate 2 for these cross section lines relative to the epicenters).

We compare the earthquake data to the kinematics of three major fault zones in the quadrangle—the Cherry Creek, Tokul Creek, and Carnation fault zones (see Appendix H for a structural overview of the individual fault zones, including the original reference source mapping of these structures). Much of the PNSN hypocenter and focal mechanism data shows a strong correlation with the kinematics of the fault zones we determined in the field.

CHERRY CREEK FAULT ZONE

The Cherry Creek fault zone (CCFZ) is mapped in the northwest corner of the study area (Plates 1 and 2; Appendix H). The Duvall earthquake swarm (M5.2) of the May 2, 1996, was located directly north of the Lake Joy 7.5-minute quadrangle; the earthquake hypocenters (max. M_L=5.3 or Md=5.4) originated mostly at a shallow depth (~2–8 km) along the CCFZ (Dragovich and others, 2010a,b, 2011a,b)(see Plate 2 of Dragovich and others, 2011b, for detailed mapping of the Duvall earthquake hypocenters). These earthquakes occurred along several faults within the CCFZ and are consistent with a left-lateral strike-slip fault zone flower structure and fault displacements and strain partitioned between both (1) left-lateral, high-angle, northeast-trending faults, *and* (2) lower-angle, northeast-trending reverse faults or thrusts in the CCFZ (Dragovich and others, 2011a,b). Dragovich and others (2011b) proposed that the thrusts and reverse faults within the CCFZ are anastomosing structures that link the high-angle faults, and thus the dominance of thrust and strike-slip focal mechanisms suggests partitioning of displacements between high-angle strike-slip faults and more shallowly dipping faults and that these faults define a flower structure. Left-lateral northeast displacement is indicated by the field mapping and outcrop structures that show that the CCFZ is dominated by northeast-trending fault splays with strike-slip kinematics. This is supported by the focal mechanism data presented in Tables G1 and G2 and Plate 2, where ~70 percent of the focal mechanisms in the Lake Joy portion of the CCFZ have a left-lateral or left-lateral-oblique northeast-trending fault solution.

TOKUL CREEK FAULT ZONE

The Tokul Creek fault zone (TCFZ) of Dragovich and others (2009b,c) cuts the southeastern part of the map area and includes the newly mapped Tolt River fault in the TCFZ (Plates 1 and 2). Similar to the CCFZ, the TCFZ is a probable left-lateral strike-slip fault zone forming a long, straight regional fault zone lineament (Appendix H). This scenario is supported by focal mechanism data that show ~70 percent of the focal mechanisms in the CCFZ in or very near the present map area have a left-lateral or left-lateral oblique northeast-trending fault plane solution (Tables G1 andG2 and Plate 2). This includes northeast-trending faults within the TCFZ in the southeastern most

part of the map area and in the northeastern part of the Snoqualmie quadrangle directly to the south of the current study area. The spatial correlation of some of the fairly shallow earthquake hypocenters with the TCFZ fault strands, as well as the relatively high density of earthquakes in this area, is suggestive of activity along this strike-slip fault zone, particularly in areas that have a tight clustering of epicenters near a mapped fault strand (Plate 2). A Quaternary tectonic fault displacing unit Qchmp deposits at significant site 108D (Plate 1; Appendix H) also suggests active faulting along the western part of the TCFZ in the center of the quadrangle. This area is the general location of the 1932 Tolt River earthquake studied by Bradford and Waters (1934), and the center of their Tolt River earthquake intensity VI contour coincides with significant site TQ2 on Plate 1. This intensity contour was partially based on the felt report—"practically impossible to stand"—at significant site TQ1 near the Regulating Basin on Plate 1. This mapping and earthquake information may indicate that Tokul Creek fault no. 4 or other TCFZ faults are currently active or potentially active.

CARNATION FAULT ZONE

Carnation faults no. 1 and no. 2 (CF-1 and CF-2) are an east-trending reverse fault (CF-1) and normal fault (CF-2), respectively, that form the Carnation fault zone (CFZ) as outlined in Appendix H. CF-1 appears to be spatially coincident with seismic activity, including small moderately shallow earthquakes (Plate 2 and Fig. G1). This seismic activity, as well as the deformation of Pleistocene deposits across the Tolt River anticline, is discussed in Appendix H. Our mapping of CF-1 as a reverse fault is supported by the high percentage of thrust or thrust-oblique focal mechanism solutions that have a general east strike and epicenters that occur along and north of the CFZ. (About 75 percent of earthquakes along the CFZ have this solution on Plate 2 and Fig. G1, assuming an east–west nodal plane). However, there is also a strong left-lateral or left-lateral-oblique component in these mechanisms using the alternate northeast-trending nodal plane, perhaps suggesting the reverse fault is a more complex structure. Another source of uncertainty is the dip of CF-1. The hypocenter data suggest a steep structure (Fig. G2), whereas some of the field mapping suggests a more moderately north-dipping structure, a contradiction leading to uncertainty about the detailed geometry of CF-1. Given all available data, CF-1 as a reverse fault may be a composite structure with both (1) shallowly dipping reverse splays (Appendix H) and (2) minor northeast-trending, left-lateral strike-slip faults that offset the master reverse fault.

Table G1. Focal mechanism data grouped by identified structures for the Lake Joy quadrangle area. (Also see Plate 2 and Table G2 for additional information about the focal mechanisms, which are listed by focal mechanism ID number). This table provides the focal mechanism ID number, as well as the strike, dip, and rake for both of the focal mechanism solutions' nodal planes. Structure is the interpreted structural domain encompassing the hypocenter; these domains include the Cherry Creek fault zone (CCFZ), Carnation fault zone (CFZ), Tokul Creek fault zone (TCFZ), and the poorly understood area around the Griffin Creek fault zone (GCF). Interpreted fault kinematics provides the preferred fault plane solution determined from the structural domain obtained in the field. The bold data are the preferred focal mechanism fault plane and fault rake orientations. Strike1=Faz-90 and Strike2= Gaz-90. (See Table G2 for Faz and Gaz values).

Focal mechanism ID number	Strike 1 (°) (=Faz-90)	Dip1 (°)	Rake1 (°)	Strike 2 (°) (=Gaz-90)	Dip 2 (°)	Rake 2(°)	Structure	Interpreted fault kinematics
FM 38	105	80	170	**197**	**80**	**10**	CCFZ	left-lateral strike-slip
FM 24	**40**	**70**	**-30**	141	62	-157	CCFZ	unknown (oblique – left-lateral strike-slip)
FM 16_2	-90	90	-170	**180**	**80**	**0**	CCFZ	left-lateral strike-slip
FM 19	-65	80	170	**27**	**80**	**10**	CCFZ	left-lateral strike-slip
FM 20	-75	80	180	**195**	**90**	**-10**	CCFZ	left-lateral strike-slip
FM 8_2	**10**	**85**	**-30**	103	60	-174	CCFZ	left-lateral strike-slip
FM 16_1	95	85	140	**189**	**50**	**6**	CCFZ	thrust (oblique – left-lateral strike-slip)
FM 17	**35**	**90**	**70**	-55	20	180	CCFZ	thrust (oblique – left-lateral strike-slip)
FM 8_1	95	50	150	**205**	**67**	**44**	CCFZ	thrust (oblique – left-lateral strike-slip)
FM 6	**40**	**20**	**60**	252	73	100	CCFZ	thrust (oblique – unknown)
FM 23	**30**	**20**	**-50**	168	75	-103	CFZ	unknown
FM 12	**55**	**90**	**10**	-35	80	180	CFZ	left-lateral – strike-slip (unknown)
FM 32_1	20	85	-20	**112**	**70**	**-175**	CFZ	right-lateral – strike-slip
FM 15	**115**	**85**	**170**	206	80	5	CFZ	right-lateral – strike-slip (unknown)
FM 27	75	55	90	**255**	**35**	**90**	CFZ	thrust
FM 9	60	50	70	**270**	**44**	**113**	CFZ	thrust
FM 29_2	35	65	20	**-64**	**72**	**154**	CFZ	thrust (oblique – right lateral strike-slip)
FM 10	95	40	131	**227**	**61**	**61**	CFZ	thrust (oblique)
FM 13	**85**	**80**	**80**	-50	14	134	CFZ	thrust (oblique)
FM 14	15	85	-50	**111**	**40**	**-172**	CFZ	thrust (oblique)
FM 18_1	**105**	**80**	**130**	207	41	16	CFZ	thrust (oblique)
FM 18_2	25	90	60	**-65**	**30**	**180**	CFZ	thrust (oblique)
FM 2	130	60	150	**236**	**64**	**34**	CFZ	thrust (oblique)
FM 29_1	**-75**	**60**	**130**	46	48	42	CFZ	thrust (oblique)
FM 30	95	35	139	**220**	**68**	**62**	CFZ	thrust (oblique)
FM 32_2	25	45	10	**-72**	**83**	**135**	CFZ	thrust (oblique)
FM 35	115	30	130	**251**	**67**	**70**	CFZ	thrust (oblique)
FM 37	**60**	**35**	**0**	-30	90	125	CFZ	thrust (oblique)
FM 5	30	55	30	**-78**	**66**	**141**	CFZ	thrust (oblique)
FM 7	25	90	-50	**115**	**40**	**180**	CFZ	thrust (oblique)
FM 28	110	45	130	**240**	**57**	**57**	CFZ	thrust
FM 31	**25**	**70**	**0**	-65	90	160	GCF	strike-slip (unknown)
FM 11	**20**	**80**	**60**	-87	31	160	GCF	thrust (oblique) (unknown)
FM 25	80	55	110	**228**	**40**	**64**	GCF	thrust (oblique) (unknown)
FM 36	**130**	**85**	**-90**	-50	5	-90	TCFZ	unknown
FM 1_2	-70	90	170	**20**	**80**	**0**	TCFZ	left-lateral – strike-slip
FM 21	**15**	**75**	**-30**	113	61	-163	TCFZ	left-lateral – strike-slip
FM 22	**15**	**70**	**-20**	112	71	-159	TCFZ	left-lateral – strike-slip
FM 3_1	**60**	**85**	**50**	-36	40	172	TCFZ	left-lateral – strike-slip
FM 3_2	-30	80	-170	**238**	**80**	**-10**	TCFZ	left-lateral – strike-slip
FM 4	125	45	-150	**13**	**69**	**-49**	TCFZ	left-lateral – strike-slip
FM 1_1	**25**	**65**	**30**	-79	63	152	TCFZ	thrust (oblique – left-lateral strike-slip)
FM 33	135	60	140	**248**	**56**	**37**	TCFZ	thrust (oblique – left-lateral strike-slip)
FM 26	**50**	**70**	**30**	-51	62	157	TCFZ	thrust (oblique)
FM 34	85	50	30	**-25**	**67**	**136**	TCFZ	thrust (oblique)

Table G2. Focal mechanism AM card data for fault plane solution analyses in the Lake Joy quadrangle area (Plate 2; www.pnsn.org; T. Yelin, PNSN, written commun., 2011). See Table G1 for additional focal mechanism data. Pick-file name, the unique identifier for the pick files containing earthquake phase data and focal mechanism solutions, as reported by the PNSN, encodes the earthquake date information [for example, 73060911113p is year (1973), month (06), day (09), hour (11), and minute (11) in the pm]. See ftp://ftp.ess.washington.edu/pub/seis_net/focal.readme for an explanation of the F, G, U, V, P and T azimuths (az), dip or plunge data, and the AM card. F, azimuth of dip and dip of first possible fault plane; G, azimuth of dip and dip of second possible fault plane; U, azimuth and plunge of the pole to the F-plane; V, azimuth and plunge of the pole to the G-plane; P, azimuth and plunge of the axis of maximum principal stress; T, azimuth and plunge of the axis of minimum principal stress. Azimuth of dip is given rather than strike of F or G; if F is the fault plane, G is the auxiliary plane and V is the slip direction on the fault. If G is the fault plane, F is the auxiliary plane and U is the slip direction on the fault. The bold data are the preferred focal mechanism fault plane orientations also described in Table G1.

Focal mechanism ID number	Latitude & Longitude (decimal degree)	F az (°)	F dip (°)	G az (°)	G dip (°)	U az (°)	U dip (°)	V az (°)	V dip (°)	P az (°)	P dip (°)	T az (°)	T dip (°)	Depth (km)	Mag. (M_c)
FM 1_1; 73060911113p	N 47.5987 W-121.8120	**115**	**65**	11	63	295	25	191	27	153	1	244	38	5.97	3.3
FM 1_2; 73060911113p	N 47.5987 W-121.8120	20	90	**110**	**80**	200	0	290	10	335	7	245	7	5.97	3.3
FM 2; 73110623112p	N 47.6747 W-121.8170	220	60	**326**	**64**	40	30	146	26	2	3	95	41	14.96	2.1
FM 3_1; 77013015003p	N 47.5992 W-121.7458	**150**	**85**	54	40	330	5	234	50	181	29	295	37	10.46	2.8
FM 3_2; 77013015003p	N 47.5992 W-121.7458	60	80	**328**	**80**	240	10	148	10	194	14	284	0	10.46	2.8
FM 4; 83040303433p	N 47.6123 W-121.7587	215	45	**103**	**69**	35	45	283	21	327	49	74	14	12.70	2.7
FM 5; 86033001330p	N 47.6643 W-121.8660	120	55	**12**	**66**	300	35	192	24	338	7	242	44	17.62	2.2
FM 6; 88061611045p	N 47.7072 W-121.8973	**130**	**20**	342	73	310	70	162	17	333	27	177	61	7.51	3.1
FM 7; 89011714090p	N 47.6407 W-121.8858	115	90	**205**	**40**	295	0	25	50	328	33	82	33	20.42	1.7
FM 8_1; 93081205325p	N 47.7200 W-121.8755	185	50	**295**	**67**	5	40	115	23	326	11	68	46	18.77	2.4
FM 8_2; 93081205325p	N 47.7200 W-121.8755	**100**	**85**	193	60	280	5	13	30	322	24	60	17	18.77	2.4
FM 9; 93112512200p	N 47.6520 W-121.8637	150	50	**360**	**44**	330	40	180	46	164	3	265	74	15.59	2.0
FM 10; 95032510412p	N 47.6707 W-121.8757	185	40	**317**	**61**	5	50	137	29	337	11	90	63	13.11	2.2
FM 11; 95082616414p	N 47.6065 W-121.8318	**110**	**80**	3	31	290	10	183	59	134	29	259	47	15.20	1.4
FM 12; 95102501120p	N 47.6707 W-121.8767	**145**	**90**	55	80	325	0	235	10	190	7	280	7	15.79	2.6
FM 13; 95102522194p	N 47.6767 W-121.8643	**175**	**80**	40	14	355	10	220	76	184	34	343	54	15.87	1.6
FM 14; 95102605024p	N 47.6685 W-121.8570	105	85	**201**	**40**	285	5	21	50	320	37	74	29	17.27	2.0
FM 15; 96011410590p	N 47.6707 W-121.8712	**205**	**85**	296	80	25	5	116	10	161	3	70	11	15.65	2.0
FM 16_1; 96050706450p	N 47.7555 W-121.8733	185	85	**279**	**50**	5	5	99	40	149	23	44	31	4.27	2.3
FM 16_2; 96050706450p	N 47.7555 W-121.8733	0	90	**270**	**80**	180	0	90	10	135	7	45	7	4.27	2.3
FM 17; 96051618334p	N 47.7568 W-121.8540	**125**	**90**	35	20	305	0	215	70	144	42	286	42	5.01	2.6
FM 18_1; 96070704204p	N 47.6710 W-121.8595	**195**	**80**	297	41	15	10	117	49	165	24	52	41	16.00	2.3
FM 18_2; 96070704204p	N 47.6710 W-121.8595	115	90	**25**	**30**	295	0	205	60	142	38	268	38	16.00	2.3
FM 19; 96102707531p	N 47.7542 W-121.8600	25	80	**117**	**80**	205	10	297	10	161	0	251	14	5.40	2.6
FM 20; 97021920523p	N 47.7552 W-121.8560	15	80	**285**	**90**	195	10	105	0	150	7	240	7	5.30	1.8

FM 21; 99092011165p	N 47.6070 W-121.7643	**105**	**75**	203	61	285	15	23	29	331	32	67	9	16.93	2.8
FM 22; 99092012005p	N 47.6045 W-121.7698	**105**	**70**	202	71	285	20	22	19	334	28	243	1	15.95	2.1
FM 23; 00110510275p	N 47.6763 W-121.8530	**120**	**20**	258	75	300	70	78	15	60	58	269	29	13.76	1.9
FM 24; 03013122472p	N 47.7438 W-121.8382	**130**	**70**	231	62	310	20	51	28	358	35	92	5	0.03	2.5
FM 25; 03092106124p	N 47.6098 W-121.8305	170	55	**318**	**40**	350	35	138	50	156	8	41	72	17.38	2.0
FM 26; 05041912304p	N 47.6650 W-121.8117	**140**	**70**	39	62	320	20	219	28	178	5	272	35	17.69	2.3
FM 27; 05042111540p	N 47.6690 W-121.8123	165	55	**345**	**35**	345	35	165	55	165	10	345	80	17.79	2.1
FM 28; 06102316533p	N 47.7022 W-121.8538	200	45	**330**	**57**	20	45	150	33	353	7	96	62	20.09	2.4
FM 29_1; 07011223281p	N 47.6700 W-121.8205	**15**	**60**	136	48	195	30	316	42	348	7	248	55	17.10	2.4
FM 29_2; 07011223281p	N 47.6700 W-121.8205	125	65	**26**	**72**	305	25	206	18	347	5	254	31	17.10	2.4
FM 30; 08052213264p	N 47.6400 W-121.8613	185	35	**310**	**68**	5	55	130	22	330	19	91	57	15.43	1.8
FM 31; 09052019063p	N 47.6037 W-121.8648	**115**	**70**	25	90	295	20	205	0	342	14	248	14	21.07	2.5
FM 32_1; 09080223160p	N 47.6717 W-121.8823	110	85	**202**	**70**	290	5	22	20	334	18	68	10	16.38	2.2
FM 32_2; 09080223160p	N 47.6717 W-121.8823	115	45	**18**	**83**	295	45	198	7	345	24	236	36	16.38	2.2
FM 33; 10013121570p	N 47.6078 W-121.7777	225	60	**338**	**56**	45	30	158	34	192	2	100	48	12.10	2.5
FM 34; 10022318133p	N 47.6210 W-121.7578	175	50	**65**	**67**	355	40	245	23	34	11	292	46	15.96	1.9
FM 35; 10052114093p	N 47.6192 W-121.8900	205	30	**341**	**67**	25	60	161	23	356	20	129	62	18.35	1.6
FM 36; 10071807164p	N 47.6070 W-121.7720	**220**	**85**	40	5	40	5	220	85	40	50	220	40	12.95	1.8
FM 37; 10110713171p	N 47.6642 W-121.9017	**150**	**35**	60	90	330	55	240	0	30	35	270	35	13.69	1.5
FM 38; unknown	N 47.6971 W-121.8741	April 21, 2012 14:25 (GMT), Event Id= 60395237 http://www.pnsn.org/event/60395237#technical-data. This earthquake occurred near the end of the Lake Joy mapping project; thus we have only partial data for this event.												2.32	2.6

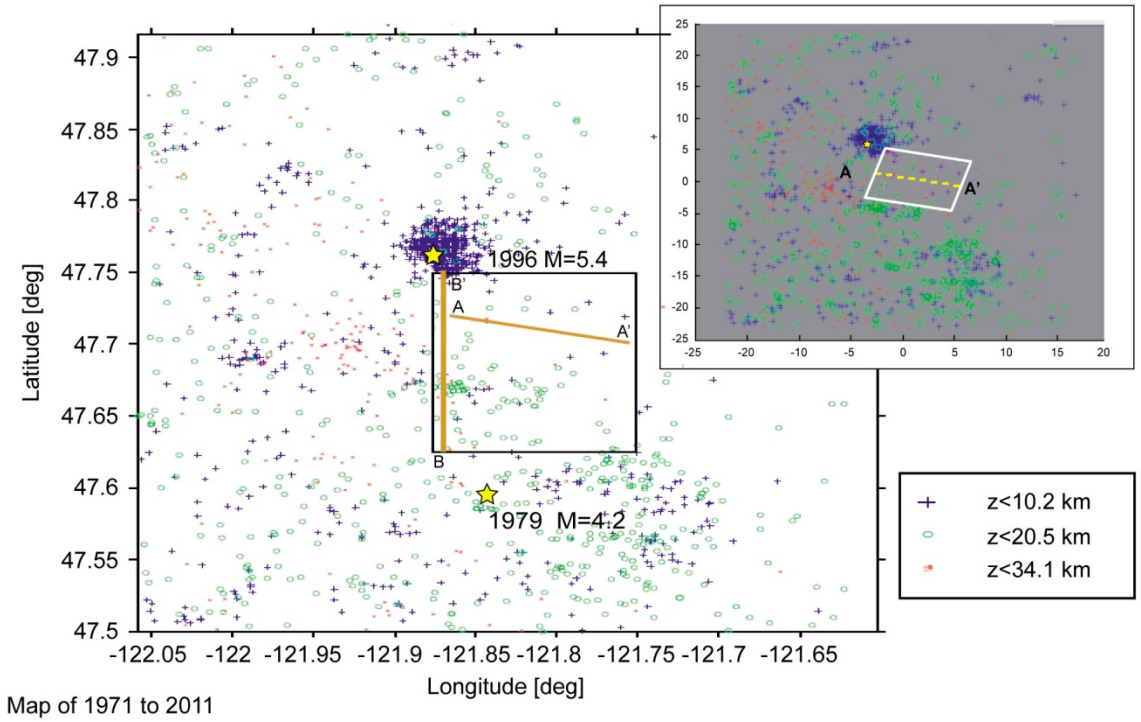

Map of 1971 to 2011

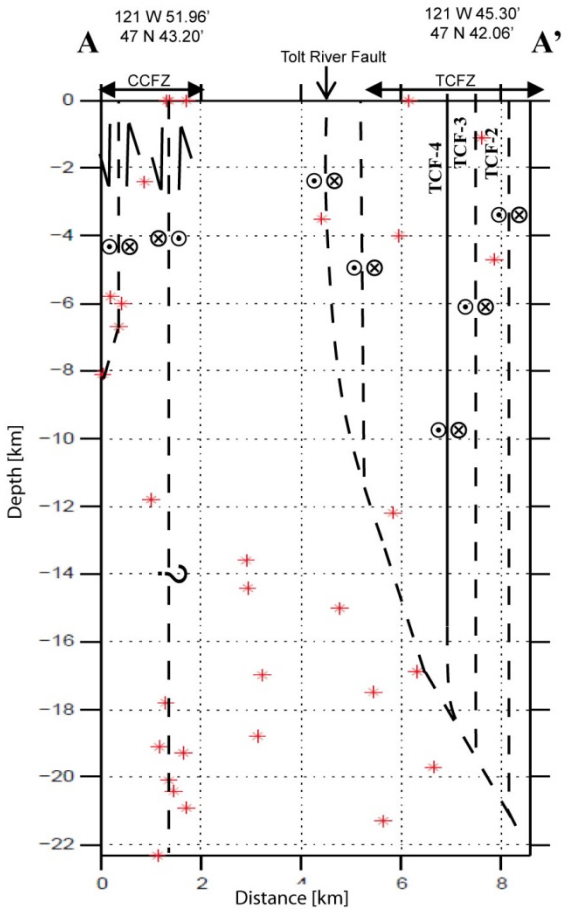

Figure G1. Cross section showing earthquake hypocenters near lithologic cross section A–A′ on Plates 1 and 2. The upper map shows regional earthquakes; the inset map shows the 8-km-wide projection area (light colored box). Lower illustration shows the earthquakes projected onto the cross section (red symbols). The projected earthquakes do not show a strong overall linear correlation with the Tokul Creek fault zone (TCFZ), including Tokul Creek faults no. 2, no. 3, and no. 4 (TCF-2, TCF-3, and TCF-4) near the cross section. However, see spatial correlation of earthquake epicenters with TCFZ fault strands on the southeastern part of Plate 2 significantly south of the cross section line area. The small concentration of earthquakes on the lower western portion of the cross section is the edge of the Duvall earthquake swarm within the Cherry Creek fault zone (CCFZ).

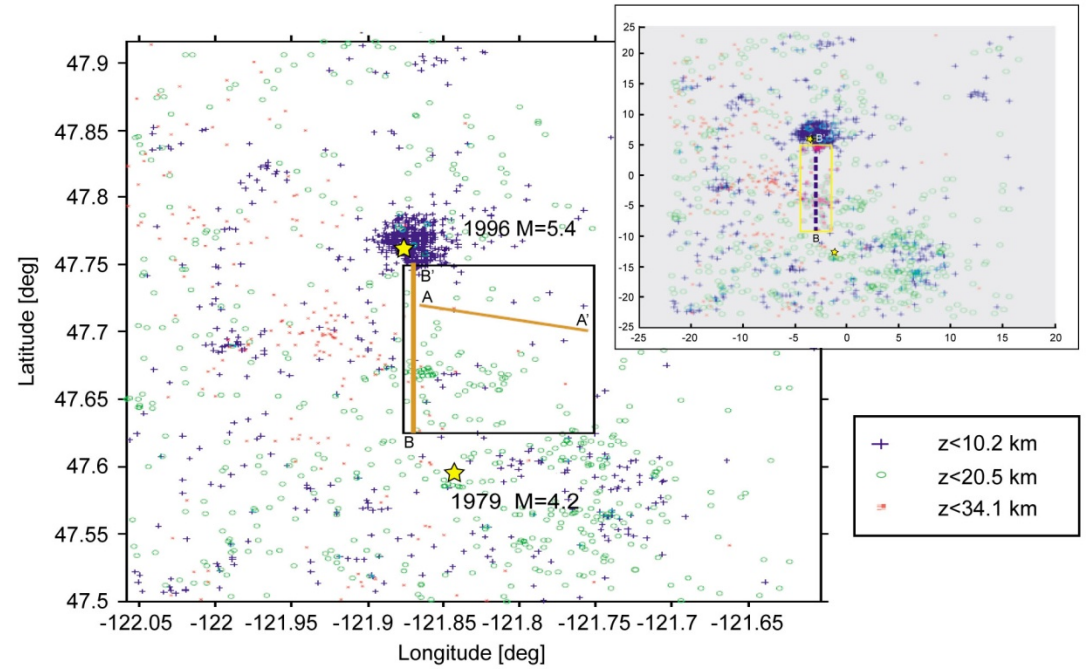

Map of 1971 to 2011

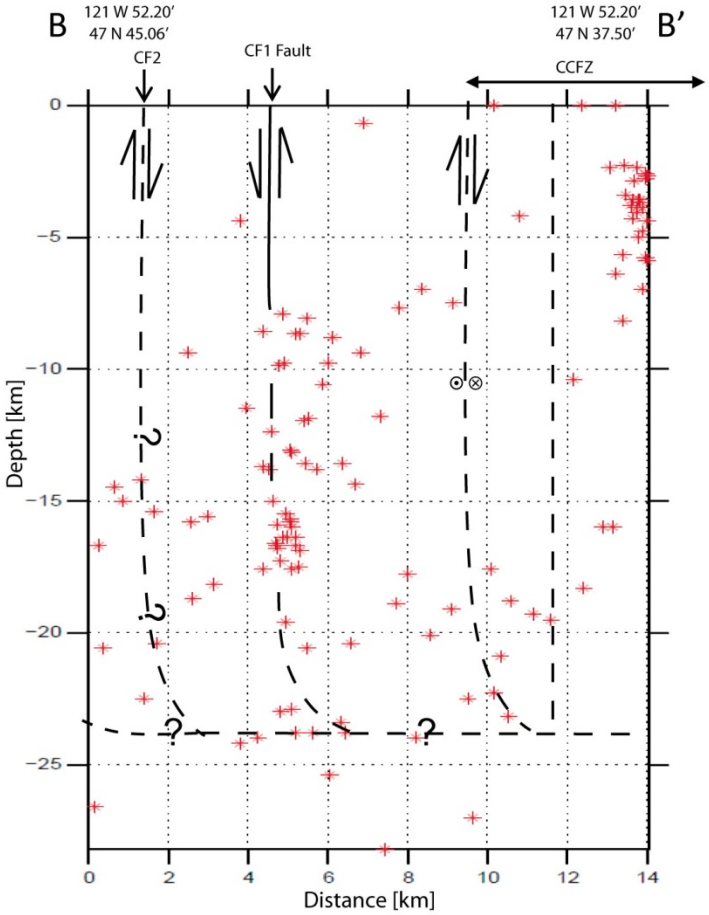

Figure G2. Cross section and maps showing all the earthquake hypocenters within a 5-km zone (2.5 km each side) parallel to lithologic cross section B–B′ on Plates 1 and 2. Two maps (top) show the regional earthquakes, Lake Joy map boundary (black square), and cross section locations (orange lines). The earthquake swarm on the regional map directly northwest of the Lake Joy map area is the Duvall swarm. The small inset map shows the cross section and 5-km-wide projection area (yellow box). Cross section (bottom) shows the projected earthquakes. Note the number and density of earthquakes hypocenters along our downward projection Carnation fault no. 1 (CF1).

Appendix H. Fault zones in the Lake Joy 7.5-minute quadrangle—some structural data and interpretations

Three fault zones are mapped in the Lake Joy 7.5-minute quadrangle: the Tokul Creek, Cherry Creek, and Carnation fault zones (see Table H1 for tabulated major characteristics of these fault zones and previous mapping references). The Tokul Creek and Cherry Creek fault zones are likely conjugate structures to the southern Whidbey Island fault zone (SWIF; Dragovich and others, 2009a,b,c, 2010a,b, 2011a,b). The Carnation fault zone is likely a strike-slip duplex reverse fault zone within and (or) adjacent to the SWIF and may be part of a broader pop-up structure. The geophysical modeling of lithologic Cross Sections A and B on Plate 1 (Figs. 1 and 2) supports our fault mapping (Appendix D). Plate 2 shows earthquake hypocenters and focal mechanisms in and around the study area. Some of these earthquake hypocenters appear to be co-located with some of the fault strands on Cross Sections A and B (Figs. G1 and G2) and are further discussed below.

Active faults display evidence for offset during the Holocene (last ~11,000 yr). The best such evidence includes displaced Holocene deposits in combination with other evidence for ongoing movement, such as hypocenters along faults. *Potentially active faults* show evidence of offset during the Quaternary (last ~2.6 my). We did not discover any displaced Holocene deposits along mapped faults in the map area; however, converging lines of evidence indicate there are potentially active faults in the Lake Joy quadrangle. Some fault zones are likely co-located with recent moderate to small earthquakes and locally displace or deform Pleistocene deposits. Complete characterization of these proposed active faults and potentially active faults awaits detailed analyses, including fault trenching, or definitive evidence of Holocene activity.

Indications of active or potentially active faulting in this quadrangle, discussed more fully below, include: (1) rare faulting of pre-Fraser nonglacial deposits, (2) localized earthquake liquefaction features in Vashon and older Quaternary deposits (for example, Fig. E8, significant site 204T, photo 288), and (3) elevation differences of ancient alluvium (Plate 1) along Carnation fault no. 1 and the adjacent Tolt River anticline, resulting in an inverted basin (Appendix F). In addition, some earthquakes appear to be co-located with mapped fault zones; that is, our direct field mapping and (or) indirect geophysical modeling (Appendix D) link the kinematics of the fault zones inferred from the focal mechanisms to the hypocenters, particularly for the high-angle fault zones (Appendix G). Examples are the left-lateral strike-slip faulting inferred for the Cherry Creek and Tokul Creek fault zones by our detailed field structural mapping, and this information correlates well with the kinematics of the fault zones (Plate 2, Appendix G). Fault activity is also suggested by the "Tolt River" and "Duvall" earthquakes in or near the study area.

FAULT SUMMARIES

Tokul Creek fault zone (TCFZ)—This is a regional oblique-left-lateral strike-slip fault zone originally mapped south of the Lake Joy quadrangle by Dragovich and others (2007, 2009b,c, 2010b) and extended into this study area. The TCFZ here includes the Tokul Creek fault main strand and the numbered strands (Tokul Creek faults 2, 3, and 4), as well as the Tolt River fault and associated structures. Oblique-slip offset along the main strand has resulted in juxtaposition of Tertiary volcanic rocks of Mount Persis against the Western mélange belt Jurassic–Cretaceous basement rocks (Tabor and others, 1993; Dragovich and others, 2009b,c). Most primary and subsidiary fault strand structures are consistent with strike-slip fault deformation and include steep northeast-trending fractures or cataclasite zones dominated by subhorizontal slickenlines (Plate 1, explanation of structural symbols). Also, the fault lineaments are straight, indicating a zone dominated by high-angle strike-slip faults. Like the CCFZ, the TCFZ contains many anastomosing structures typical of strike-slip fault zones, such as cross faults between the main fault strands. Although no distinct lineaments were observed in the lidar or Quaternary deformation along the Tokul Creek fault zone was noted by Dragovich and others (2009b,c), the location of several earthquake hypocenters near the Tokul Creek fault zone suggests a locally active structure. As discussed in Appendix G, earthquake focal mechanisms in the TCFZ are dominated by left-lateral strike-slip solutions, assuming a northeast-trending fault plane. The spatial coincidences of Tokul Creek fault no. 4 with some local Quaternary faults and the 1932 Tolt River earthquake suggest this structure might be active. Figure E13 (photo 1046) shows Pleistocene nonglacial deposits at significant site 108D (Plate 1; sec. 33, T26N R8E) displaced by a tectonic fault. The Tolt River earthquake intensity VI contour (Bradford and Waters, 1934), centered on significant site TQ2 on Plate 1 (sec. 20, T26N R8E), was partially based on a felt report—"practically impossible to stand"—at significant site TQ1 (sec. 33, T26N R8E) near

the Tolt Regulating Basin. Although spatially poorly constrained, available information suggests a causal relation of that earthquake with Tokul Creek fault no. 4. We speculate that the seismic energy of the Tolt River earthquake relieved strain along this portion of the TCFZ and loaded nearby faults. This speculation assumes: (1) the location of the 1932 Tolt River epicenter near the Tolt Regulating Basin is generally correct, and (2) the TCFZ and CCFZ are kinematically tied by east- and northwest-trending cross faults in the Lake Joy quadrangle (Plates 1 and 2). This conjecture is supported by the presence of fewer earthquake epicenters surrounding the Tolt Regulating Basin area than along the TCFZ directly south of the map area and by the number of epicenters along the CCFZ in the northwest part of Plate 2. In this scenario the TCFZ and CCFZ are kinematically tied via the many cross faults in the northern part of the study area.

Cherry Creek fault zone (CCFZ)—Dragovich and others (2010a,b) gave the informal name Cherry Creek fault zone to a family of subparallel faults in the northeastern Carnation quadrangle. The northeast-trending CCFZ may be a conjugate fault zone to the overall northwest-trending SWIF. This arrangement is strikingly similar to the relation between the Tokul Creek fault zone and the Rattlesnake Mountain fault zone (RMFZ) in the Snoqualmie quadrangle to the southeast, where the northeast-trending Tokul Creek fault zone merges with the northwest-trending RMFZ east of the city of Snoqualmie. In both the Snoqualmie and Carnation areas, the northeast-trending faults may be conjugate faults to the RMFZ-SWIF composite structure. We interpret the focal mechanisms associated with the shallow Duvall earthquake swarm to indicate a positive flower structure associated with a transpressional left-lateral strike-slip fault zone (Appendix G). Dragovich and others (2010a,b) tentatively relate local Quaternary deformation of unit Qc$_{ol}$ to tectonism within the CCFZ in the Carnation quadrangle to the west. We found no direct field evidence for an active fault zone along the CCFZ strands in the northeast part of the Lake Joy quadrangle. However, the distinct spatial correspondence of the shallow Duvall earthquakes (2–10 km depth) with a high-angle fault zone is strongly suggestive of an active fault, and the lack of tectonic scarps might be due to vegetative cover and mass wasting along the steep slopes that are common within the fault zone (Dragovich and others (2011a,b). See Plates 1 and 2 of Dragovich and others (2011b) for more information about the Duvall earthquake main shock and aftershocks.

Carnation Fault Zone (CFZ)—The Carnation fault zone was originally mapped by Dragovich and others (2010a,b) on the basis of geophysical (gravity, magnetic, and seismic reflection) and structural data and contains two strands—Carnation faults no. 1 and no. 2 (CF-1, CF-2). Although there is some geophysical evidence for projecting CF-2 into the study area from the west (Plate 1, Figs. 1 and 2), the more compelling structure in the present study area is CF-1. CF-1 is evidenced by several independent data sources including: (1) the direct mapping of bedrock cataclasite, mylonites along the fault (unit tz on Plate 1), (2) direct mapping of primary bedding along the fault (Tolt River anticline on Plate 1), (3) gravity and aeromagnetic geophysical data (Plate 1, Figs. 1 and 2; Villeneuve, 2012), (4) seismic cluster data (Appendix G), and (5) geomorphic and stratigraphic anomalies directly north of the fault. Some of the cataclasites and mylonites formed along CF-1 are shown in Figures E4 and E5 (site 28D, photos 143, 147 and 149). The mylonitic foliations in unit tz along this fault (Plate 1) generally have a moderate northerly dip consistent with brittle-ductile shear along an east-striking reverse fault. Slickenlines on the shear surfaces generally plunge moderately to the north, consistent with overall southerly vergence, and parallel the south-directed offset. We suggest the Tolt River anticline is a flexural slip fold related to southerly verging reverse offset along CF-1. Available Quaternary bedding information is consistent with folding of ancient alluvium (units Qc$_{ws}$ and Qc$_{hmp}$) around this potentially active anticline—fold tightening may have uplifted ancient alluvium in the fold axis area. Our geophysical modeling along Cross Section B (Plate 1) supports significant vertical (north side up) offset along CF-1. This geophysical dataset is consistent with the hypocenter information suggestive of a subvertical active fault along the CF-1 trend. The difference in fault dip suggested by the hypocenter data (subvertical) and the direct mylonitic fabric data in unit tz along CF-1 may indicate a more complex fault that consists of a steep master fault and more shallowly dipping subsidiary faults that taper into the master fault. The upper plate of this reverse fault also hosts topographic and stratigraphic anomalies near significant site 5W that are mapped to an elevation of ~900 ft (274 m) (Plate 1; sec. 7, T25N R8E). This area exposes anomalously high ancient Snoqualmie alluvium of unit Qc$_{ws}$ that we hypothesize was uplifted via a combination of CF-1 vertical offset and (or) folding along the Tolt River anticline (Plate 1, Cross Section B). We also speculate that the anomalously high ridge elevations around significant site 5W (~30 ft higher than surrounding fluted ridge tops) observable on lidar elevation data are the result of Holocene reverse offset along CF-1. Finally, although large, deep-seated landslides are common in the region, the Carnation fault zone is spatially coincident with several landslide complexes, including the Tolt River landslide complex (Plate 1). Seismically induced landslides commonly have a lateral spread style of failure, similar to the

style of deep-seated landsliding in this area. Finally, a regional pop-up structure is indicated by the dual nature of the Carnation fault zone southerly vergence versus the northerly vergence of the Monroe faults north of the study area (see also Dragovich and others, 2011a,b). This broadly defined pop-up structure is coincident with shallow or exposed bedrock between these oppositely verging reverse structures in the general Monroe–Duvall–Lake Joy area. This proposed pop-up structure begs several questions: What is the relation between this pop-up structure and the kinematics of the SWIF? Also, is this pop-up structure related to the slight bend in the SWIF azimuth northwest of Carnation? Finally, are the reverse faults that bound the pop-up structure strike-slip duplex reverse faults within and (or) adjacent to the SWIF, or are they more discrete structures that verge into the SWIF from the east? In other words, is the pop-up bound by the SWIF as reverse faults between strike-slip strands of the SWIF, or does a reverse fault complex merge from the east into the SWIF?

Table H1. Characteristics of the major fault zones in the Lake Joy 7.5-minute quadrangle. See text above for further fault zone information.

Fault zone name; overall sense of displacement	Original reference(s)	Activity and other structure notes
Tokul Creek fault zone (TCFZ); left-lateral strike- slip fault zone (possible flower structure)	Originally named by Dragovich and others (2009b,c) directly to the south in the Snoqualmie 7.5-minute quadrangle	Potentially active. Spatial correlation of the earthquake hypocenters with some of the fault strands, particularly in the northeastern part of the adjacent Snoqualmie 7.5-minute quadrangle (Plate 2), suggests some strands may be active. Probable tectonic displacement of Pleistocene deposits along the TCF-4 fault as discussed above. The TCFZ appears to be a regional fault zone that juxtaposes basement with Tertiary volcanic rocks (Dragovich and others, 2009a,b; this study). Part of the Tokul Creek fault was originally mapped by Tabor and others (1993), who mapped an unnamed fault along the TCFZ trend subparallel to the TCF main strand.
Cherry Creek fault zone (CCFZ); left-lateral strike- slip fault zone (possible flower structure)	Originally mapped by Dragovich and others (2010a,b) and extended by Dragovich and others (2011a,b) in the Carnation and Monroe 7.5-minute quadrangles	Correlation of seismicity with the CCFZ suggests an overall active fault. (See Duvall earthquake above.) Further work is required to correlate individual strands of the CCFZ with surface fault structures formed in the Holocene (see Dragovich and others (2011a,b). Mapped strands of the CCFZ in the Lake Joy quadrangle locally contain unit tz cataclasite, but better exposures of this fault zone are in the adjacent Carnation and Monroe quadrangles. The CCFZ trends into the Sultan quadrangle (J. Dragovich, unpub. data) directly north of the Lake Joy quadrangle, where it appears to be coincident with fault-like geomorphic features such as elongate tributary valleys and other lineaments.
Carnation fault zone (CFZ); reverse fault or fault zone	Dragovich and others (2010a,b) originally mapped Carnation faults no. 1 and no. 2 (CF-1, CF-2) directly west in the Carnation 7.5-minute quadrangle	Correlation of seismicity with CF-1, as well as potential geomorphic and stratigraphic anomalies directly north of the fault, suggest that this structure is active. Folding and (or) uplift of Pleistocene beds also strongly suggest this fault is potentially active, as does the apparent uplift of Whidbey Formation ancient Snoqualmie River alluvium. CF-2 is poorly constrained, and its dip-slip offset is inferred from geophysical evidence. The westerly projection of CF-1 on the basis of geophysical information (Plate 1, Figs. 1 and 2), earthquake hypocenters (Appendix G), and subsurface data (Plate 1, Cross Sections A and B) in the Lake Joy quadrangle suggests that CF-1 was mismapped by Dragovich and others (2010a) in the easternmost part of the Carnation quadrangle as illustrated on the western part of Plate 2. CF-1 was projected to the eastern part of the adjacent Carnation quadrangle on the basis of indirect information (magnetic susceptibility data and bedrock top elevation information), but newer mapping information suggests this fault occurs north of where it was mapped in the Carnation quadrangle. (See Plate 2 and locations of CF-1 in the two adjacent quadrangles.)